USGS
science for a changing world

Prepared in cooperation with the Harris-Galveston Subsidence District, City of Houston, Fort Bend Subsidence District, Lone Star Groundwater Conservation District, and Brazoria County Groundwater Conservation District

Treatment of the Chicot and Evangeline Aquifers as a Single Hydrogeologic Unit and Use of Geostatistical Interpolation Methods To Develop Gridded Surfaces of Water-Level Altitudes and Water-Level Changes in the Chicot and Evangeline Aquifers (Undifferentiated) and Jasper Aquifer, Greater Houston Area, Texas, 2021

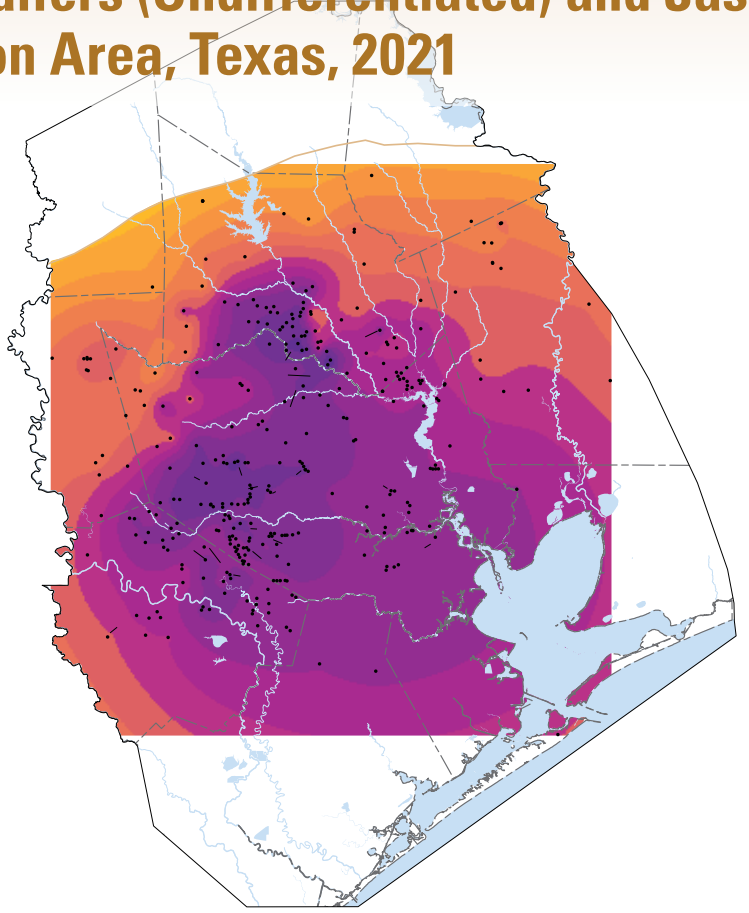

Scientific Investigations Report 2022–5064

U.S. Department of the Interior
U.S. Geological Survey

Treatment of the Chicot and Evangeline Aquifers as a Single Hydrogeologic Unit and Use of Geostatistical Interpolation Methods To Develop Gridded Surfaces of Water-Level Altitudes and Water-Level Changes in the Chicot and Evangeline Aquifers (Undifferentiated) and Jasper Aquifer, Greater Houston Area, Texas, 2021

By Jason K. Ramage, Christopher L. Braun, and John H. Ellis

Prepared in cooperation with the Harris-Galveston Subsidence District, City of Houston, Fort Bend Subsidence District, Lone Star Groundwater Conservation District, and Brazoria County Groundwater Conservation District

Scientific Investigations Report 2022–5064

U.S. Department of the Interior
U.S. Geological Survey

U.S. Geological Survey, Reston, Virginia: 2022

For more information on the USGS—the Federal source for science about the Earth, its natural and living resources, natural hazards, and the environment—visit https://www.usgs.gov or call 1–888–ASK–USGS.

For an overview of USGS information products, including maps, imagery, and publications, visit https://store.usgs.gov/.

Any use of trade, firm, or product names is for descriptive purposes only and does not imply endorsement by the U.S. Government.

Although this information product, for the most part, is in the public domain, it also may contain copyrighted materials as noted in the text. Permission to reproduce copyrighted items must be secured from the copyright owner.

Suggested citation:
Ramage, J.K., Braun, C.L., and Ellis, J.H., 2022, Treatment of the Chicot and Evangeline aquifers as a single hydrogeologic unit and use of geostatistical interpolation methods to develop gridded surfaces of water-level altitudes and water-level changes in the Chicot and Evangeline aquifers (undifferentiated) and Jasper aquifer, greater Houston area, Texas, 2021: U.S. Geological Survey Scientific Investigations Report 2022–5064, 51 p., https://doi.org/10.3133/sir20225064.

Associated data for this publication:
Ramage, J.K., 2022, Depth to groundwater measured from wells completed in the Chicot and Evangeline (undifferentiated) and Jasper aquifers, greater Houston area, Texas, 2021: U.S. Geological Survey data release, https://doi.org/10.5066/P9R6CX2T.

U.S. Geological Survey, 2022, USGS water data for the Nation: U.S. Geological Survey National Water Information System database, https://doi.org/10.5066/F7P55KJN.

ISSN 2328-0328 (online)

Contents

Figures

Tables

Conversion Factors

U.S. customary units to International System of Units

Multiply	By	To obtain
	Length	
foot (ft)	0.3048	meter (m)
mile (mi)	1.609	kilometer (km)
	Area	
square foot (ft^2)	0.09290	square meter (m^2)
square mile (mi^2)	2.590	square kilometer (km^2)
	Transmissivity	
foot squared per day (ft^2/d)	0.09290	meter squared per day (m^2/d)

International System of Units to U.S. customary units

Multiply	By	To obtain
	Length	
meter (m)	3.281	foot (ft)
meter (m)	1.094	yard (yd)
	Area	
square meter (m^2)	0.0002471	acre
square kilometer (km^2)	247.1	acre
square meter (m^2)	10.76	square foot (ft^2)
square kilometer (km^2)	0.3861	square mile (mi^2)

Datum

Vertical coordinate information is referenced to either the National Geodetic Vertical Datum of 1929 (NGVD 29) or the North American Vertical Datum of 1988 (NAVD 88).

Horizontal coordinate information is referenced to the North American Datum of 1983 (NAD 83).

Abbreviations

>	greater than
BCGCD	Brazoria County Groundwater Conservation District
bls	below land surface
FBSD	Fort Bend Subsidence District
HGSD	Harris-Galveston Subsidence District
LOO	leave-one-out
LSGCD	Lone Star Groundwater Conservation District
NAVD 88	North American Vertical Datum of 1988
p-value	probability value
RMSE	root mean square error
R-squared	coefficient of determination
USGS	U.S. Geological Survey

Treatment of the Chicot and Evangeline Aquifers as a Single Hydrogeologic Unit and Use of Geostatistical Interpolation Methods To Develop Gridded Surfaces of Water-Level Altitudes and Water-Level Changes in the Chicot and Evangeline Aquifers (Undifferentiated) and Jasper Aquifer, Greater Houston Area, Texas, 2021

By Jason K. Ramage, Christopher L. Braun, and John H. Ellis

Abstract

The greater Houston area of Texas includes approximately 11,000 square miles and encompasses all or part of 11 counties (Harris, Galveston, Fort Bend, Montgomery, Brazoria, Chambers, Grimes, Liberty, San Jacinto, Walker, and Waller). From the early 1900s until the mid-1970s, groundwater withdrawn from the three primary aquifers that compose the Gulf Coast aquifer system—the Chicot, Evangeline, and Jasper aquifers—had been the primary source of water for the greater Houston area. The withdrawal of groundwater was unregulated prior to 1975, resulting in land-surface subsidence caused by large water-level declines in the greater Houston area.

This report, prepared by the U.S. Geological Survey in cooperation with the Harris-Galveston Subsidence District, City of Houston, Fort Bend Subsidence District, Lone Star Groundwater Conservation District, and Brazoria County Groundwater Conservation District, describes updates to the ways in which water-level altitudes and water-level changes in the greater Houston area are presented relative to previous U.S. Geological Survey reports. The first update involves presenting water-level altitudes and water-level changes as a combined (undifferentiated) representation of the Chicot and Evangeline aquifers. The second update concerns the methods used to depict water-level altitudes and water-level changes in the greater Houston area in interpretive reports, with geostatistical interpolation methods replacing manual contouring methods.

The Chicot and Evangeline aquifers have historically been described as distinct hydrogeologic units for the purpose of water-level mapping. A confining unit does not separate these two aquifers in the study area, and water-level data from colocated wells screened in these aquifers indicate that there is likely a substantial degree of hydrogeologic connection. From a groundwater-flow perspective, these two aquifer units predominantly function as a single unit. Hence, the decision was made to combine the Chicot and Evangeline aquifers into a single, undifferentiated hydrogeologic unit for the purposes of assessing water-level altitudes and water-level changes over time. The 2020 water-level altitudes for the Chicot, Evangeline, and Jasper aquifers were re-created in this report from computer algorithms of the contoured datasets as gridded surfaces to demonstrate the similarity of results from geostatistical interpolation methods to those from manual contouring methods.

Introduction

The greater Houston area of Texas includes approximately 11,000 square miles (mi^2) and encompasses all or part of 11 counties (Harris, Galveston, Fort Bend, Montgomery, Brazoria, Chambers, Grimes, Liberty, San Jacinto, Walker, and Waller) (fig. 1). Until the implementation of groundwater regulations in the mid-1970s, groundwater withdrawn from the three primary aquifers that compose the Gulf Coast aquifer system—the Chicot, Evangeline, and Jasper aquifers—had been the primary source of water for municipal supply, commercial and industrial use, and irrigation in the greater Houston area since the early 1900s (Kasmarek and Robinson, 2004). The unregulated withdrawal of groundwater from the Chicot and Evangeline aquifers, prior to 1975, caused water levels in the aquifers to steadily decline year over year, resulting in land-surface subsidence in the greater Houston area (Coplin and Galloway, 1999). By 1977, the withdrawals had resulted in distinct areas in southeastern Harris County where water levels in the Chicot and Evangeline aquifers were as much as 300 and 350 feet (ft), respectively, below the National Geodetic Vertical Datum of 1929 (NGVD 29)

(Gabrysch, 1979). Large water-level declines such as those in southeastern Harris County are the primary reason that the land surface has subsided by several feet in a large part of the study area and by as much as 9 ft in isolated parts of the greater Houston area (Gabrysch and Bonnet, 1975; Kasmarek, Gabrysch, and Johnson, 2009).

To address concerns regarding land-surface subsidence in Harris and Galveston Counties, the 64th Texas State Legislature authorized the establishment of the Harris-Galveston Subsidence District (HGSD) in 1975 (Harris-Galveston Subsidence District, 2021) to regulate and reduce groundwater withdrawals. After establishing the HGSD, the Texas State Legislature established an additional subsidence district (Fort Bend Subsidence District [FBSD]) and four groundwater conservation districts (Lone Star Groundwater Conservation District [LSGCD], Brazoria County Groundwater Conservation District [BCGCD], Bluebonnet Groundwater Conservation District, and Lower Trinity Groundwater Conservation District) in the greater Houston area (figs. 1 and 2) to enable the regulation of groundwater withdrawals within their respective jurisdictions. Each district maintains a website describing their history and groundwater management plan (Fort Bend Subsidence District, 2013, 2021; Harris-Galveston Subsidence District, 2013; Brazoria County Groundwater Conservation District, 2017, 2021; Bluebonnet Groundwater Conservation District, 2018, 2021; Lower Trinity Groundwater Conservation District, 2019, 2021; Lone Star Groundwater Conservation District, 2020, 2021). Regulatory plans to gradually decrease groundwater withdrawals have been in place in some parts of Harris and Galveston Counties since 1976; plans to regulate groundwater withdrawals (in conjunction with increased usage of alternative surface-water supplies) are currently (2022) being phased in throughout most of the study area (as of 2022, no plans to reduce groundwater withdrawals in Liberty and Chambers Counties have been promulgated) (figs. 1 and 2).

Since the late 1970s, the U.S. Geological Survey (USGS), in cooperation with the HGSD, has monitored water-level altitudes and published reports depicting the status of water-level altitudes and long-term water-level changes in aquifers in the greater Houston area. Following their establishment by the Texas State Legislature, the FBSD, LSGCD, and BCGCD, as well as the City of Houston, also became cooperative participants in the project. An extensive monitoring-well network was first established by the USGS in 1977, and water-level data were collected and used to create the first published water-level-altitude maps of the Chicot and Evangeline aquifers in the greater Houston area for the reporting period of spring 1977 and spring 1978 (Gabrysch, 1979). A comprehensive water-level-altitude report for the Chicot and Evangeline aquifers was first published by the USGS in 1991 (Barbie and others, 1991), and in 2001, the first published water-level-altitude map of the Jasper aquifer (Coplin, 2001) was added to the annual series of reports depicting the status of water-level altitudes and long-term water-level changes in aquifers in the greater Houston area. Additional information on the history of water-level-altitude monitoring and of the annual series of USGS reports published to document water-level altitudes and water-level changes in aquifers in the greater Houston area is provided in Kasmarek and Ramage (2017).

This report, prepared by the USGS in cooperation with the HGSD, City of Houston, FBSD, LSGCD, and BCGCD, describes two substantial updates to the ways in which water-level altitudes and water-level changes in the greater Houston area are presented relative to previous USGS reports (for example, Kasmarek and Houston, 2008; Kasmarek, Houston, and Ramage, 2009; Kasmarek and others, 2010, 2012, 2013, 2014, 2015, 2016; Johnson and others, 2011; Kasmarek and Ramage, 2017; Shah and others, 2018; Braun and others, 2019; Braun and Ramage, 2020). The Chicot and Evangeline aquifers have traditionally been depicted as separate aquifers (figs. 1, 3, and 5). The first update involves presenting water-level altitudes and water-level changes as a combined (undifferentiated) representation of the Chicot and Evangeline aquifers (figs. 4 and 5). For the purpose of depicting water-level altitudes and long-term water-level changes, the Chicot and Evangeline aquifers are not presented as separate hydrogeologic units herein or in the companion 2021 annual report on water-level altitudes and water-level changes in the study area (Braun and Ramage, 2022), nor are they planned to be presented as separate in the annual series of reports hereafter. The rationale for referring to the Chicot and Evangeline aquifers as the "Chicot and Evangeline aquifers (undifferentiated)" (figs. 2, 4, and 5) is explained in this report. The second update concerns the methods used to depict water-level altitudes and water-level changes in the greater Houston area in interpretive reports. Instead of the manual contouring methods that have historically been used in the annual USGS interpretive report series (for example, Braun and others, 2019; Braun and Ramage, 2020), geostatistical interpolation methods are used to develop gridded surfaces of water-level altitudes and water-level changes starting with the 2021 annual report (Braun and Ramage, 2022). As part of the second update, the areal extent of the gridded surfaces is refined through the use of a masking process. In the masking process, grid cells with either extrapolated or interpolated location-specific values representing areas of reduced well density within the well network distribution are not shown. This masking process is used for removing, or hiding, grid cells with estimates of high uncertainty provided by the interpolation. Estimates of high uncertainty are defined as those grid cells in which the standard error of the kriging estimate exceeds the overall mean standard error for the entire gridded surface. The standard error most often exceeds the overall mean standard error (as provided by the kriging estimates) in areas of reduced well density or areas where the estimate is extrapolated beyond where there is good data control (such as near the grid boundaries) (Olea, 1975, 2009; Dunlap and Spinazola, 1984).

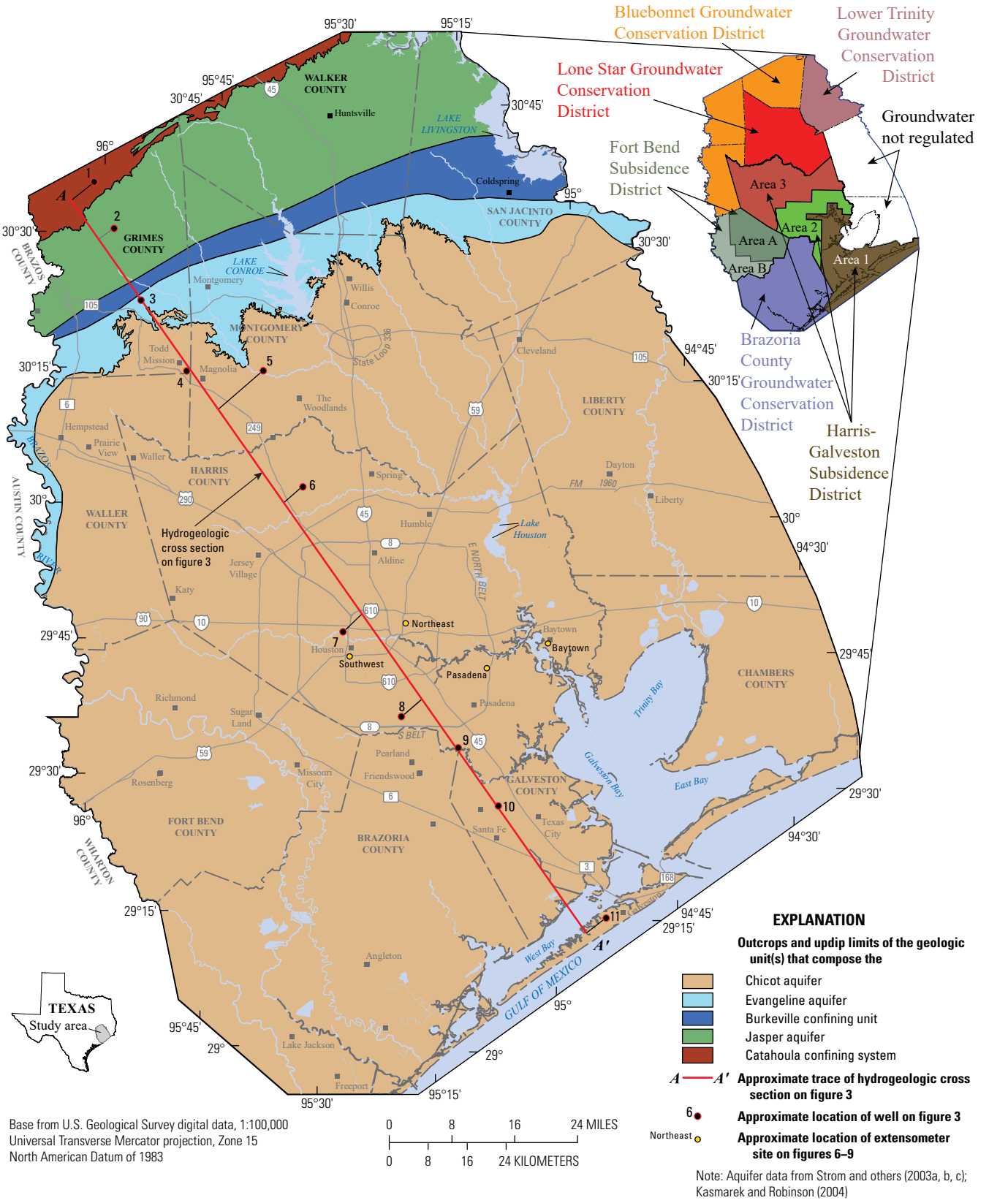

Figure 1. Jurisdictions of groundwater conservation and subsidence districts with the approximate trace of hydrogeologic cross section *A*–*A*′ spanning traditional depictions of the outcrops and updip limits of the geologic units of the Gulf Coast aquifer system in the greater Houston study area, Texas.

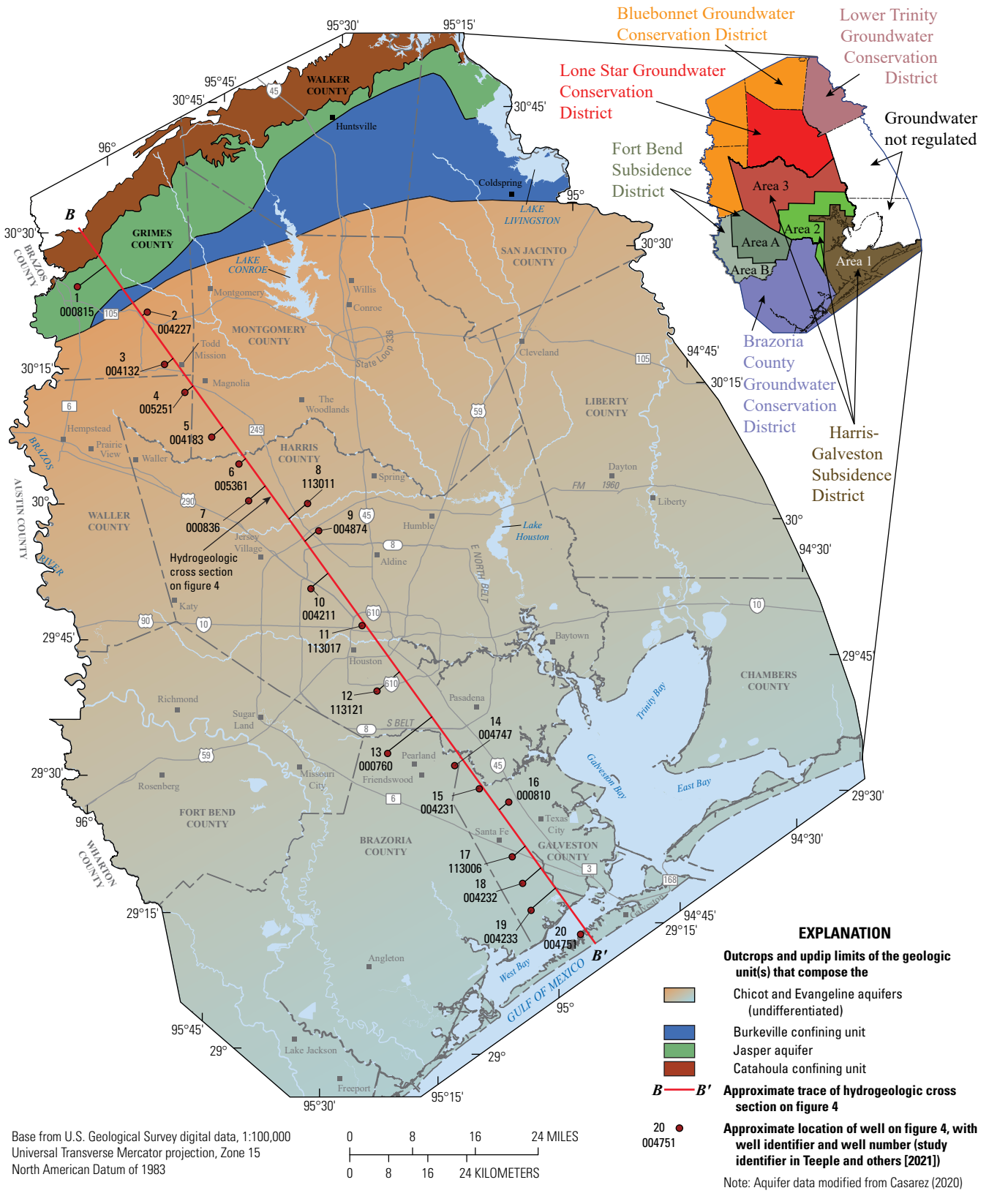

Figure 2. Jurisdictions of groundwater conservation and subsidence districts with the approximate trace of hydrogeologic cross section *B*–*B*′ spanning an updated depiction of the outcrops and updip limits of the geologic units of the Gulf Coast aquifer system in the greater Houston study area, Texas.

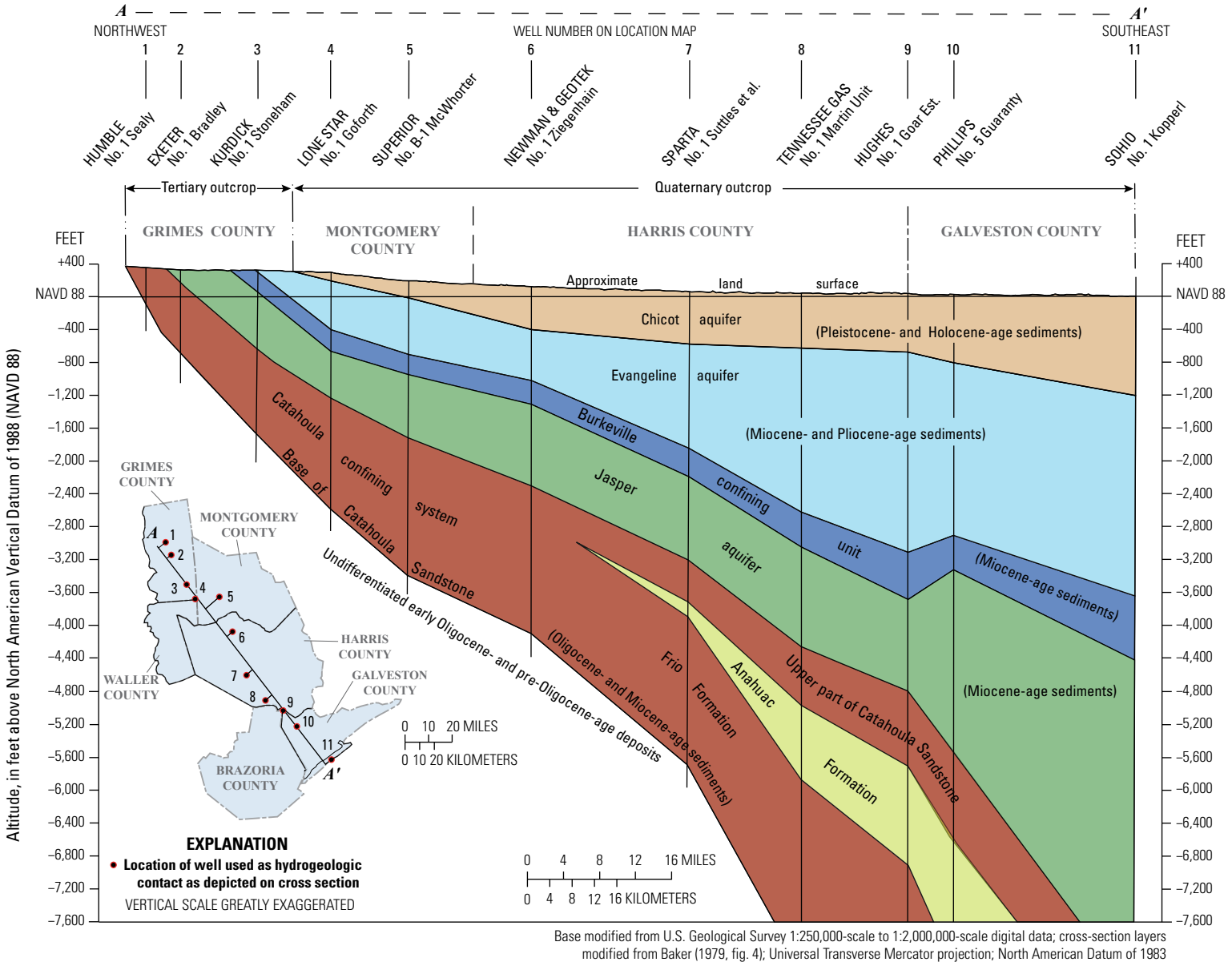

Figure 3. Traditional hydrogeologic cross section *A–A′* of the Gulf Coast aquifer system in Grimes, Waller, Montgomery, Harris, Brazoria, and Galveston Counties, Texas.

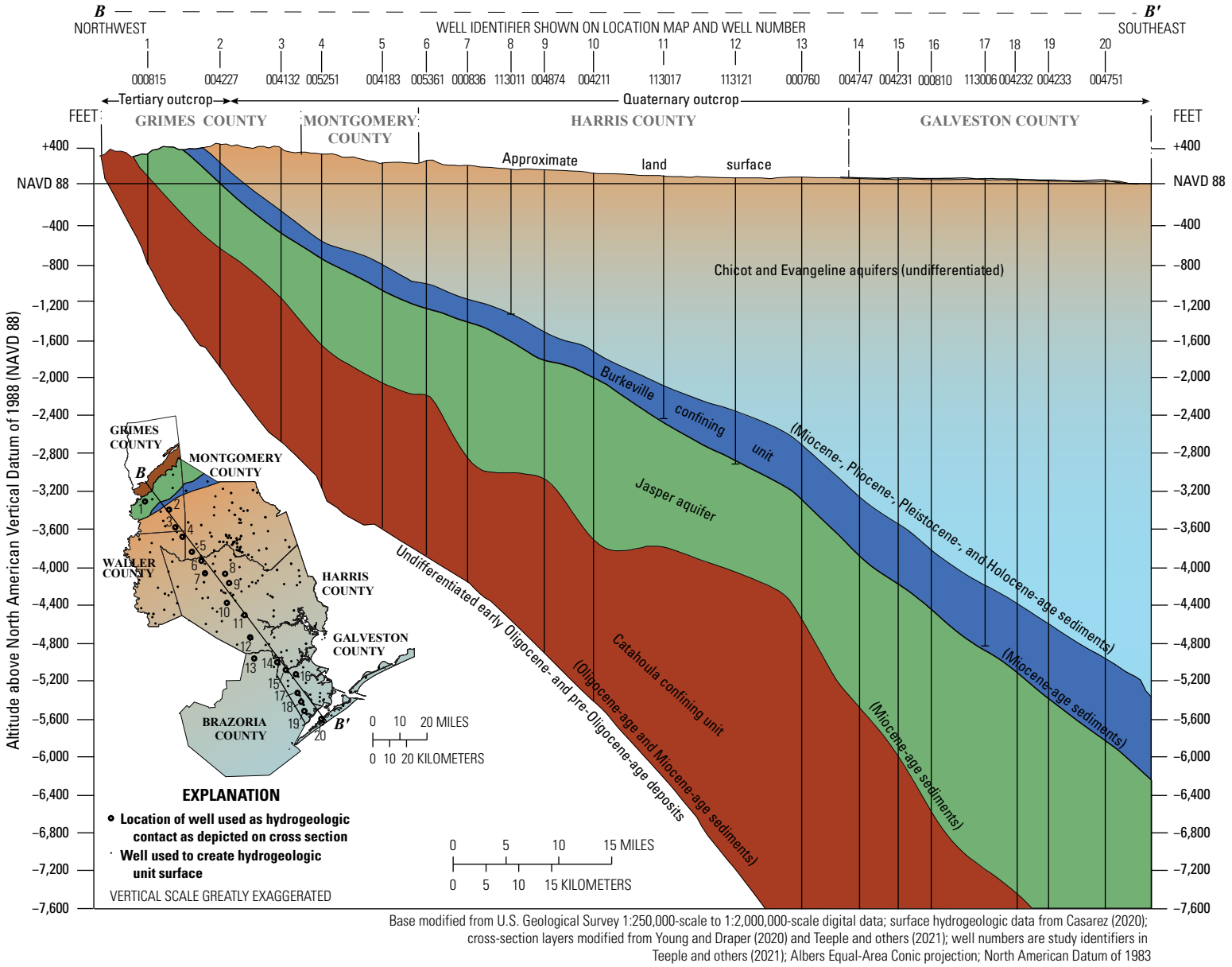

Figure 4. Updated hydrogeologic cross section *B–B′* of the Gulf Coast aquifer system in Grimes, Waller, Montgomery, Harris, Brazoria, and Galveston Counties, Texas.

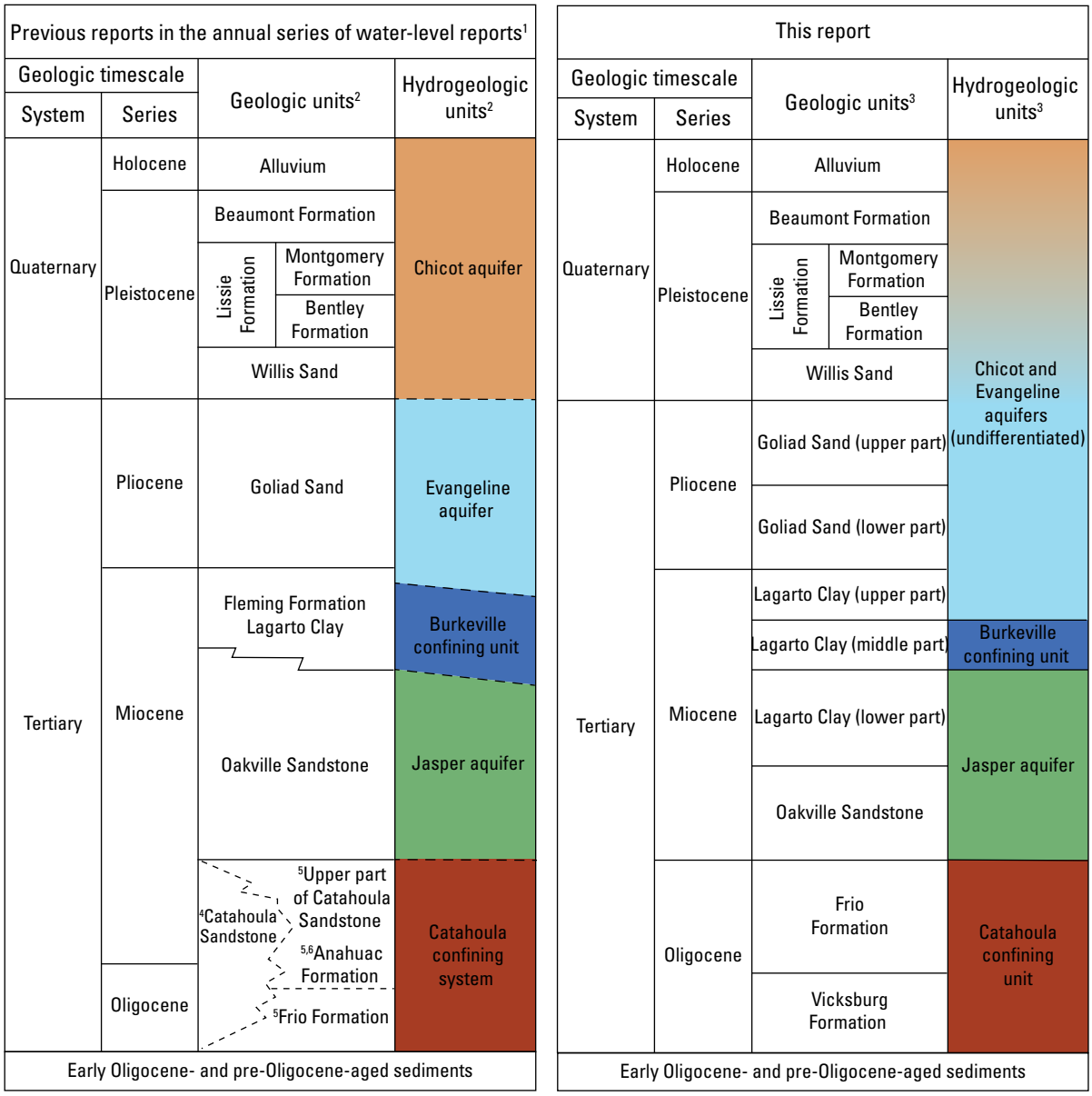

[1]For example, Braun and others (2019) and Braun and Ramage (2020).
[2]Modified from Sellards and others (1932), Baker (1979), and Meyer and Carr (1979).
[3]Modified from Young and others (2012, 2014) and Young and Draper (2020).
[4]Located in the outcrop.
[5]Located in the subcrop.
[6]"Anahuac Formation" is not an approved U.S. Geological Survey unit name but has been referred to previously in a U.S. Geological Survey report by Swanson and others (2013).

Note: Dashed lines shown between hydrogeologic units in previous reports in the annual series indicate that the geologic units shown as containing the hydrogeologic units in question are not absolute.

Figure 5. Traditional and updated depictions of the geologic and hydrogeologic units of the Gulf Coast aquifer system in the greater Houston study area, Texas.

Purpose and Scope

The primary purpose of this report is to describe an updated process for depicting water-level altitudes and long-term water-level changes in the greater Houston area of Texas. Results from the updated process are compared to the results from traditional, manual contouring methods used to depict water levels in the greater Houston area. Differences between the updated process and the traditional, manual methods used in the annual USGS reports on water-level altitudes and water-level changes include (1) the treatment of the Chicot and Evangeline aquifers as a single hydrogeologic unit as opposed to separate aquifers and (2) the use of geostatistical kriging interpolation methods (Olea, 1975, 2009; Dunlap and Spinazola, 1984) to develop gridded surfaces of water-level altitudes and water-level changes instead of manually drawn contour lines.

Geology and Hydrogeology of the Study Area

The following overview of the geology and hydrogeology of the study area is modified from Kasmarek and Ramage (2017) and Braun and Ramage (2020). The Gulf Coast aquifer system hydrogeologic units include the Chicot aquifer, the Evangeline aquifer, the Burkeville confining unit, the Jasper aquifer, and the Catahoula confining unit (figs. 2, 4, and 5). Baker (1979) used 11 stratigraphic cross sections to describe the Gulf Coast aquifer system hydrogeologic units defined by Turcan and others (1966) from where the hydrogeologic units that contain the aquifer units crop out to the Gulf of Mexico nearshore. Baker (1979) was also among the first reports contributing to an aquifer-wide hydrostratigraphic framework and subsurface delineation of the previously mentioned hydrogeologic units. Carr and others (1985) provided further refinement of the Baker (1979) cross sections in the Houston area and has been much used to describe the stratigraphy of the Gulf Coast aquifer system since publication.

The three primary aquifers in the Gulf Coast aquifer system (the Chicot, Evangeline, and Jasper aquifers) are composed of laterally discontinuous deposits of gravel, sand, silt, and clay (Baker, 1979). The percentage of clay and other fine-grained, clastic material generally increases downdip (Baker, 1979). The uppermost aquifer, the Chicot aquifer, is contained in Holocene- and Pleistocene-age (Quaternary-age) sediments, and the underlying Evangeline aquifer is contained in Pliocene- and Miocene-age (Tertiary-age) sediments (fig. 5). In the companion report on 2021 water-level altitudes and water-level changes in the greater Houston area (Braun and Ramage, 2022), the Chicot and Evangeline aquifers were treated as a single, undifferentiated hydrogeologic unit. The most deeply buried of the three aquifers, the Jasper aquifer, is contained in Miocene-age sediments (fig. 5) (Baker, 1979, 1986). The stratigraphic relations between the hydrogeologic units in the study area are shown on hydrogeologic cross sections *A–A′* (figs. 1 and 3) and *B–B′* (figs. 2 and 4) of the Gulf Coast aquifer system, which extends through the greater Houston area from northwestern Grimes County southeastward through Waller, Montgomery, Harris, and Brazoria Counties before terminating at the coast in Galveston County.

Young and Draper (2020) updated the Gulf Coast aquifer system geologic stratigraphy and hydrogeologic unit thicknesses; their report featured a coupled chronostratigraphic and lithostratigraphic approach. The approach used by Young and Draper (2020) built on an existing hydrogeologic framework proposed by Young and others (2014), which in turn was based on the work of Young and others (2012) and differs from the hydrogeologic framework in earlier publications (Baker, 1979; Carr and others, 1985; Strom and others, 2003a, b, c) that exclusively used a lithostratigraphic approach. Using information from Young and others (2012) that included sedimentary marker beds and evidence of coastal onlap observed in geophysical logs, Young and Draper (2020) subdivided the Lagarto Clay into upper, middle, and lower parts and depicted the upper part of the Lagarto Clay as one of the formations that contain the Evangeline aquifer (fig. 5). In previous reports (Turcan and others, 1966; Jorgensen, 1975; Baker, 1979; Carr and others, 1985), the Evangeline aquifer was described as being contained in the Goliad Sand and a small section of the uppermost part of the Lagarto Clay. Additionally, in Young and Draper (2020) the Goliad Sand was subdivided into upper and lower parts following Young and others (2012). In the updated hydrogeologic framework, the upper and lower parts of the Goliad Sand collectively contain part of the Chicot and Evangeline aquifers (undifferentiated) (fig. 5). The base of the Chicot aquifer was defined as the base of the Willis Sand in previous reports; however, additional geophysical logs (approximately 650 versus 290 original logs) were used by Young and others (2012) to characterize the contact between the Chicot and Evangeline aquifers. Thus, the thicknesses of the Chicot and Evangeline aquifers in this study differ substantially in some areas compared to previous studies. The implications of this recharacterization of the thicknesses of the Chicot and Evangeline aquifers are discussed in the "Distribution of Groundwater Wells" section of this report. In Baker (1979) and other reports (fig. 5), the Jasper aquifer was depicted as being contained entirely in the Oakville Sandstone. In addition to the Oakville Sandstone, the lower part of the Lagarto Clay was included in the updated definition of the hydrogeologic units that contain the Jasper aquifer, similarly to Turcan and others (1966).

Over the course of geologic time, geologic and hydrologic processes created accretionary sediment wedges (stacked sequences of sediments) more than 7,600 ft thick at the coast (Chowdhury and Turco, 2006); these sediments, which compose the Gulf Coast aquifer system, were deposited by fluvial-deltaic processes and subsequently were eroded and redeposited by worldwide episodic changes in sea level that occurred as a result of oscillations between glacial and interglacial climate conditions (Lambeck and others, 2002). The Gulf Coast aquifer system consists of hydrogeologic units that dip and thicken from northwest to southeast; the hydrogeologic units

representing the aquifers and confining units thus crop out in bands inland from and approximately parallel to the coast and become progressively more deeply buried and confined toward the coast (figs. 3 and 4) (Kasmarek and others, 2013; Casarez, 2020). The aquifers receive recharge where the hydrogeologic units composing the aquifers crop out (Kasmarek and Robinson, 2004). The Burkeville confining unit is stratigraphically positioned between the Chicot and Evangeline aquifers (undifferentiated) and Jasper aquifer (figs. 3–5), thereby restricting groundwater flow between the undifferentiated Chicot and Evangeline aquifers and the underlying Jasper aquifer. There is no confining unit between the Chicot and Evangeline aquifers; therefore, these two aquifers have substantial hydraulic connection, which allows groundwater flow between them (Kasmarek and others, 2010; Liu and others, 2019). Because of this hydraulic connection, water-level changes (changes in the depth to water in feet below land surface) that occur in one aquifer can affect water levels in the adjoining aquifer (Kasmarek and others, 2010). Supporting evidence of the interaction of groundwater flow between the Chicot and Evangeline aquifers includes maps of long-term water-level changes that show areas where rises and declines are approximately spatially coincident and colocated wells with different screened-interval depths where rises or declines in water levels are approximately coincident in time (for example, Braun and others, 2019; Braun and Ramage, 2020). Additional evidence of the hydraulic connection between the Chicot and Evangeline aquifers is provided by Borrok and Broussard (2016, p. 330); their geochemical evaluation of the Chicot aquifer system from 1993 to 2015 in Louisiana indicated that in some years (1998, 2008, and 2011) certain wells screened in the Chicot aquifer "appeared to be tapping water with a geochemistry (temperature, salinity, alkalinity, [and so forth]) matching the underlying Evangeline aquifer." Further evidence for hydraulic connection is provided in Young and others (2014, sec. 3, p. 2), which summarizes the work of previous authors (Hammond, 1969; Sandeen and Wesselman, 1973; Loskot and others, 1982) who documented vertical hydraulic gradients from the Evangeline aquifer to the Chicot aquifer. Lang and others (1950) have also noted similarities in water-level fluctuations between shallower and deeper wells and the absence of extensive clay zones whereby the Chicot and Evangeline aquifers could be considered as a single unit. Hill (1901) hypothesized that prior to large-scale groundwater withdrawals in the region the aquifers of the coastal plain were under sufficient artesian pressure for the groundwater to rise above land surface, which indicates that there was likely unimpeded vertical flow between the Evangeline and Chicot aquifers. Winslow and Wood (1959, p. 1032) stated that although "the principal water-producing zones in the upper Gulf Coast region are more or less distinct locally, they are all in hydraulic connection and regionally may be considered as a unit." More evidence for hydraulic connection is given in White and others (1944) where patterns of groundwater levels in wells completed at varying depth intervals were documented to be similar across water-production zones in parts of the greater Houston area.

Hydraulic properties of the Chicot aquifer do not differ appreciably from those of the hydrogeologically similar Evangeline aquifer but can be identified by subtle differences in hydraulic conductivity (Carr and others, 1985, p. 10). From aquifer-test data, Meyer and Carr (1979) estimated that the transmissivity of the Chicot aquifer ranges from 3,000 to 25,000 feet squared per day (ft^2/d) and that the transmissivity of the Evangeline aquifer ranges from 3,000 to 15,000 ft^2/d; however, despite these slight differences in transmissivities, there is a logical rationale for combining the aquifers for the purposes of providing status updates of water-level altitudes and long-term water-level changes as explained in the "Treatment of the Chicot and Evangeline Aquifers as a Single Hydrogeologic Unit" section of this report. The outcrops and updip limits of the geologic units that contain the Chicot aquifer are shown in figure 1. Proceeding updip and inland of the Quaternary-age sediments containing the Chicot aquifer, the older geologic units (containing the Evangeline aquifer, the Burkeville confining unit, the Jasper aquifer, and the Catahoula confining system) sequentially crop out (figs. 1 and 2). In the updip areas the Jasper aquifer can be differentiated from the Evangeline aquifer on the basis of the depths to water below land-surface datum, which are shallower (closer to land surface) in the Jasper aquifer compared to those in the Evangeline aquifer (Kasmarek and Ramage, 2017). Additionally, in the downdip areas the Jasper aquifer can be differentiated from the Evangeline aquifer on the basis of stratigraphic position relative to the altitude of the Burkeville confining unit (figs. 3 and 4).

Precipitation falling on the land surface overlying the Gulf Coast aquifer system returns to the atmosphere as evapotranspiration, discharges to streams, or infiltrates as groundwater recharge to the unconfined updip sediments composing the different aquifers (Kasmarek and Robinson, 2004). The infiltrating water moves downgradient toward the coast, reaching the intermediate and deep zones of the aquifers southeastward of the outcrop areas, where the water can then be withdrawn and discharged by wells or is naturally discharged by diffuse upward leakage in topographically low areas near the coast. Water in the coastal, deep zones of the aquifers is denser, and this higher density water causes the fresher, lower density water that has not been captured and withdrawn by wells to be redirected as diffuse upward leakage to shallow zones from the confined downdip areas of the aquifer system.

Previous Studies

An extensive monitoring-well network was established by the USGS in 1977, and water-level data were collected and used to create the first published maps of water-level altitudes for the Chicot and Evangeline aquifers in the greater Houston area in 1979 (Gabrysch, 1979). In cooperation with the FBSD, which adopted its groundwater management plan in 1990 (Fort Bend Subsidence District, 2013), an increased number of wells were inventoried by the USGS in Fort Bend, Harris, Brazoria, and Waller Counties in 1989 and 1990. A more comprehensive water-level-altitude report for the Chicot and Evangeline aquifers was published by the USGS in 1991 (Barbie and others, 1991) and was revised in 1997 when updated well data became available (Kasmarek, 1997). After the establishment of the LSGCD in 2001, the USGS began publishing water-level-altitude maps for the Jasper aquifer in the greater Houston area (primarily Montgomery County) (Coplin, 2001). In 2004, 2006, and 2007, as additional wells with reliable water-level data were inventoried, revised water-level-altitude maps for the Jasper aquifer were prepared (Kasmarek and Lanning-Rush, 2004; Kasmarek and others, 2006; Kasmarek and Houston, 2007). Since 2007, comprehensive maps for the Jasper aquifer have been included in the annual series of water-level reports for the greater Houston area (Kasmarek and Houston, 2008; Kasmarek, Houston, and Ramage, 2009; Kasmarek and others, 2010, 2012, 2013, 2014, 2015, 2016; Johnson and others, 2011; Kasmarek and Ramage, 2017; Shah and others, 2018; Braun and others, 2019; Braun and Ramage, 2020).

Treatment of the Chicot and Evangeline Aquifers as a Single Hydrogeologic Unit

This section describes the rationale and methods for (1) combining the Chicot and Evangeline aquifers into a single hydrogeologic unit; (2) replacing traditional, manual contouring with geostatistical kriging interpolation methods to depict water-level altitudes and long-term water-level changes as gridded surfaces; and (3) defining the interpolated areal extent. The methods described were used in the 2021 report in the annual series of reports published to document water-level altitudes and water-level changes in the study area (Braun and Ramage, 2022).

Since the formalization of the present-day naming of the Gulf Coast aquifer system aquifers and confining units in Turcan and others (1966), the Chicot and Evangeline aquifers have been described as distinct hydrogeologic units for the purpose of water-level mapping. The delineation of these units was largely based on stratigraphic position, grain size, water quality, drill cuttings, and permeability (Turcan and others, 1966). More recently, Young and Draper (2020) updated the Gulf Coast aquifer system geologic stratigraphy and hydrogeologic unit thicknesses by using a coupled chronostratigraphic and lithostratigraphic approach. A confining unit does not separate these two aquifers in the study area, and water-level data from colocated wells screened in these aquifers at several Harris County extensometer sites (discussed in the "Colocated Well Analysis" section and detailed in table 1 of this report) indicate that there is likely a substantial degree of hydrogeologic connection (figs. 6–9). Therefore, from a groundwater-flow perspective, these two aquifer units predominantly function as a single unit. Additionally, on the basis of the update to the Gulf Coast aquifer system unit thicknesses from Young and Draper (2020), the distribution of wells screened in the Chicot and Evangeline aquifers changed considerably, whereby many wells previously classified as being screened in the Evangeline aquifer were reclassified as being screened in the Chicot aquifer (figs. 10 and 11). As a result, the updated distribution of wells identified as being screened in the Evangeline aquifer was diminished to such a degree that substantial parts of the study area lacked the water-level data needed to make reliable water-level-altitude maps for the Evangeline aquifer. Additionally, because of the redistribution and reduction of wells screened in the Evangeline aquifer as a result of updates to the Gulf Coast aquifer system unit thicknesses, water-level altitudes from the Chicot and Evangeline aquifers that were derived from the updated well distribution could no longer be readily compared to water-level altitudes derived from previously used well distributions for each aquifer. After considering all of these factors, the decision was made to combine the Chicot and Evangeline aquifers into a single, undifferentiated hydrogeologic unit for the purposes of assessing water-level altitudes and water-level changes over time.

Colocated Well Analysis

Several colocated wells exist in the study area, several of which are in Harris County at extensometer sites (figs. 1, 2, and 6–9; table 1). To illustrate the hydrogeologic connection between the Chicot and Evangeline aquifers, water levels at wells screened at differing vertical depth intervals at four sites were analyzed (figs. 6–9). These sites are distributed across Harris County and are considered representative of patterns in water levels across the study area. Patterns in water levels common to the sites in figures 6–9 include (1) minimal changes in water levels over time in wells that are shallower than about 125 ft below land surface (bls) and in which the groundwater is under atmospheric pressure and (2) increasing water levels with substantial degree of similarity over time in wells that are deeper than about 225 ft bls and in which the groundwater is under artesian pressure. A transition zone between atmospheric and artesian pressure exists between about 125 and 250 ft bls, whereby wells screened above this zone are considered not to be a part of the Chicot and Evangeline aquifers (undifferentiated).

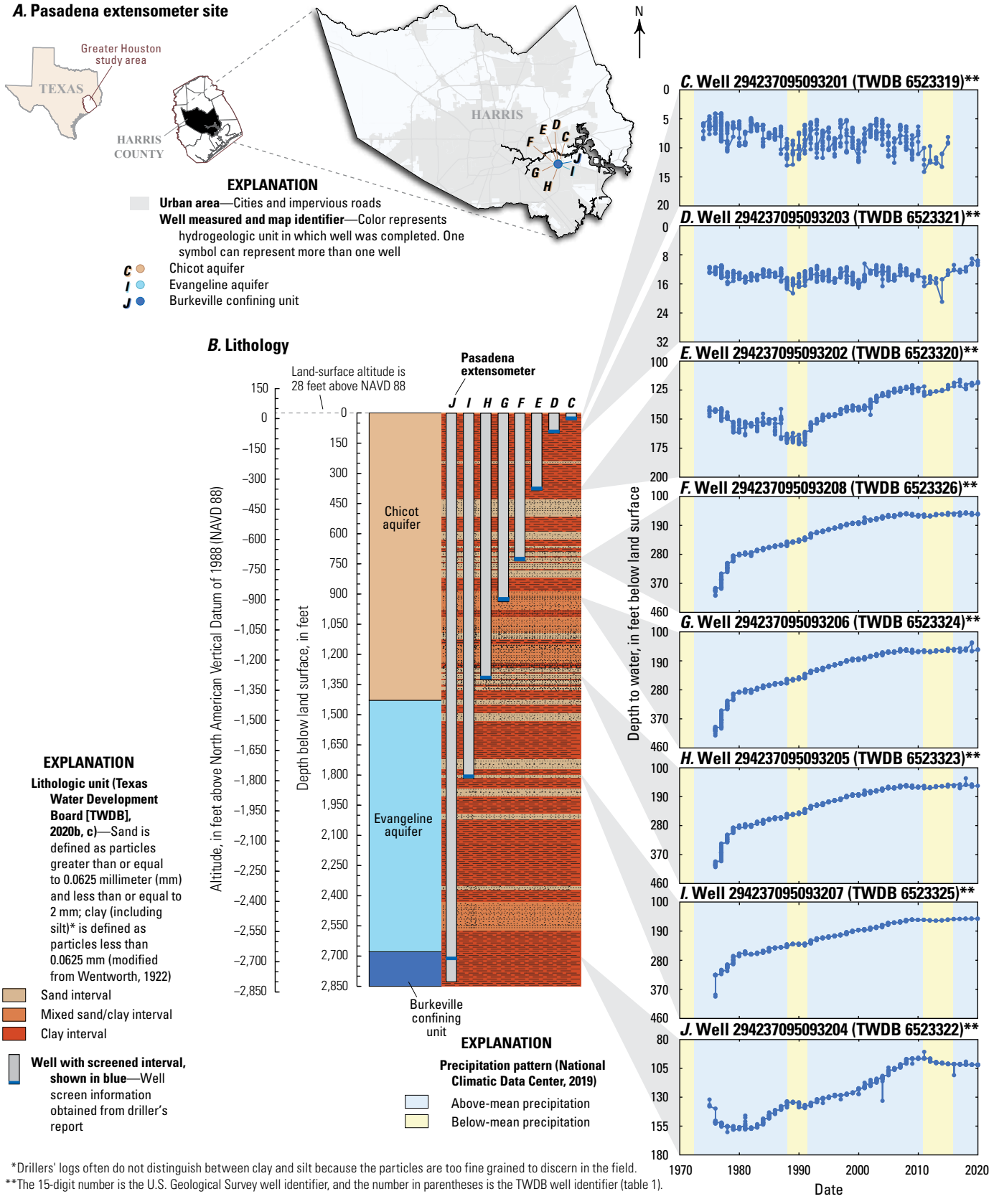

*Drillers' logs often do not distinguish between clay and silt because the particles are too fine grained to discern in the field.
**The 15-digit number is the U.S. Geological Survey well identifier, and the number in parentheses is the TWDB well identifier (table 1).

Figure 6. *A*, Map showing location of the Pasadena extensometer site (294237095093204) in Harris County in the greater Houston study area, Texas, and *B*, lithologic section with graphs *C*, *D*, *E*, *F*, *G*, *H*, *I*, and *J* showing depths to water and precipitation patterns during the periods of record between 1970 and 2020 at the colocated wells at the site.

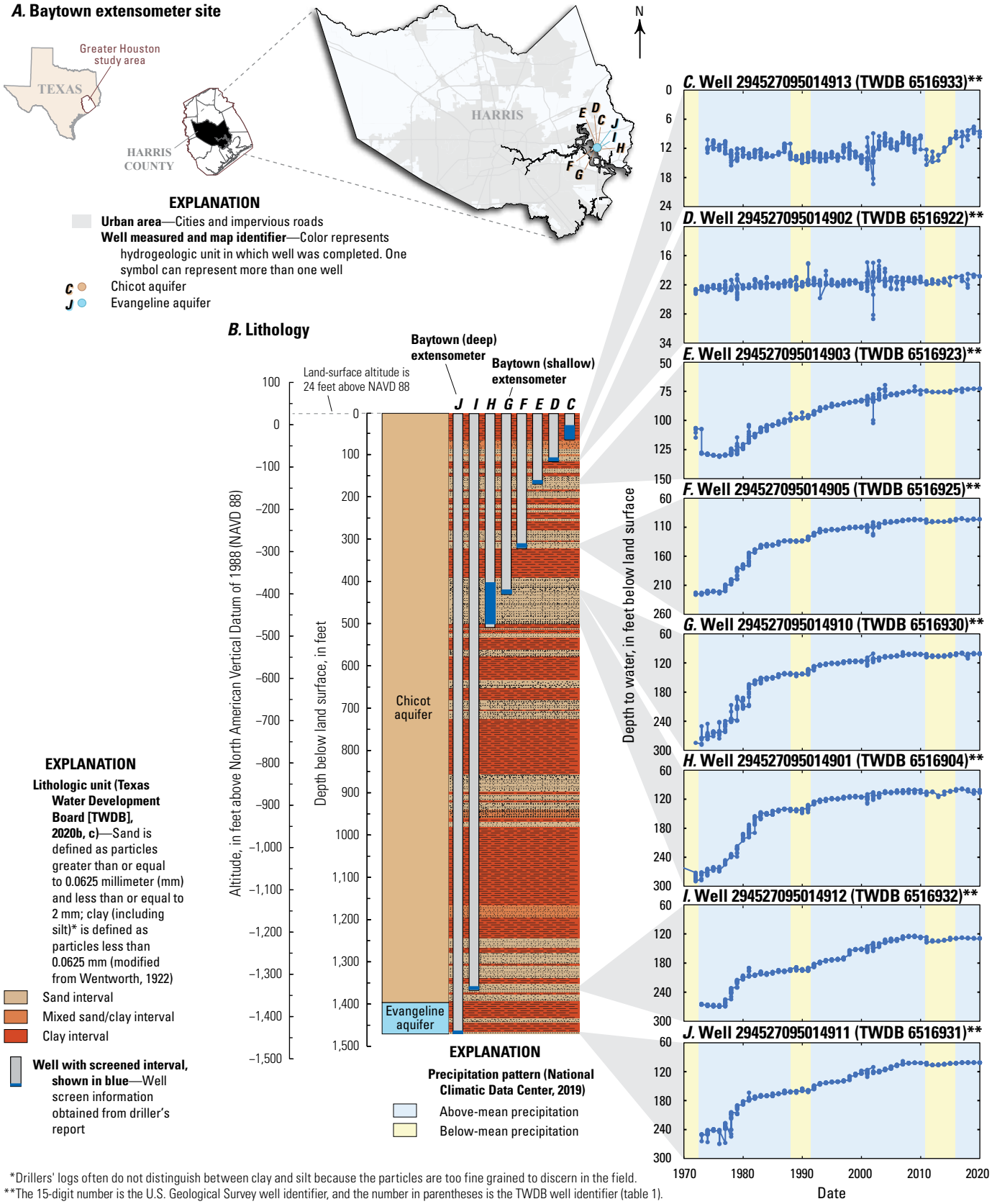

*Drillers' logs often do not distinguish between clay and silt because the particles are too fine grained to discern in the field.
**The 15-digit number is the U.S. Geological Survey well identifier, and the number in parentheses is the TWDB well identifier (table 1).

Figure 7. *A*, Map showing location of the Baytown extensometer site (294527095014911) in Harris County in the greater Houston study area, Texas, and *B*, lithologic section with graphs *C*, *D*, *E*, *F*, *G*, *H*, *I*, and *J* showing depths to water and precipitation patterns during the periods of record between 1970 and 2020 at the colocated wells at the site.

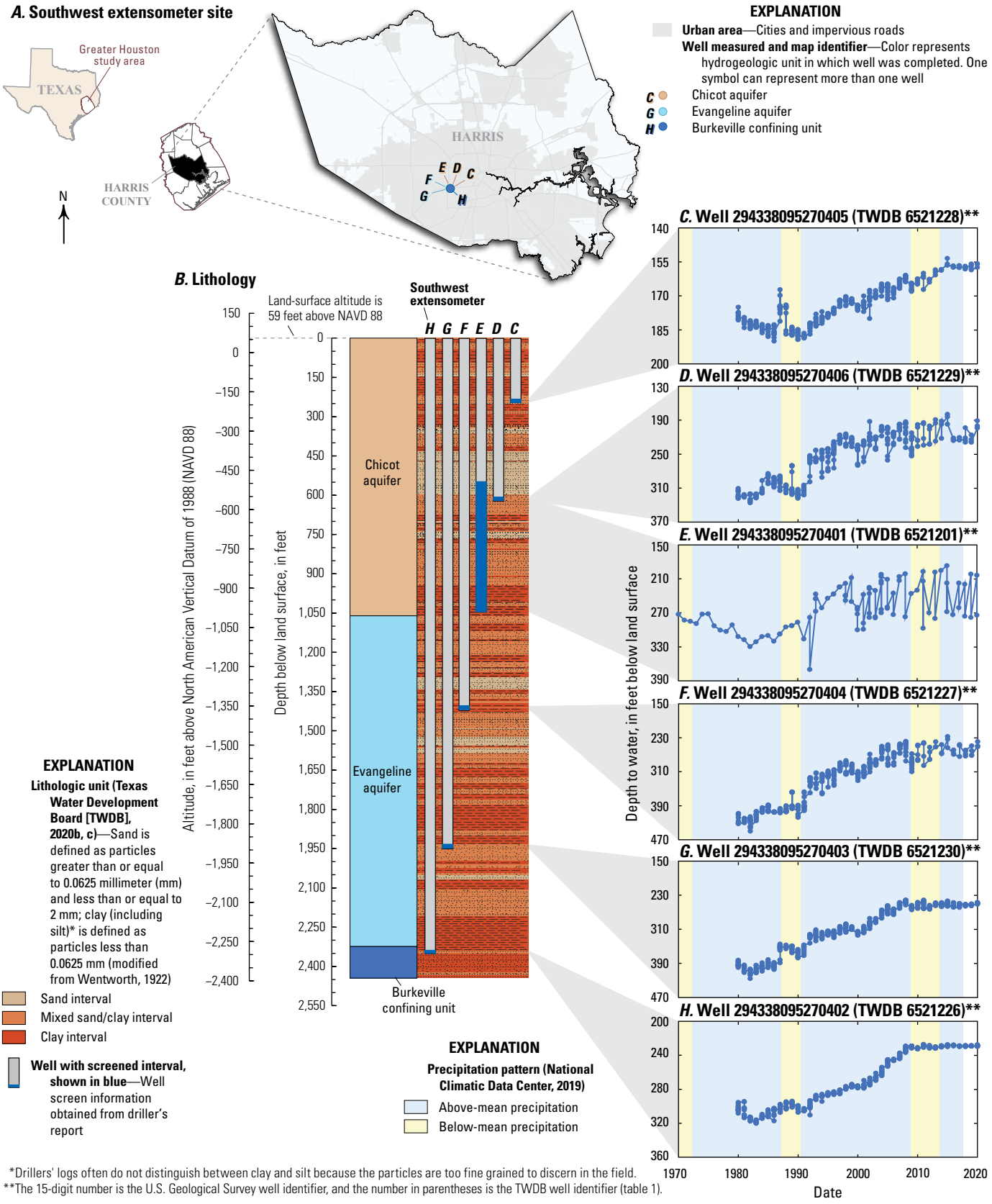

*Drillers' logs often do not distinguish between clay and silt because the particles are too fine grained to discern in the field.
**The 15-digit number is the U.S. Geological Survey well identifier, and the number in parentheses is the TWDB well identifier (table 1).

Figure 8. *A*, Map showing location of the Southwest extensometer site (294338095270402) in Harris County in the greater Houston study area, Texas, and *B*, lithologic section with graphs *C*, *D*, *E*, *F*, *G*, and *H* showing depths to water and precipitation patterns during the periods of record between 1970 and 2020 at the colocated wells at the site.

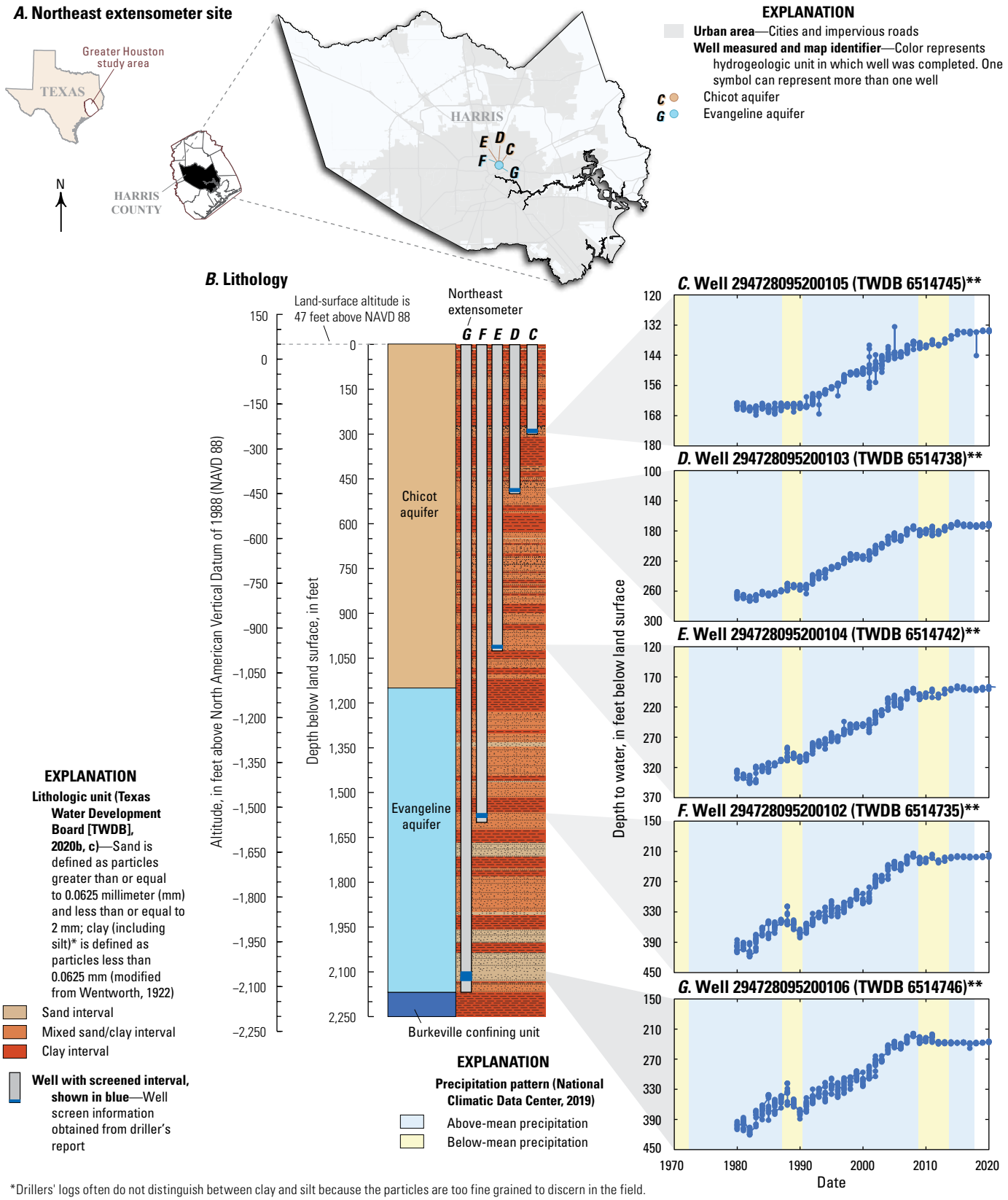

*Drillers' logs often do not distinguish between clay and silt because the particles are too fine grained to discern in the field.
**The 15-digit number is the U.S. Geological Survey well identifier, and the number in parentheses is the TWDB well identifier (table 1).

Figure 9. *A*, Map showing location of the Northeast extensometer site (294728095200106) in Harris County in the greater Houston study area, Texas, and *B*, lithologic section with graphs *C*, *D*, *E*, *F*, and *G* showing depths to water and precipitation patterns during the periods of record between 1970 and 2020 at the colocated wells at the site.

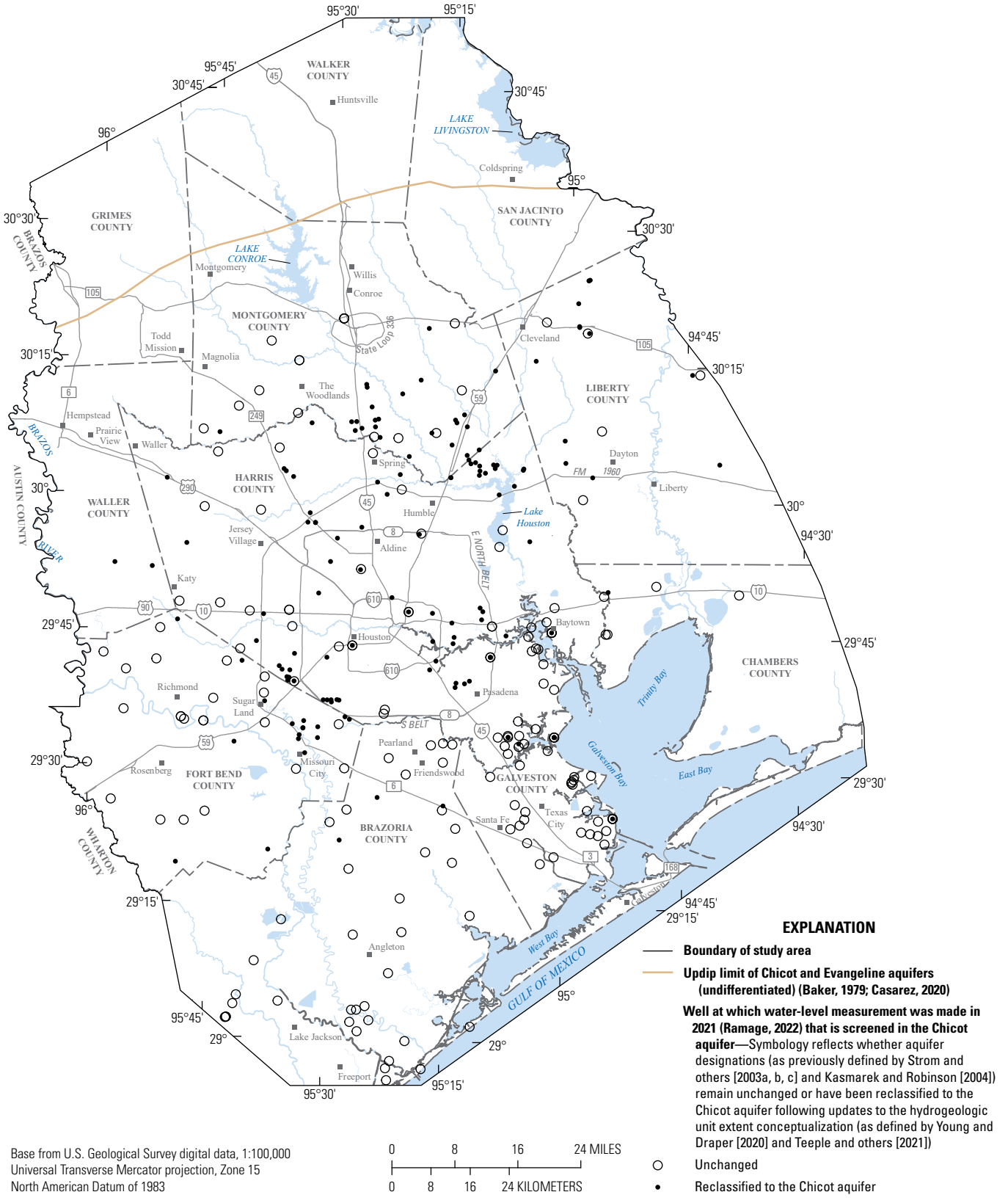

EXPLANATION

- **Boundary of study area**
- **Updip limit of Chicot and Evangeline aquifers (undifferentiated) (Baker, 1979; Casarez, 2020)**
- **Well at which water-level measurement was made in 2021 (Ramage, 2022) that is screened in the Chicot aquifer**—Symbology reflects whether aquifer designations (as previously defined by Strom and others [2003a, b, c] and Kasmarek and Robinson [2004]) remain unchanged or have been reclassified to the Chicot aquifer following updates to the hydrogeologic unit extent conceptualization (as defined by Young and Draper [2020] and Teeple and others [2021])
  - ○ Unchanged
  - • Reclassified to the Chicot aquifer

Base from U.S. Geological Survey digital data, 1:100,000
Universal Transverse Mercator projection, Zone 15
North American Datum of 1983

0 8 16 24 MILES
0 8 16 24 KILOMETERS

Figure 10. Wells at which water-level measurements were made in 2021 that were either unchanged or reclassified as being screened in the Chicot aquifer in the greater Houston study area, Texas.

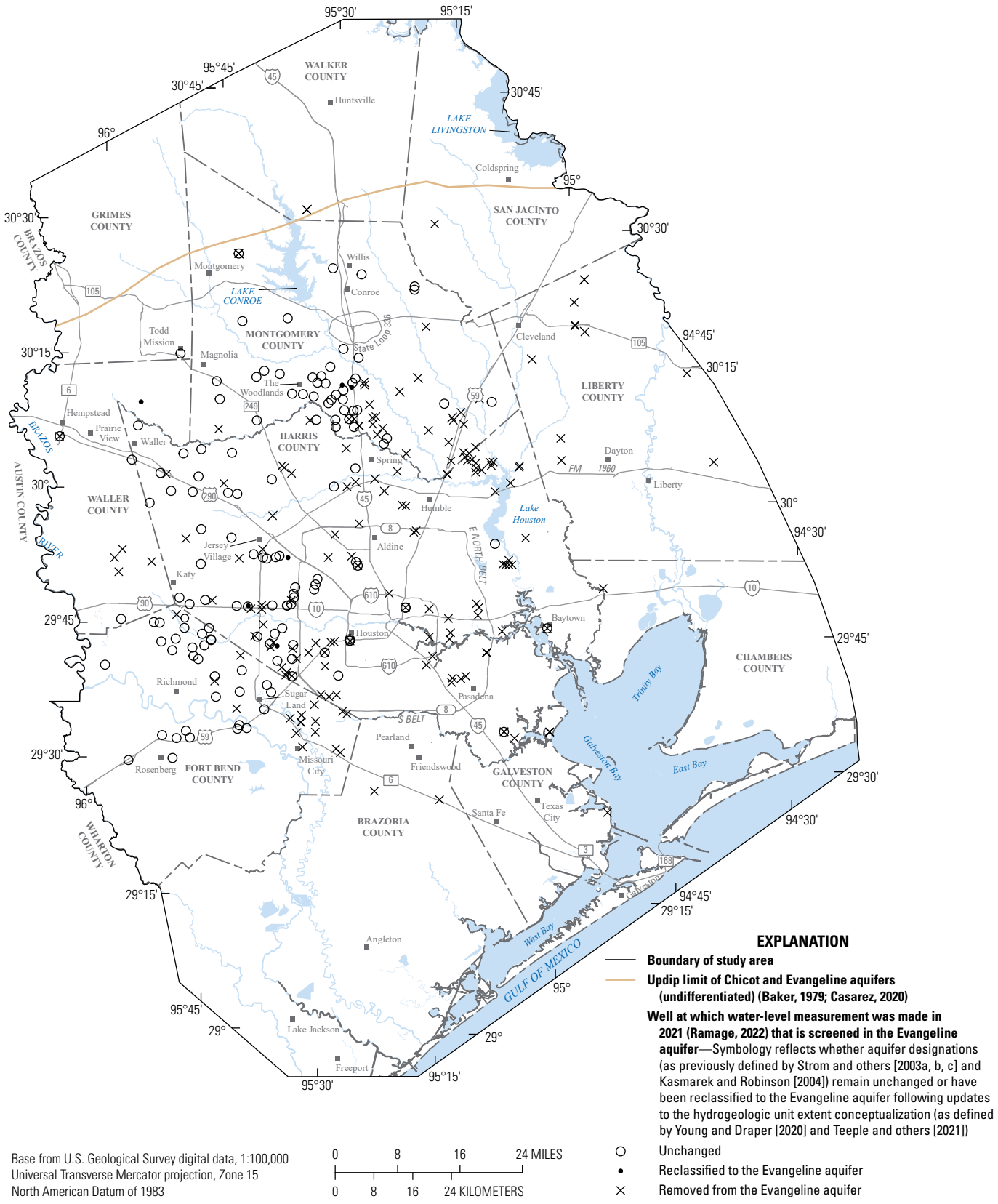

Figure 11. Wells at which water-level measurements were made in 2021 that were unchanged, were reclassified to, or were reclassified from (designated as "removed from") being screened in the Evangeline aquifer in the greater Houston study area, Texas.

Table 1. Colocated well locations and construction information for extensometer sites in Harris County in the greater Houston study area, Texas.

[Information from Texas Water Development Board (2020b, c) and U.S. Geological Survey (2021). USGS, U.S. Geological Survey; TWDB ID, Texas Water Development Board well identifier; NAVD 88, North American Vertical Datum of 1988]

Short name (figs. 6–9)	Well identifier (figs. 6–9)	USGS site identifier	TWDB ID	Aquifer unit[1] (figs. 6–9)	Latitude, in decimal degrees	Longitude, in decimal degrees	Well depth (in feet below land surface) (figs. 6–9)	Top of screen (in feet below land surface)[2]	Bottom of screen (in feet below land surface)[2]	Top of screen (altitude in feet above NAVD 88)[2]	Bottom of screen (altitude in feet above NAVD 88)[2]
Pasadena extensometer (fig. 6)	C	294237095093201	6523319	Chicot aquifer	29.71056	−95.15917	34	24	34	4	−6
	D	294237095093203	6523321	Chicot aquifer	29.71056	−95.15917	100	90	100	−62	−72
	E	294237095093202	6523320	Chicot aquifer	29.71056	−95.15917	390	380	390	−352	−362
	F	294237095093208	6523326	Chicot aquifer	29.71056	−95.15917	730	715	725	−687	−697
	G	294237095093206	6523324	Chicot aquifer	29.71056	−95.15917	936	921	931	−893	−903
	H	294237095093205	6523323	Chicot aquifer	29.71056	−95.15917	1,328	1,313	1,323	−1,285	−1,295
	I	294237095093207	6523325	Evangeline aquifer	29.71056	−95.15917	1,817	1,802	1,812	−1,774	−1,784
	J	294237095093204	6523322	Evangeline aquifer[3]	29.71016	−95.15928	2,831	2,707	2,717	−2,679	−2,689

Table 1. Colocated well locations and construction information for extensometer sites in Harris County in the greater Houston study area, Texas.—Continued

[Information from Texas Water Development Board (2020b, c) and U.S. Geological Survey (2021). USGS, U.S. Geological Survey; TWDB ID, Texas Water Development Board well identifier; NAVD 88, North American Vertical Datum of 1988]

Short name (figs. 6–9)	Well identifier (figs. 6–9)	USGS site identifier	TWDB ID	Aquifer unit[1] (figs. 6–9)	Latitude, in decimal degrees	Longitude, in decimal degrees	Well depth (in feet below land surface) (figs. 6–9)	Top of screen (in feet below land surface)[2]	Bottom of screen (in feet below land surface)[2]	Top of screen (altitude in feet above NAVD 88)[2]	Bottom of screen (altitude in feet above NAVD 88)[2]
Baytown extensometer (fig. 7)	C	294527095014913	6516933	Chicot aquifer	29.75778	−95.03056	60	30	60	−6	−36
	D	294527095014902	6516922	Chicot aquifer	29.75778	−95.03056	110	102	110	−78	−86
	E	294527095014903	6516923	Chicot aquifer	29.75778	−95.03056	170	162	170	−138	−146
	F	294527095014905	6516925	Chicot aquifer	29.75778	−95.03056	324	316	324	−292	−300
	G	294527095014910	6516930	Chicot aquifer	29.75784	−95.03065	431	420	430	−396	−406
	H	294527095014901	6516904	Chicot aquifer	29.75778	−95.03056	512	418	500	−394	−476
	I	294527095014912	6516932	Chicot aquifer	29.75778	−95.03056	1,365	1,355	1,365	−1,331	−1,341
	J	294527095014911	6516931	Evangeline aquifer	29.75784	−95.03065	1,475	1,455	1,465	−1,431	−1,441
Southwest extensometer (fig. 8)	C	294338095270405	6521228	Chicot aquifer	29.72750	−95.45139	253	238	248	−182	−192
	D	294338095270406	6521229	Chicot aquifer	29.72750	−95.45139	627	612	622	−556	−566
	E	294338095270401	6521201	Chicot aquifer	29.72750	−95.45139	1,051	554	1,031	−498	−975
	F	294338095270404	6521227	Evangeline aquifer	29.72750	−95.45139	1,433	1,418	1,428	−1,362	−1,372
	G	294338095270403	6521230	Evangeline aquifer	29.72750	−95.45139	1,943	1,928	1,938	−1,872	−1,882
	H	294338095270402	6521226	Evangeline aquifer[3]	29.72700	−95.45078	2,358	2,316	2,336	−2,257	−2,277

Table 1. Colocated well locations and construction information for extensometer sites in Harris County in the greater Houston study area, Texas.—Continued

[Information from Texas Water Development Board (2020b, c) and U.S. Geological Survey (2021). USGS, U.S. Geological Survey; TWDB ID, Texas Water Development Board well identifier; NAVD 88, North American Vertical Datum of 1988]

Short name (figs. 6–9)	Well identifier (figs. 6–9)	USGS site identifier	TWDB ID	Aquifer unit[1] (figs. 6–9)	Latitude, in decimal degrees	Longitude, in decimal degrees	Well depth (in feet below land surface) (figs. 6–9)	Top of screen (in feet below land surface)[2]	Bottom of screen (in feet below land surface)[2]	Top of screen (altitude in feet above NAVD 88)[2]	Bottom of screen (altitude in feet above NAVD 88)[2]
Northeast extensometer (fig. 9)	C	294728095200105	6514745	Chicot aquifer	29.79139	−95.33389	298	283	293	−237	−247
	D	294728095200103	6514738	Chicot aquifer	29.79139	−95.33389	487	472	482	−426	−436
	E	294728095200104	6514742	Chicot aquifer	29.79139	−95.33389	1,035	1,020	1,030	−974	−984
	F	294728095200102	6514735	Evangeline aquifer	29.79139	−95.33389	1,596	1,567	1,577	−1,521	−1,531
	G	294728095200106	6514746	Evangeline aquifer	29.79089	−95.33397	2,170	2,099	2,119	−2,053	−2,073

[1]Indicates the aquifer unit present at the screened interval of the well. The aquifer units on this table retain the previous separate classification of the Chicot and Evangeline aquifers depicted on figure 1 of this report.

[2]Wells may have one or more screened intervals within this range as shown on figures 6–9.

[3]The screens of these wells intersect the Burkeville confining unit (shown on fig. 1); however, these wells have historically been classified as having been completed in the Evangeline aquifer, so this classification is retained.

At the Pasadena extensometer site (hereinafter referred to as the "Pasadena site") (fig. 6; table 1), the water levels (represented as depths to water in feet below land surface) in wells C and D were generally stable with less than 12 ft of change and showed little association with water levels in the wells screened at greater depths (wells F through J). Water levels at wells C and D were similarly affected by changes in precipitation; for example, water levels in wells C and D rose during periods of above-mean precipitation and declined during periods of below-mean precipitation (fig. 6*C*, *D*). Prior to about 1985, the pattern in water levels over time in well E was similar to the pattern observed in wells C and D. However, after about 1990, the water-level pattern in well E was most similar to the pattern observed in the wells screened at greater depths (wells F through J at the Pasadena site), although the water-level change in well E was less than 55 ft compared to greater water-level changes in the wells screened at greater depths, where water levels ranged from about 70 to 289 ft. The pattern observed in water levels for wells F through J at the Pasadena site was somewhat similar over time; however, the magnitude of the water-level changes in wells F through I was appreciably greater compared to the magnitude of the water-level changes in well J. A likely explanation for the differences in the magnitude of water-level changes in wells F through I compared to well J at the Pasadena site is that well J is screened in the Burkeville confining unit and thus surrounded by a substantial clay layer that decreases the hydraulic connection between well J and the overlying aquifer units. In most cases, drillers' logs obtained during the installation of wells do not distinguish between clay and silt because the particles are too fine grained to discern in the field and instead record all fine-grained sediment as clay. Fine-grained intervals are therefore referred to as clay intervals in figures 6–9. After about 1990, the pattern of water-level changes in well E was different from the pattern for wells C and D at the Pasadena site, indicating that a transition zone from a shallow zone where groundwater is under atmospheric pressure to a deeper zone where groundwater is under artesian pressure occurs at a depth interval of about 125–200 ft bls.

The similarity of water levels at different depth intervals for wells at the Pasadena site (fig. 6) was observed as far back as 1937. As explained in the "Introduction" section of this report, prior to 1975, the withdrawal of groundwater from the Chicot and Evangeline aquifers was unregulated, and water levels in the aquifers were steadily declining year over year. In 1937, water-level declines in the area where the extensometer at the Pasadena site is installed differed by the depth of the screened intervals, with smaller declines in the more deeply screened wells and larger declines in the more shallowly screened wells (White and others, 1944). However, the pattern of water-level declines in all of the wells was nearly the same even though thick clay beds separated many of the water-production zones (White and others, 1944). Thus, a hydraulic connection among many of the water-production zones at various depth intervals exists (White and others, 1944), which is evident on the basis of water levels measured at the different depth intervals for the wells at the Pasadena site with the exception of the water levels measured in the two shallowest wells (wells C and D) (fig. 6).

Water-level patterns observed in wells at the Pasadena site (fig. 6) were similar to water-level patterns observed in wells at the other three extensometer sites (Baytown, Southwest, and Northeast; figs. 7–9). Unlike the wells at the other extensometer sites, the wells at the Baytown extensometer site (hereinafter referred to as the "Baytown site") are not screened at regularly spaced intervals representing the full extent of the aquifers in which they are screened (fig. 7). Instead, six wells are screened between 30 and 500 ft bls, and two wells are screened between 1,355 and 1,465 ft bls (fig. 7; table 1). Despite the large differences in screened-interval depths at the Baytown site, the water-level patterns observed at all but the two shallowest wells at the site (wells C and D) were similar. Water levels in the shallowest wells at the Baytown site (wells C and D) increased or decreased in response to changes in precipitation, whereas water levels in well E were similar to those in wells F through J (fig. 7). Therefore, a transition zone likely exists at a depth of about 125–150 ft bls, where the groundwater changes from a shallower zone under atmospheric pressure to a deeper zone under artesian pressure.

At the Southwest extensometer site (hereinafter referred to as the "Southwest site"), water levels were similar throughout nearly 2,350 vertical feet of aquifer sediment (fig. 8; table 1). The shallowest well at the Southwest site (well C; fig. 8) is screened in the deeper zone under artesian pressure, and water levels in this well generally were not responsive to changes in precipitation. The water levels at the Southwest site measured in wells screened in the Chicot and Evangeline aquifers exhibited a high degree of similarity, differing only slightly in the magnitude of the water-level change over time. The shallowest well at the Southwest site is screened between 238 and 248 ft bls (table 1), whereas the Pasadena and Baytown sites each include two shallow wells screened at or above 110 ft bls. The absence of shallow wells at the Southwest site similar to the screened intervals of the two shallowest wells at the Pasadena and Baytown sites (table 1) complicates the estimation of a transition zone. However, on the basis of the available data, it is estimated that the transition zone occurs at a depth of about 125–175 ft bls.

At the Northeast extensometer site (hereinafter referred to as the "Northeast site"), water-level patterns were similar across all colocated wells (fig. 9; table 1), consistent with the patterns in water levels measured at the other three extensometer sites. The shallowest well at the Northeast site (well C) is screened between 283 and 293 ft bls, and water levels in this well are not generally responsive to changes in precipitation (fig. 9*C*; table 1). The maximum water-level change in the shallowest wells at the Northeast and Southwest sites (each well C) is about 35 ft (figs. 8 and 9) during the 1980–2015 period of record at these sites. Similar to the Southwest site, the absence of shallow wells at the Northeast site complicates the estimation of a transition zone. However, on the basis of the available data, it is estimated that the transition zone at the Northeast site occurs at a depth of about 175–225 ft bls.

Colocated well data at the four extensometer sites indicate that a transition zone from a shallower zone under atmospheric pressure to a deeper zone under artesian pressure exists between about 125 and 225 ft bls. Above the depth interval 125–225 ft bls, water levels have remained relatively stable over time and have not been affected by pressure-head changes within the aquifer that are found when the groundwater is under artesian pressure; any small differences in water levels measured in wells screened above the depth interval 125–225 ft bls are primarily driven by changes in precipitation. The water levels measured in shallow wells (screened at a depth interval from 24 to 110 ft bls) remain largely static over time and are primarily driven by changes in precipitation (figs. 6*C*, *D* and 7*C*, *D*; table 1). Groundwater from land surface down to a depth of about 125–225 ft bls functions as a "perched" system. This perched system is not indicative of water levels within the Chicot and Evangeline aquifers (White and others, 1939, 1944; Lang and others, 1950; Kasmarek and Strom, 2002). Therefore, wells screened above the transition zone that extends to about 250 ft bls were not classified as wells screened in the Chicot and Evangeline aquifers (undifferentiated). Accordingly, the 2021 annual report on water-level altitudes and water-level changes in the study area (Braun and Ramage, 2022) did not classify wells screened above the transition zone as wells screened in the Chicot and Evangeline aquifers (undifferentiated), and wells screened above the transition zone are not planned to be classified as wells screened in the Chicot and Evangeline aquifers (undifferentiated) henceforth for assessing water-level altitudes and water-level changes in the study area.

At all of the extensometer sites, water levels among all wells screened in the Chicot and Evangeline aquifers below about 125–225 ft bls under artesian pressure were similar on an overall basis during a 40- to 50-year period (figs. 6–9). The extensometer sites were installed between 1973 and 1980, so the period of record varies for each extensometer site depending on the year of installation. The similar water-level patterns among the sites demonstrate a hydraulic connection across a range of depth intervals that has persisted from at least 1980 to 2020 in the Chicot and Evangeline aquifers. This hydraulic connection was also noted in Kasmarek and Ramage (2017); the patterns observed in water-level measurements from Kasmarek and Ramage (2017) support the hypothesis that the Chicot and Evangeline aquifers function as one integrated hydrogeologic unit rather than as distinct aquifers.

Distribution of Groundwater Wells

Young and Draper (2020) used data from approximately 650 geophysical logs to redefine the contact between the Chicot and Evangeline aquifers and to redefine the top and bottom of the Burkeville confining unit. Teeple and others (2021) compiled data from the same geophysical logs used by Young and Draper (2020) to define the tops and bottoms of the hydrogeologic units of the Gulf Coast aquifer system as gridded surfaces, which were then intersected with the screened intervals associated with wells in the long-term monitoring-well network. As a result of the work by Young and Draper (2020) and Teeple and others (2021), a large number of wells in the study area were reclassified as being screened in a different aquifer (figs. 10–12). Figures 10, 11, and 12 depict the wells in the long-term monitoring-well network at which water-level measurements were made in 2021 that are currently (as defined by hydrogeologic unit extent conceptualization compiled from Teeple and others [2021] and Young and Draper [2020]) or were previously (as defined by hydrogeologic unit extent conceptualization compiled from Strom and others [2003a, b, c] and Kasmarek and Robinson [2004]) screened in the Chicot, Evangeline, or Jasper aquifers, respectively.

As a result of the change in thickness of the hydrogeologic units, a large proportion of wells in the long-term monitoring-well network required reclassification. Specifically, about 125 wells that were classified as Evangeline aquifer wells were reclassified as Chicot aquifer wells, resulting in substantial portions of the Evangeline aquifer (from an areal extent) that no longer had available wells with which to describe water-level changes over time (figs. 10 and 11). Thus, after establishing that the two aquifers have similar hydraulic properties and effectively function as one hydrogeologic unit, combining the Chicot and Evangeline aquifers into a single, undifferentiated hydrogeologic unit was a way to ensure a spatially distributed network of wells with a sufficient distribution of long-term water-level measurements for mapping purposes. Although the water-level-change maps from the previously published reports cannot be directly compared to the maps of the newly combined Chicot and Evangeline aquifers (undifferentiated), comparison at individual wells can reasonably be made, particularly for identification of areas where groundwater demands are greatest and where water-level changes over time are most pronounced.

Use of Geostatistical Interpolation Methods To Develop Gridded Surfaces of Water-Level Altitudes and Water-Level Changes

The 2020 water-level altitudes for the Chicot, Evangeline (with the Chicot and Evangeline aquifers treated as separate aquifers, as was done in Braun and Ramage, 2020), and Jasper aquifers were re-created in this report from computer algorithms of the contoured datasets as gridded surfaces by using the same source data (Ramage and Braun, 2020) to demonstrate the similarity of results from geostatistical interpolation methods to those from manual contouring methods. The gridded surfaces used to depict water levels for 2020 were created independently of the previously published contoured maps and provide a means for comparison between the manual contouring methods and the geostatistical interpolation methods.

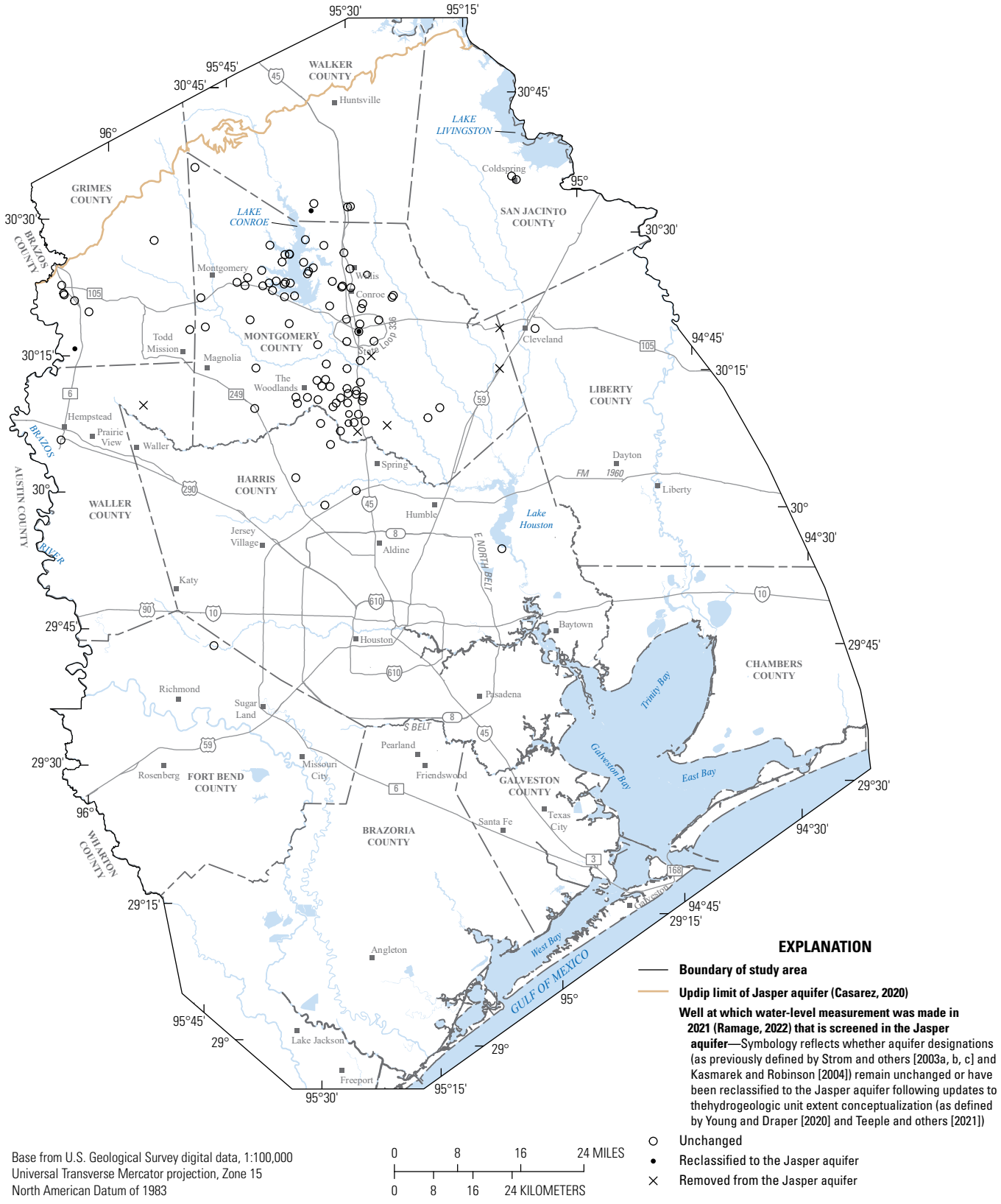

Figure 12. Wells at which water-level measurements were made in 2021 that were unchanged, were reclassified to, or were reclassified from (designated as "removed from") being screened in the Jasper aquifer in the greater Houston study area, Texas.

Braun and Ramage (2022) used geostatistical interpolation methods to create gridded surface representations of 2021 water-level altitudes and long-term water-level changes over time across the study area. Long-term water-level changes are created by subtracting one gridded surface from another where each gridded surface shares a common spatial extent (for example, the gridded surface of altitudes from the current year minus the gridded surface of altitudes from the historical year).

Defining the areal extent through kriging interpolation of the water-level-altitude and water-level-change depictions provides a mechanism for indicating areas of high uncertainty (large standard error), which generally coincide with areas of reduced well density within the well network distribution. Areas are masked when the standard errors exceed the overall mean standard error provided by the kriging process for each aquifer.

Kriging is a well-established geostatistical method (Matheron, 1963; Paramasivam and Venkatramanan, 2019) that provides an optimized unbiased linear prediction with a minimum mean estimation error. Kriging, like other interpolation methods, uses a weighted average of all measured values to predict values at unmeasured locations. The weights assigned to measured values are spatially dependent. The spatial dependency is quantified by the spatial correlation of the measured locations and is assumed to be more similar in spatial proximity and diverge as spatial distance increases. Correlation between measured locations and their spatial distance relative to one another is described by the experimental semivariogram and the best fit model designed to minimize the estimation error (Olea, 1975, 2009). Kriging methods for depicting water-level altitudes and water-level changes provide several advantages compared to the manual contouring methods described in Kasmarek and Ramage (2017). One of the advantages of kriging methods over traditional, manual contouring methods is that kriging provides estimated values of the variable of interest at unmeasured locations. Additionally, kriging provides a means of quantifying the estimation uncertainty (standard deviation or square root of the provided variance), thereby allowing for evaluation of the estimation reliability (Yamamoto, 2000). This estimation uncertainty can be useful for determining the spatial variability of the data and for allowing for possible optimization of the monitoring-well network. Dunlap and Spinazola (1984) provided a detailed description of the advantages of interpolating water-level-altitude data by using kriging methods.

A fundamental assumption associated with the use of kriging methods is that the data are stationary; that is, the mean and variance of the data do not differ appreciably in space (Bohling, 2005). Inspection of reports by Kasmarek and Ramage (2017) and Braun and Ramage (2020), however, indicates that spatial changes over time where mean and variance are not spatially consistent (that is, sharp changes in water-level altitude) do occur in localized areas within the monitoring-well network depicted in these previously published reports (the same is expected to be true of the other annual water-level reports for the greater Houston area). Therefore, before beginning the kriging process, it is important to assess spatial changes in the data, represented as a planar function of coordinate variables, by completing what is referred to as the "trend-surface analysis" step. As explained in Dunlap and Spinazola (1984, p. 5), "trend-surface analysis commonly fits a medium- to high-order polynomial to the entire set of data points. Therefore, a value at an estimated point is interpolated from the entire set of data points instead of only its closest neighbors (Olea, 1975)" so that statistically significant trends (if any) are removed prior to beginning the kriging process.

In this report, planar surfaces were analyzed in the trend-surface analysis step by fitting first- and second-order polynomial equations of water-level altitude as a function of X and Y coordinate pairs. First-order polynomial equations (Olea, 1975, 2009) (eq. 1) produced planar surfaces for the Chicot, Evangeline, and Jasper aquifers (app. 1, figs. 1.1–1.3) that exhibited declining water-level altitudes in the downdip direction (generally from northwest to southeast), which likely corresponds with the general flow of groundwater in the region toward the Gulf of Mexico coast. The first-order polynomial equation to compute water-level altitude is

$$WLALT = a + bX + cY \quad (1)$$

where

- $WLALT$ is the computed water-level altitude in feet,
- X and Y are the coordinate variables for each measured point in meters, and the following coefficients are
  - a is in feet,
  - b is in feet per meter, and
  - c is in feet per meter.

A second-order polynomial equation (Olea, 1975, 2009) (eq. 2) was used to refine the planar surfaces from equation 1 for the Chicot, Evangeline, and Jasper aquifers (app. 1, figs. 1.4–1.6) to provide a better fit to the water-level-altitude data collected in 2020 by including exponential terms and additional variables in the equation. The second-order polynomial equation to compute water-level altitude is

$$WLALT = a + bX + cY + dX^2 + eY^2 + fXY \quad (2)$$

where

- $WLALT$ is the computed water-level altitude in feet,
- X and Y are the coordinate variable pair for each measured point in meters, and the following constant coefficients are
  - a is in feet,
  - b is in feet per meter,
  - c is in feet per meter,
  - d is in feet per meter squared,
  - e is in feet per meter squared, and
  - f is in feet per meter squared.

The planar surfaces produced from second-order polynomial equations (that is, regression equations for the Chicot, Evangeline, and Jasper aquifers computed by using eq. 2)

show similar patterns where a central part of the gridded area for each of the three aquifers contains the deepest water-level altitudes that shallow radially outward (app. 1, figs. 1.4–1.6). The patterns depicted likely represent both a major component represented by an area of concentrated groundwater withdrawals near densely populated areas and a minor component representing the underlying general flow of groundwater in a southeasterly direction toward the coast. Additionally, summary statistics for the first- and second-order regression equations for each of the three aquifers reveal that probability values (*p*-values) and adjusted coefficient of determination (*R*-squared) values used to identify statistically significant trends are greatly improved (that is, smaller *p*-values and larger adjusted *R*-squared values) by including the extra terms in the second-order polynomial equation (eq. 2) (table 2).

In this report, universal kriging methods (Dunlap and Spinazola, 1984) were used to produce the re-created 2020 water-level-altitude maps for the Chicot, Evangeline, and Jasper aquifers. In universal kriging, the kriging process accounts for any statistically significant trends (by kriging the residuals after the trend is removed and then adding those residuals back to the provided estimations), thereby producing the gridded surfaces from detrended datasets. The second-order polynomial equation (eq. 2) was used in the universal kriging process to produce the re-creation of the 2020 water-level-altitude maps.

The process for re-creating gridded surface representations of the previously published 2020 water-level altitudes of the Chicot, Evangeline, and Jasper aquifers in the greater Houston area (Braun and Ramage, 2020) began with the data in Ramage and Braun (2020). Before kriging is implemented, a rectangular grid over which-to interpolate is established. For this report, as well as the annual report presenting water-level altitudes and water-level-altitude changes for 2021 (Braun and Ramage, 2022), rectangular grids with cell dimensions of 60 by 60 meters (m) were created for each of the three aquifers. These rectangular grids over which the interpolation was made extended to the outermost extents defined by the monitoring-well network for each aquifer (Chicot, Evangeline, and Jasper aquifers). The grid cell resolution of 197 by 197 ft (60 by 60 m) was selected as a compromise between optimizing run time for the kriging process (finer resolutions require more computing power and consequently more run time) and minimizing errors associated with differences between estimated grid cell values and measured water-level altitudes at wells (coarser resolutions result in higher estimation errors). The 2020 rectangular grids for the Chicot, Evangeline, and Jasper aquifers contained 5,775,728; 5,161,584; and 2,517,048 cells, respectively. The 5,775,728 cells in the Chicot aquifer grid represent an area of approximately 8,028 mi^2 (20,792 square kilometers [km^2]); the 5,161,584 cells in the Evangeline aquifer grid represent an area of approximately 7,175 mi^2 (18,582 km^2); and the 2,517,048 cells in the Jasper aquifer grid represent an area of approximately 3,498 mi^2 (9,061 km^2).

Development of the Semivariogram

Semivariograms, which mathematically describe the spatial relation of measured point pairs (Dunlap and Spinazola, 1984) commonly referred to as the "semivariance" (the sum of squared differences of measured point pairs separated by lag distance), were determined using the detrended datasets (residual water-level altitudes after removing the spatial trend) for each of the three aquifers. Dunlap and Spinazola (1984, p. 5) explained, "the most important item in the application of kriging is the semivariogram. The semivariogram is a graph of the variability of the difference of the regionalized data versus the distance between data points * * * the semivariogram is a plot of the squared differences in water-table altitudes at pairs of observation wells that are separated by a certain distance." The data used in the semivariance analysis are coordinate point data projected in Universal Transverse Mercator zone 15 (measured in meters), a standard map projection used as a "representation of all or part of the surface of a round body, especially the Earth, on a plane" (Snyder, 1987, p. 3). All distance calculations are therefore originally computed in meters. However, the dependent variable of water-level altitude is measured in feet, which means that the native model parameters are all computed in units of feet except for range, which is measured in meters. Range and lag distance is therefore converted from meters to feet to provide a consistent set of units.

The R programming language (ver. 3.6.2) (R Core Team, 2019) was used for all kriging processes. Semivariograms and their associated parameters were developed by using the R package automap version 1.0–14 (Hiemstra, 2013). The autofitVariogram function within the automap package uses the detrended water-level altitudes to estimate the kriging parameters and select the best theoretical model fit (common model types include exponential, Gaussian, spherical, and

Table 2. Summary statistics for first- and second-order polynomial regression equations of 2020 measured water-level altitudes (Ramage and Braun, 2020) for wells completed in the Chicot, Evangeline, or Jasper aquifers in the greater Houston study area, Texas.

[*R*-squared, coefficient of determination; *p*-value, probability value; E, exponent (for example, 1.8E−06 means "1.8×10^{-6}")]

Aquifer	Adjusted *R*-squared value		*p*-value	
	First order	Second order	First order	Second order
Chicot	0.134	0.683	1.8E−06	2.2E−16
Evangeline	0.180	0.539	4.8E−15	2.2E−16
Jasper	0.650	0.872	2.2E−16	2.2E−16

Matérn [Matérn, 1960; Olea, 2009]) to a given dataset. The kriging parameters are referred to as the "nugget," "sill" or "partial sill," "range," and "kappa value" (Olea, 2009; Sarma, 2009). The nugget describes the small-scale variability of the data over short distances that are less than the smallest distance between measurements and measurement error (Philip and Kitanidis, 1989, p. 857). The sill describes the maximum variability between point pairs (the partial sill is the sill minus the nugget), and the range describes the distance at which point pairs are no longer spatially correlated. The kappa value is a smoothing parameter applied to Matérn class variogram models (Diggle and Ribeiro, 2007; Hiemstra, 2013). A caveat to this process is that autofitVariogram function does not consider anisotropy in the data, which means that any directional trend in the data is not accounted for in the kriging parameters and interpolation. Because in universal kriging it is assumed that the mean of the measured attribute is neither constant nor known (Olea, 2009) and that detrended data using the second-order polynomial equation (eq. 2) are being modeled, it is not necessary to consider the directional trend.

The empirical and theoretical semivariogram for measured water-level altitudes in the Chicot aquifer (Ramage and Braun, 2020) is shown in figure 13. The nugget of 89 square feet (ft^2) indicates some small-scale variability in land-surface elevations, measurement error, and other unmeasured variables such as duration and rate of pumping prior to measurement. The empirical semivariogram points were fit with a theoretical Stein model (Stein, 1999), which is a modification of the Matérn model, with a sill of 3,569 ft^2, range of 267,970 ft, and kappa value of 0.8. The range was fixed as half the maximum distance between point pairs. The theoretical semivariogram has a good closeness of fit with the empirical semivariogram up to a lag distance of about 210,000 ft (about 40 miles [mi]); kriging requires a high degree of autocorrelation in the data in order to work effectively (Olea, 1975), and beyond a lag distance of about 40 mi the degree of autocorrelation in the data begins to decrease markedly.

The empirical and theoretical semivariogram for measured water-level altitudes in the Evangeline aquifer (Ramage and Braun, 2020) is shown in figure 14. The empirical semivariogram points were fit with a theoretical Stein model with a nugget of 71 ft^2, which indicates that there is good continuity of water-level altitudes within short distances. The computed sill is 11,203 ft^2; the range is 235,932 ft (about 45 mi), fixed as half the maximum distance between point pairs; and the kappa value is 0.3.

The empirical and theoretical semivariogram for measured water-level altitudes in the Jasper aquifer (Ramage and Braun, 2020) is shown in figure 15. The relatively large nugget of 117 ft^2 indicates that there are some small-scale variabilities that are likely caused by measurement or land-surface-elevation errors, or other errors associated with unmeasured variables such as duration and rate of pumping prior to measurement. The empirical semivariogram points were fit with a theoretical Stein model with a sill of 5,991 ft^2; a fixed range of 175,539 ft (about 33 mi), or half the maximum distance between point pairs; and a kappa value of 1.6. Measured data for two wells, one in Fort Bend County (site number 294327095445301) and one in Harris County near the southern end of Lake Houston (site number 295449095084101), were excluded from the calculation of maximum distance between point pairs for the semivariogram range owing to their large distance from the rest of the Jasper aquifer monitoring-well network.

Removing Selected Colocated Measurements

After kriging parameters were determined by the autofitVariogram function, selected colocated measurements were removed for instances in which more than one well exists at the same location. This process is necessary because the kriging function requires a single target value at any given measured location in order to calculate semivariance and match the supplied target value (Olea, 2009, p. 114). Multiple wells at the same location and screened in the same aquifer most often are nested piezometers (colocated wells) (figs. 6–9, for example). A processing script written in the R language was used to automatically determine which wells were grouped together within a grid cell and to retain the deepest water level from that group. The reason for retaining the deepest water level within the group is that the deepest water levels at colocated well sites are generally more closely correlated with water levels measured in nearby wells, as shown in the water-level data for the screened wells below the transition zone and above the Burkeville confining unit in the colocated wells in figures 6–9. In most cases, the deepest well in a nested piezometer site will have the deepest water level and is screened at a depth interval that is most similar to nearby production wells, which are often deeper than private wells or monitoring wells and make up the largest proportion of the monitoring-well network. An additional reason for selecting the deepest water level is that it most closely aligns with the underlying assumption of kriging, that data that are spatially close are more similar than data that are spatially farther apart.

As an example of a location where there are multiple wells and a single measurement was selected for use in the kriging process, table 3 lists five wells at a nested piezometer site (indicated by the footnote assigned to selected index wells in the index well column) in Galveston County and three wells within a 9,843-ft (3,000-m) radius of the nested piezometer site. For the purposes of declustering the wells at the nested piezometer site for use in kriging interpolation, the well with an index well number of 46 was the well retained. Index well 46 has the deepest depth to water within the nest and is the deepest (depth of well) of the five nested wells, and when comparing its depth to water to those of the three wells (index wells 36, 40, and 47) most proximal to the five nested wells, their water levels are most similar to index well 46, as are their well depths. In most cases (with the exception of wells completed in the Jasper aquifer in parts of Montgomery County), the well with the deepest well depth has the deepest depth to water among all wells within a given nest or cluster group.

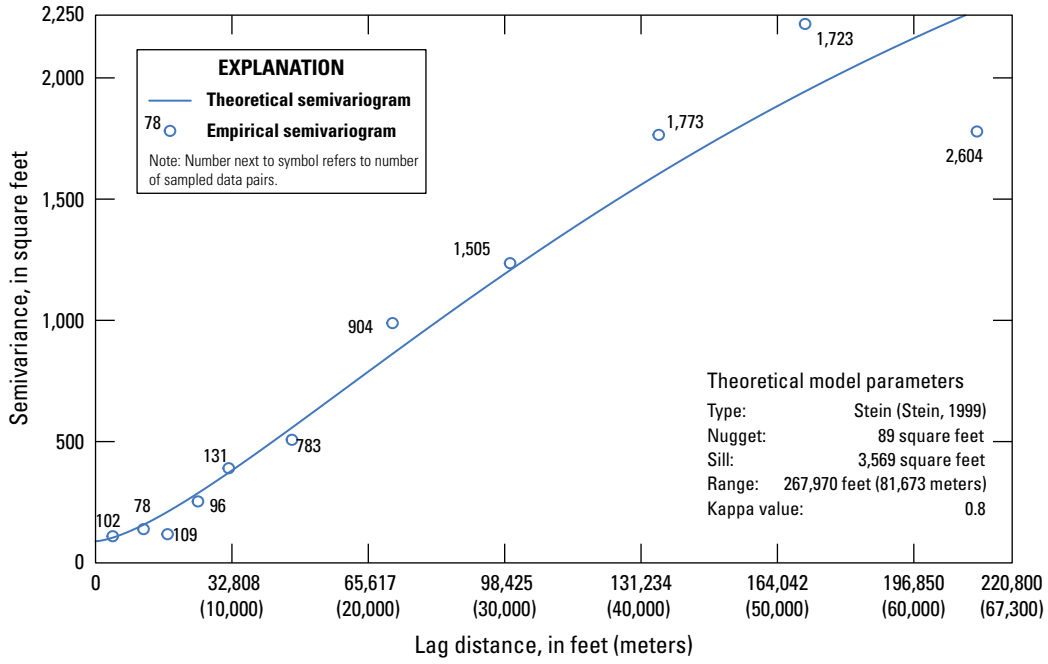

Figure 13. Empirical and theoretical semivariogram for measured water-level altitudes in the Chicot aquifer (Ramage and Braun, 2020) in the greater Houston study area, Texas, December 2019 to March 2020.

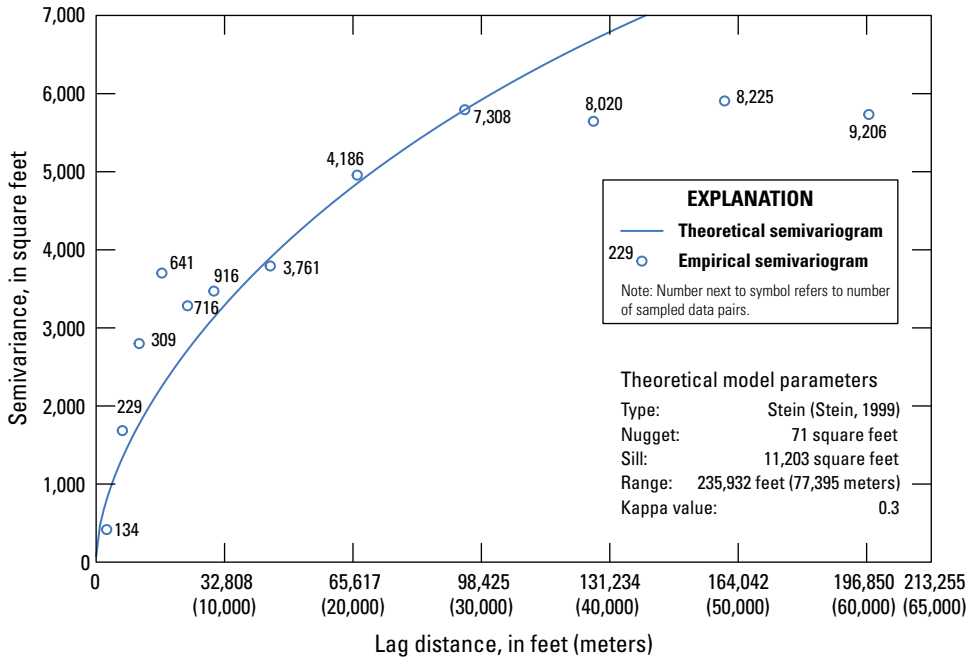

Figure 14. Empirical and theoretical semivariogram for measured water-level altitudes in the Evangeline aquifer (Ramage and Braun, 2020) in the greater Houston study area, Texas, December 2019 to March 2020.

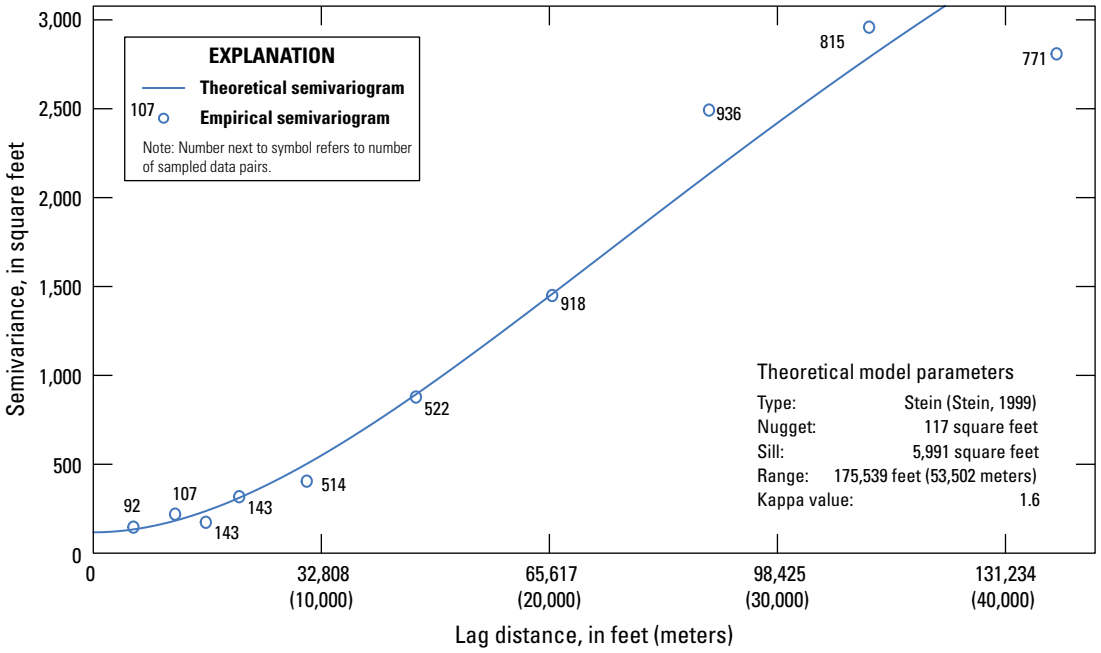

Figure 15. Empirical and theoretical semivariogram for measured water-level altitudes in the Jasper aquifer (Ramage and Braun, 2020) in the greater Houston study area, Texas, December 2019 to March 2020.

For the Chicot aquifer, 164 of the 173 wells used to measure water levels in the aquifer were retained for kriging purposes. For the Evangeline aquifer, 321 of 326 wells were retained. For the Jasper aquifer, all (112) wells were retained, as there were no nested piezometer wells used in the creation of the original 2020 water-level-altitude map.

Kriging Interpolation

After the selected colocated measurements were removed, the kriging interpolation process was performed using the detrended water-level-altitude data in conjunction with the previously determined semivariogram parameters over the established gridded surface. Universal kriging was selected because during the interpolation process it can incorporate the inherent directional trend in the data, which varies by coordinate location (Olea, 2009). Figures 16–18, which show gridded representations of water-level altitudes for 2020 in the Chicot, Evangeline, and Jasper aquifers, respectively, were color shaded in 50-ft increments to match the interval associated with the overlain contours (Braun and Ramage, 2020) for comparison purposes. Kriging interpolation was performed by using R version 3.6.2 (R Core Team, 2019), the R package gstat version 2.0–6 (Pebesma, 2020), the R packages sf version 0.9–8 (Pebesma, 2005) and sp version 1.4–2 (Pebesma, 2005) for spatial point data, the R package raster version 3.3–7 (Hijmans, 2020) for raster data, and the R package automap (Hiemstra, 2013) as discussed in the "Development of the Semivariogram" section of this report.

Use of Universal Kriging Geostatistical Interpolation Methods To Depict Water-Level Altitudes

For the Chicot aquifer in 2020, the universal kriging geostatistical interpolation methods used to develop the estimated gridded surface of water-level altitudes resulted in estimated water-level altitudes that ranged from –169 to greater than (>) 200 ft above the North American Vertical Datum of 1988 (NAVD 88) (fig. 16), and standard error ranged from 10.3 to 97.6 ft with a mean of 21.4 ft. The estimated gridded surface representing 2020 Evangeline aquifer water-level altitudes ranged in estimated water-level altitudes from –285 to >200 ft above NAVD 88 (fig. 17), and standard error ranged from 13.1 to 141.0 ft with a mean of 61.1 ft. The estimated gridded surface representing 2020 Jasper aquifer water-level altitudes ranged in estimated water-level altitudes from –206 to >250 ft above NAVD 88 (fig. 18), and standard error ranged from 11.3 to 84.8 ft with a mean of 23.4 ft.

In a comparison of the outputs from manual contouring and from kriging interpolation for the 2020 Chicot aquifer water-level-altitude map (fig. 16), generally the estimated gridded surface derived from kriging interpolation agrees well with the most recently published manual contours of the Chicot aquifer water-level altitudes (fig. 4 in Braun and Ramage [2020]). Several areas deviate slightly, particularly in the northwestern portion of the mapped area, where the gridded surface extends into areas where available well data are sparse. The gridded area near Beltway 8 and Highway 249 in northwestern Harris County extends slightly beyond the

Table 3. Water levels measured in wells at a nested piezometer site and in wells within a 9,843-foot (3,000-meter) radius of the nested piezometer site in Galveston County in the greater Houston study area, Texas, December 2019 to March 2020.

[USGS, U.S. Geological Survey; TWDB ID, Texas Water Development Board identifier]

Index well number	USGS site identifier	TWDB ID	Depth to water measured in 2020 (in feet below land surface)[1]	Well depth (in feet below land surface)[2]
36	292337094542801	6433901	42.67	772
40	292439094553101	6433804	50.09	785
43[3]	292458094534201	6433915	19.65	210
44[3]	292458094534202	6433916	28.64	302
45[3]	292458094534203	6433917	31.55	400
46[3]	292458094534204	6433918	43.22	535
47	292458094534206	6433920	45.87	800
48[3]	292458094534207	6433921	8.47	24

[1]Depth-to-water data are documented in Ramage and Braun (2020).

[2]Well-depth data are published in the U.S. Geological Survey National Water Information System (U.S. Geological Survey, 2021).

[3]Indicates wells colocated at the nested piezometer site.

contours to the north and northwest, as well as in an area near the border of Harris and Montgomery Counties, seemingly in response to a single well encircled by the –50-ft contour in south-central Montgomery County. Another slight discrepancy can be seen in the area of northern Fort Bend and Brazoria Counties near the –50-ft contour where the kriging estimates are in the range of –50 to –100.

Much like that of the Chicot aquifer water-level altitudes, the estimated gridded surface of the 2020 Evangeline aquifer water-level altitudes (fig. 17) generally agree favorably with the most recently published manual contours of the Evangeline aquifer water-level altitudes (fig. 6 in Braun and Ramage [2020]). The 50-ft increments of the gridded surface closely follow the contour lines in most cases, only deviating where the lack of control points allows the estimates to extend beyond the contours. Several areas of the gridded surface show this behavior, such as in central Harris County where the –200- to –250-ft shaded region extends beyond the –200-ft contour towards the east and in areas of south-central Montgomery County where steep gradients of water-level altitude are indicated. Also, like those of the Chicot aquifer (fig. 16), as gridded estimates of the Evangeline aquifer water-level altitudes move toward the boundaries of the grid and away from control points, in areas with the largest standard errors, estimates begin to deviate from contours. Kriging uses a weighted average of all measured values to estimate values at unmeasured locations; the weights assigned to measured values are spatially dependent. Hence, transitions in gridded surfaces tend to be more gradual than are often represented with contours. For example, on figure 17, a 50-ft contour bends sharply to "wrap around" a well point, whereas the gridded surface assigns the immediate area at and around the well point with a value approximating the actual measured water-level altitude at that location.

The estimated gridded surface of the 2020 Jasper aquifer water-level altitudes (fig. 18) is also in good agreement with the most recently published manual contours of the Jasper aquifer water-level altitudes (fig. 8 in Braun and Ramage [2020]). Areas where the contours and the gridded surface do not agree are often associated with areas where there is lack of data control, in particular the southern part of the mapped area across much of Harris and Waller Counties where control points are sparse. Another area where the contours and the gridded surface deviate is in the northwestern part of the mapped area, where shaded areas and measured water-level altitudes differ. This area is marked by a less dense well network than is present across the central part of the mapped area and shows that there is variability in the data. The area on the border of Harris and Montgomery Counties also shows some disagreement between the contours and the gridded surface. Within this area there are several wells with measured water-level altitudes that range from –188 to –196 ft (Ramage and Braun, 2020); however, estimates from the gridded surface indicate water-level altitudes up to and less than −200 ft below NAVD 88 and therefore disagree slightly with both measured values at these wells and contours in this area. The outer areas of the mapped area are not as well defined because of a lack of data control, unlike the mapped area associated with the denser network of wells in the central and southern parts of Montgomery County, where there is good data control. Lack of data control can also affect how manual contours are drawn and interpreted, often resulting in approximately equidistant spacing when other control points do not exist to define how the contours should be drawn. In contrast to the shortcomings of developing manual contours when control points are sparse, kriging interpolation includes spatial parameters supplied by the semivariogram to determine how grid cell estimates of water-level altitudes are computed.

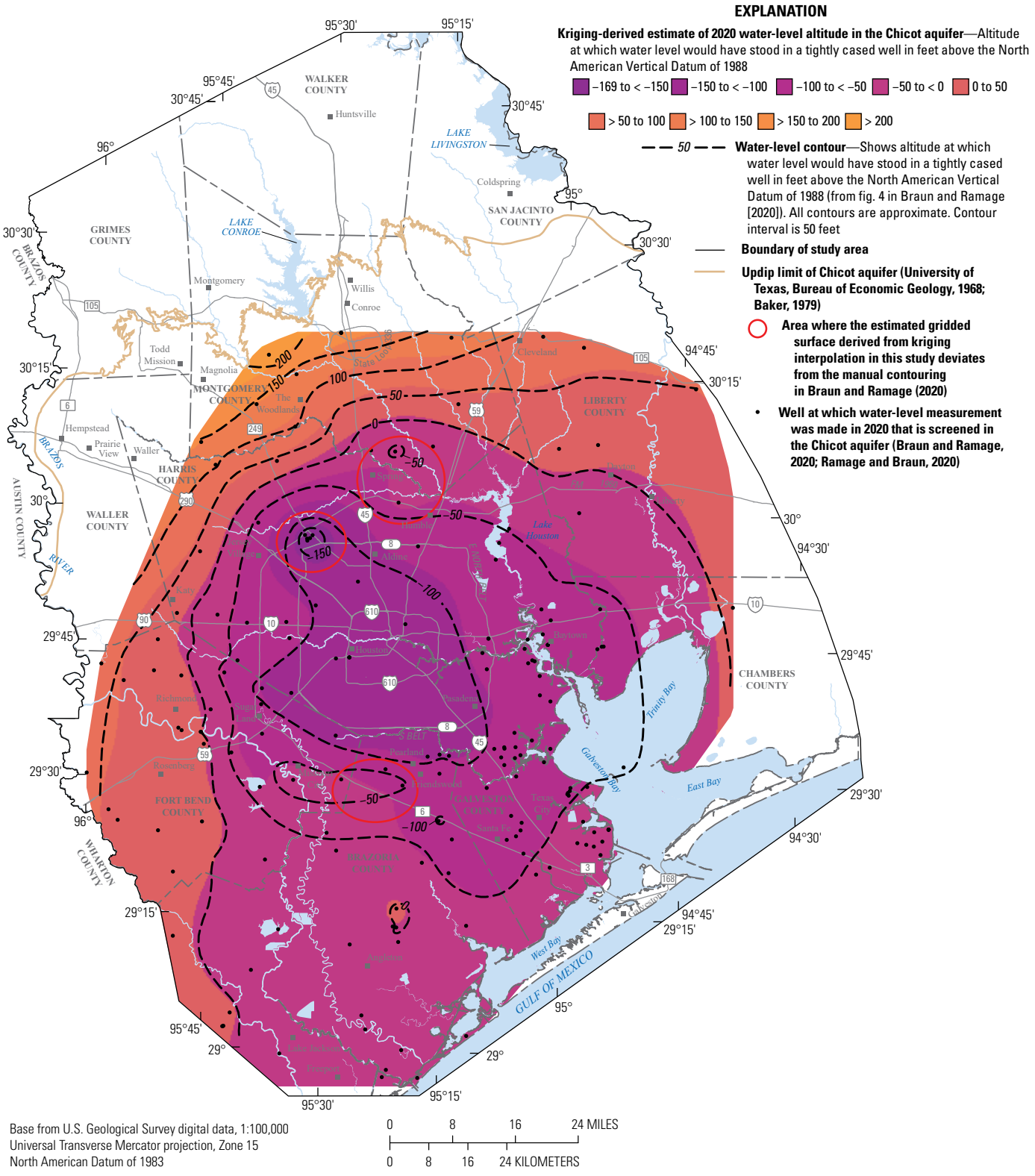

Figure 16. Estimated gridded surface representing 2020 water-level altitudes for the Chicot aquifer in the greater Houston study area, Texas, overlain with previously published contours.

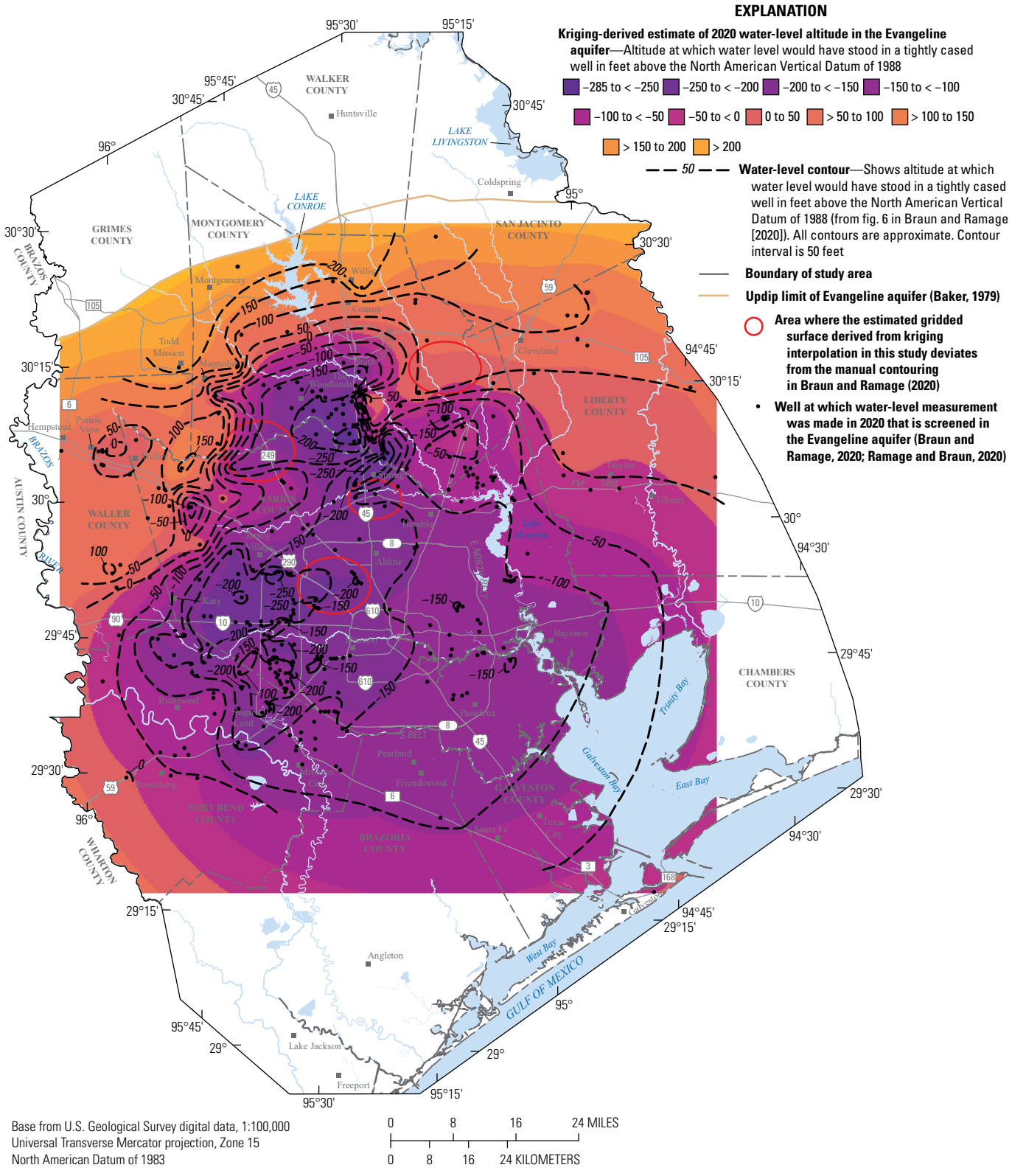

Figure 17. Estimated gridded surface representing 2020 water-level altitudes for the Evangeline aquifer in the greater Houston study area, Texas, overlain with previously published contours.

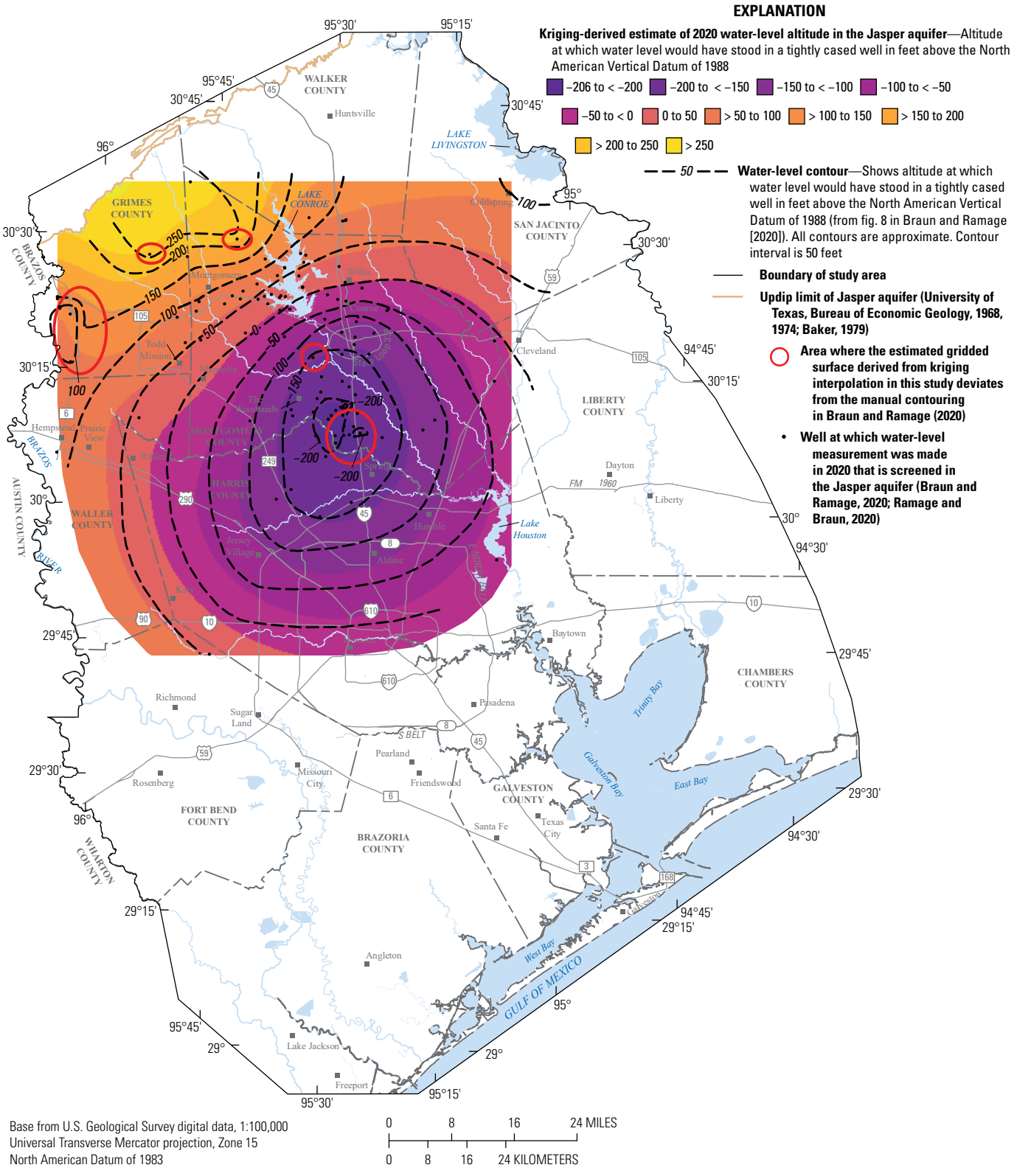

Figure 18. Estimated gridded surface representing 2020 water-level altitudes for the Jasper aquifer in the greater Houston study area, Texas, overlain with previously published contours.

Uncertainty Associated With Kriging Interpolation

When performing kriging interpolation, the estimated water-level-altitude value and variance associated with each grid cell are both computed. The standard error, which provides a measure of the uncertainty associated with the estimated value for each grid cell, can be calculated from the square root of the variance. Standard error is smallest at measured locations and increases as distance increases from measured locations (typically largest in areas of lowest measurement density).

Data Quality Control

Leave-one-out (LOO) cross validation (Olea, 2009) was performed on each dataset to verify the validity of the fitted semivariogram model and to determine where the estimated values deviated appreciably from the measured water-level altitudes. The process of LOO cross validation entails removing a single measured value and then computing the estimated value at that location by kriging the remaining data. The process is then repeated for each measured water-level altitude, and a residual is computed by subtracting the estimated value from the measured value at each removed site. This process also requires that a subset of individually located (that is, non-colocated) wells be used (164, 321, and 112 wells for the Chicot, Evangeline, and Jasper aquifers, respectively). Performing this process provides a measure of the validity of the fitted semivariogram model to the data and determines if there is conditional bias, which can be the result of kriging estimates having a different variability than the measured values (Philip and Kitanidis, 1989; Fisher, 2013).

The relation between estimated and measured water-level altitudes for 2020 obtained from the LOO cross validation for the Chicot, Evangeline, and Jasper aquifers is shown in figure 19*A–C*, respectively. For the Chicot aquifer, the slope of the regression line is 0.93 foot per foot (ft/ft), which is similar to the 1 ft/ft slope of the 1:1 line, indicating a close correlation between the estimated and measured water-level altitudes. The close fit of the regression line to the 1:1 line also indicates that the estimated water-level altitudes are not conditionally biased (Philip and Kitanidis, 1989; Fisher, 2013). For the Evangeline aquifer, the slope of the regression line is 0.81 ft/ft and thus differs from the 1:1 line, indicating that the estimated water-level-altitude values for the Evangeline aquifer differ somewhat from the measured values and may be slightly conditionally biased. Differences for the Evangeline aquifer between the estimated and measured water-level altitudes could be the result of the two large areas of substantial drawdown; that is, areas where water-level altitudes are lower than 200 ft below NAVD 88 and where tightly spaced gradients of water-level altitudes occur (fig. 17) in south-central Montgomery County and north-central and western Harris County. For the Jasper aquifer, the slope of the regression line is 0.98 ft/ft, indicating a nearly perfect fit to the 1:1 line. A few estimated water-level altitudes for the Jasper aquifer deviated appreciably from the measured values at the upper end of the range of measured values. These appreciable deviations from measured water-level altitudes are likely related to wells near the outermost extent of the gridded area and distant from other measured wells where data are sparse and where standard errors associated with kriging estimates tend to be largest (Philip and Kitanidis, 1989; Fisher, 2013).

Graphs of the differences between residual values and estimated water-level altitudes obtained from the LOO cross validation for the Chicot, Evangeline, and Jasper aquifers are shown in figure 20*A–C*, respectively. Small residuals indicate the absence of systematic errors that could lead to biased estimations from the kriging process (Fisher, 2013). For the Chicot aquifer, the residuals for estimated water-level altitudes ranged from –55.7 to 66.1 ft with a mean estimation error of 0.39 ft and a standard deviation of estimation error of 18.3 ft. For the 164 wells where water levels were retained for the Chicot aquifer, the absolute residual was larger than two times the standard deviation (36.6 ft) at only 9 wells (about 5 percent of the total number of measured wells). For the Evangeline aquifer, the residuals for estimated water-level altitudes ranged from –197.8 to 165.6 ft with a mean estimation error of 0.28 ft and a standard deviation of estimation error of 46.0 ft. For the 321 wells where water levels were retained for the Evangeline aquifer, the absolute residual was larger than two times the standard deviation (92.0 ft) at only 23 wells (about 7 percent of the total number of measurements). For the Jasper aquifer, the residuals for estimated water-level altitudes ranged from –133.2 to 109.8 ft with a mean estimation error of 0.97 ft and a standard deviation of estimation error of 28.9 ft. For the 112 wells where water levels were measured for the Jasper aquifer, the absolute residual was larger than two times the standard deviation (57.8 ft) at only 8 wells (about 7 percent of the total number of measurements).

Interpolated Areal Extent

Kriging interpolation provides both an estimated value at each grid cell location and an estimation error (variance) that can be used to quantify the uncertainty or quality of the associated estimate (Yamamoto, 2000). Uncertainty is often highest in areas that lack good data control (that is, areas where well points are separated by relatively large distances, as defined by the shape of the theoretical kriging model fit and range of autocorrelation) (Matérn, 1960; Matheron, 1963; Olea, 1975, 2009). In the 2021 annual report on water-level altitudes and water-level changes in the study area (Braun and Ramage, 2022), certain grid cells with high uncertainties were masked out. As explained in the “Introduction” section of this report, grid cells with either extrapolated or interpolated location-specific values representing areas of reduced well density within the well network distribution are masked out herein. For grid cells with high uncertainties, standard errors were calculated from the square root of the variance associated with each grid cell. All grid cells with standard errors exceeding

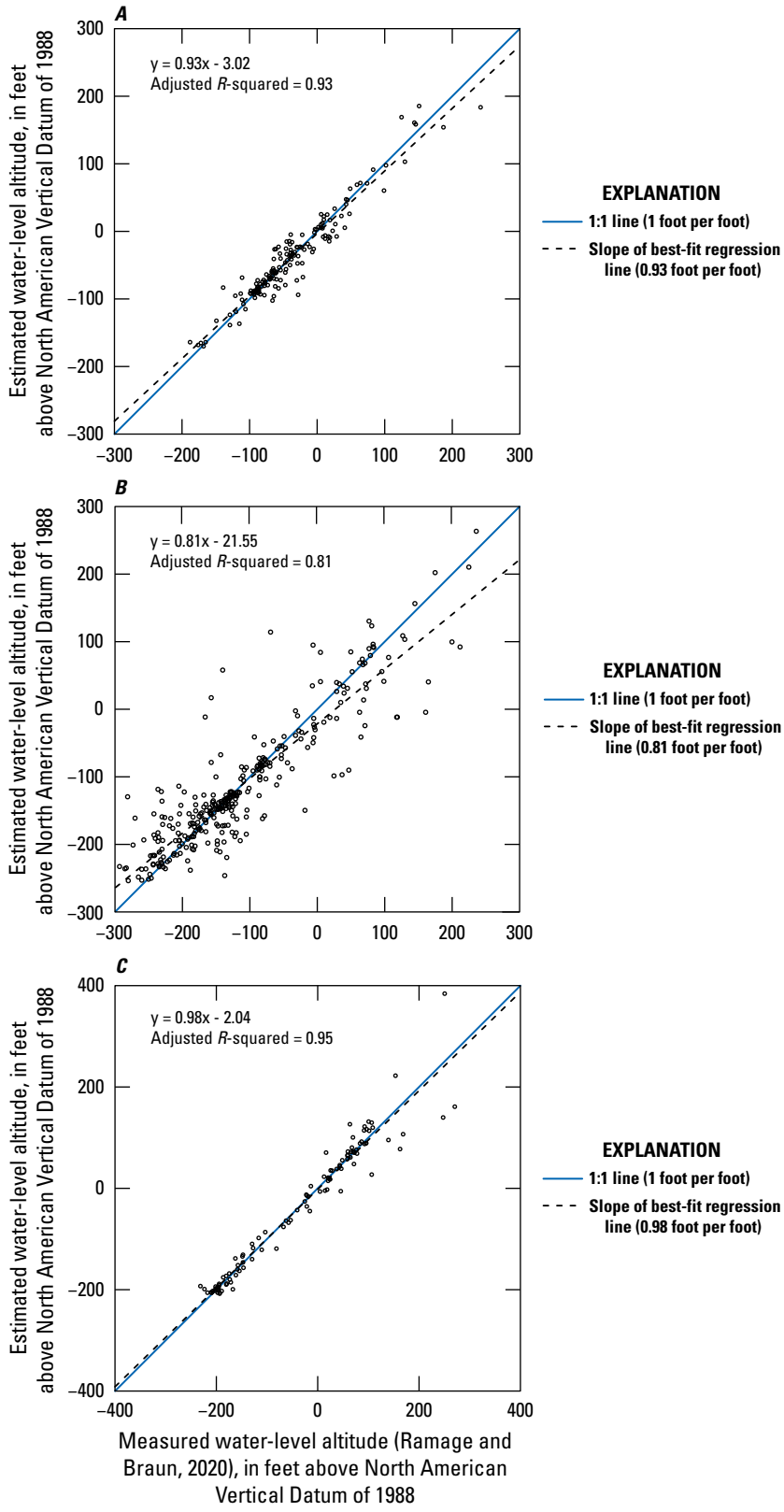

Figure 19. Relation between estimated (y) and measured (x) water-level altitudes during 2020 obtained from the leave-one-out cross validation for *A*, the Chicot aquifer, *B*, the Evangeline aquifer, and *C*, the Jasper aquifer in the greater Houston study area, Texas.

the overall mean standard error were hidden (assigned a value of "NA," or not applicable). Mean standard error for the 2020 Chicot aquifer water-level altitudes was 21.4 ft. Of the 5,775,728 grid cells in the estimated gridded surface of the Chicot aquifer water-level altitudes, about 27.8 percent (1,608,052) of the grid cells exceeded the mean standard error. Mean standard error for the 2020 Evangeline aquifer water-level altitudes was 61.1 ft. The estimated gridded surface of the Evangeline aquifer water-level altitudes is composed of 5,161,584 cells, and about 43.0 percent (2,219,120) exceeded the mean standard error. The higher mean standard error for the 2020 Evangeline aquifer water-level altitudes is likely the result of a denser network of wells within the center of the Evangeline aquifer grid combined with relatively large distances to wells near the boundaries of the grid that leave large areas with lack of data control. Mean standard error for the 2020 Jasper aquifer water-level altitudes was 23.4 ft. The estimated gridded surface of the Jasper aquifer water-level altitudes is composed of 2,517,048 cells, about 38.3 percent (963,738) of which exceeded the mean standard error. For all three aquifer gridded surfaces, areas of high uncertainty often exist where there is lack of data control or near the boundaries of the interpolated grid where wells are spaced farther apart.

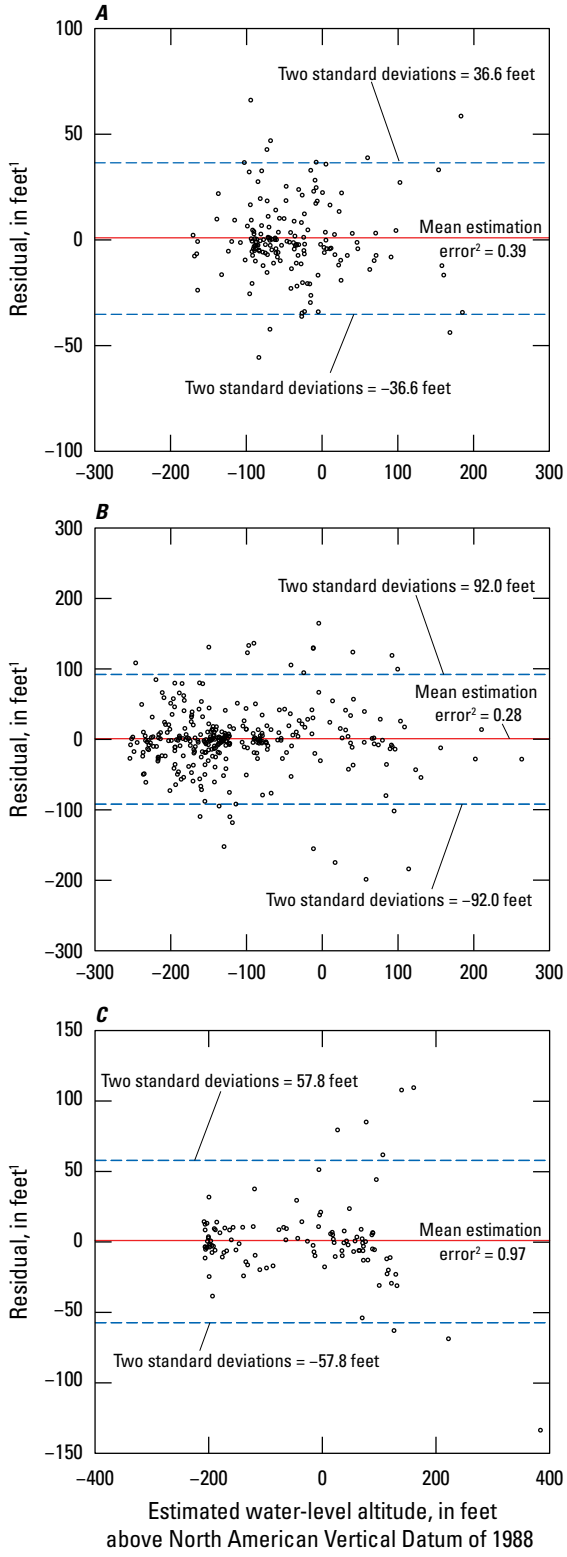

[1]Residual is the difference between measured and estimated water-level altitudes obtained from the LOO cross validation.
[2]Mean estimation error is calculated as the mean of the residuals.

Figure 20. Relation between residuals and estimated water-level altitudes during 2020 obtained from the leave-one-out cross validation for *A*, the Chicot aquifer, *B*, the Evangeline aquifer, and *C*, the Jasper aquifer in the greater Houston study area, Texas.

Quality Assurance

After the grids of water-level altitudes were created, estimated water-level altitudes at well locations in the gridded surface for each of the three aquifers were extracted and compared against measured water-level altitudes at the same wells to determine correlations between them (figs. 21–23). For the 2020 Chicot aquifer water-level altitudes, 173 values were extracted from the estimated gridded surface and produced a mean absolute error of 5.61 ft with a Pearson's correlation coefficient between estimated and measured water-level-altitude values of 0.99 and a root mean square error (RMSE) of 8.13 ft (fig. 21). For the 2020 Evangeline aquifer water-level altitudes, 326 values were extracted from the estimated gridded surface and produced a mean absolute error of 2.68 ft with a Pearson's correlation coefficient between estimated and measured water-level-altitude values of 0.99 and an RMSE of 4.06 ft (fig. 22). For the 2020 Jasper aquifer water-level altitudes, 112 values were extracted from the estimated gridded surface and produced a mean absolute error of 8.96 ft with a Pearson's correlation coefficient between estimated and measured water-level-altitude values of 0.99 and an RMSE of 13.4 ft (fig. 23).

Computer Software

Computer software used to process data, perform kriging analysis, and create the figures depicted in this report was written in the R programming language (ver. 3.6.2) (R Core Team, 2019). In addition to the base packages included with R, the following packages (available on the Comprehensive R Archive Network [CRAN] at https://cran.r-project.org) were used:

- **sf:** Standardized support for spatial vector data (Pebesma, 2018, 2021).
- **sp:** Classes and methods for spatial data (Pebesma, 2005).
- **raster:** Geographic data analysis and modeling of raster data (Hijmans, 2020).
- **gstat:** Spatial and temporal geostatistical modeling, prediction, and simulation (Pebesma, 2004).
- **automap:** Automatic determination of semivariogram parameters for kriging analysis (Hiemstra, 2013).

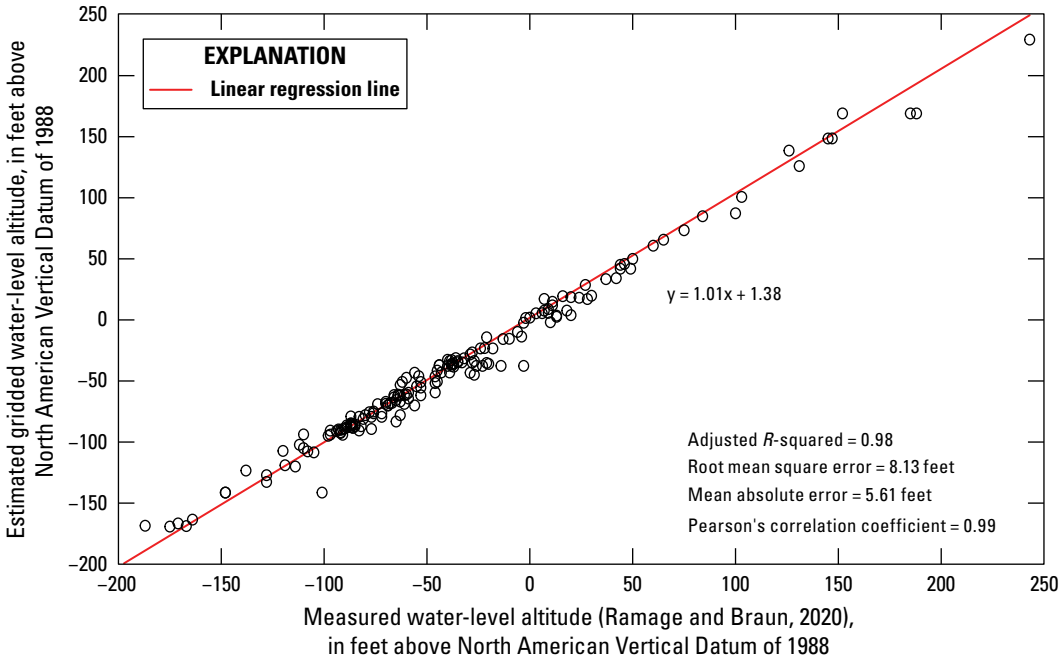

Figure 21. Correlation between 2020 Chicot aquifer estimated water-level altitudes (y) from the gridded surface and measured water-level altitudes (x) in the greater Houston study area, Texas.

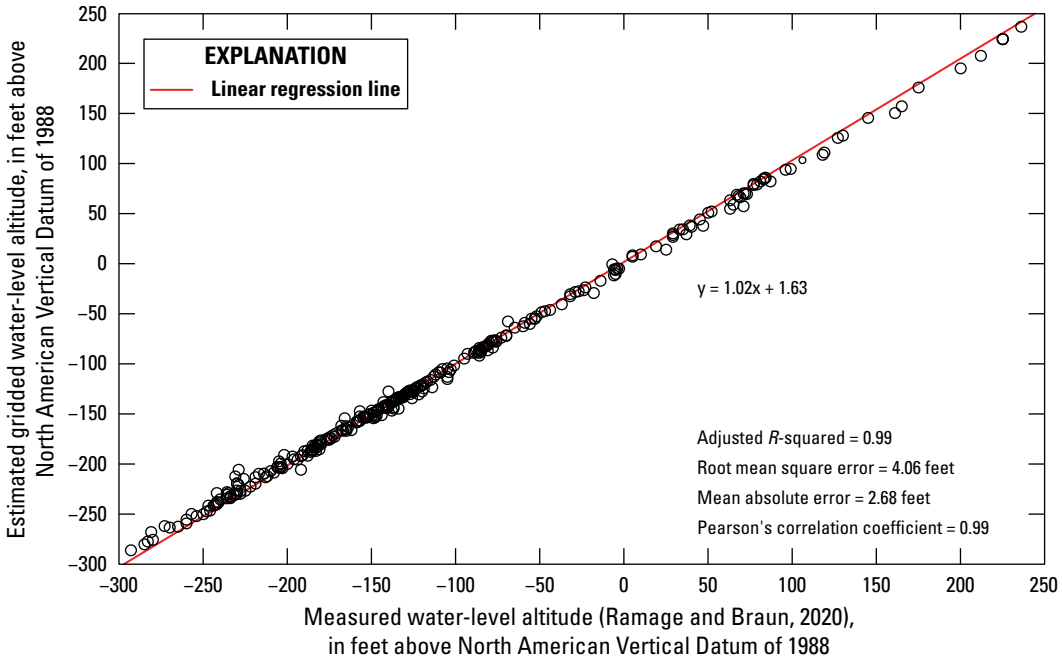

Figure 22. Correlation between 2020 Evangeline aquifer estimated water-level altitudes (y) from the gridded surface and measured water-level altitudes (x) in the greater Houston study area, Texas.

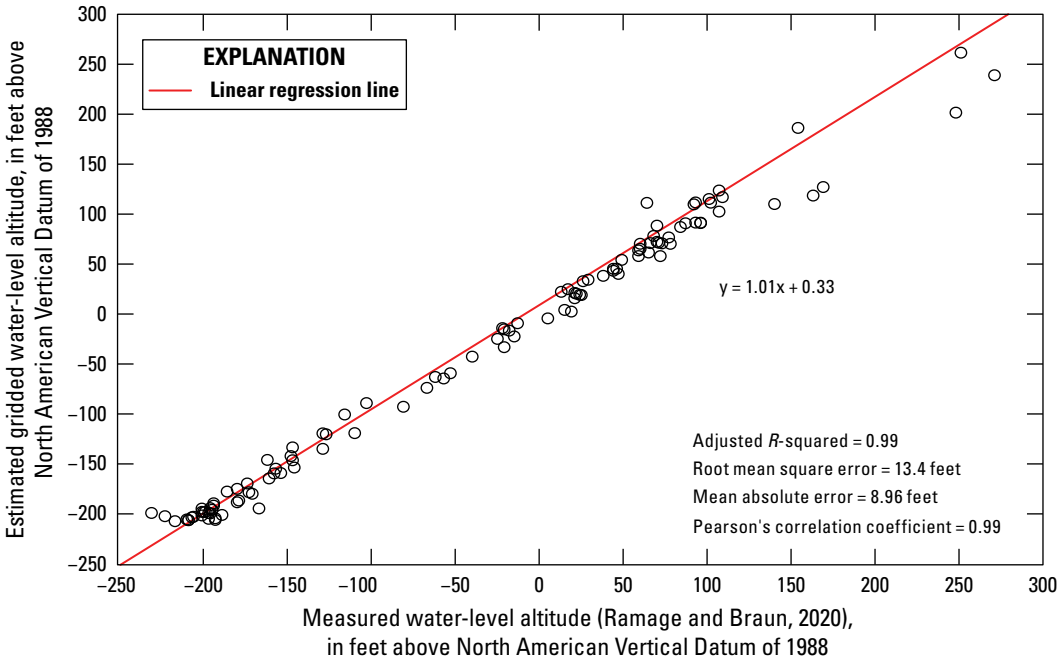

Figure 23. Correlation between 2020 Jasper aquifer estimated water-level altitudes (y) from the gridded surface and measured water-level altitudes (x) in the greater Houston study area, Texas.

Summary

The greater Houston area of Texas includes approximately 11,000 square miles and encompasses all or part of 11 counties (Harris, Galveston, Fort Bend, Montgomery, Brazoria, Chambers, Grimes, Liberty, San Jacinto, Walker, and Waller). Until the implementation of groundwater regulations in the mid-1970s, groundwater withdrawn from the three primary aquifers that compose the Gulf Coast aquifer system—the Chicot, Evangeline, and Jasper aquifers—had been the primary source of water for municipal supply, commercial and industrial use, and irrigation in the greater Houston area since the early 1900s. The unregulated withdrawal of groundwater from the Chicot and Evangeline aquifers, prior to 1975, caused water levels in the aquifers to steadily decline year over year, resulting in land-surface subsidence in the greater Houston area. By 1977, the withdrawals had resulted in distinct areas in southeastern Harris County where water levels in the Chicot and Evangeline aquifers were as much as 300 and 350 feet, respectively, below the National Geodetic Vertical Datum of 1929.

To address concerns regarding land-surface subsidence in Harris and Galveston Counties, the 64th Texas State Legislature authorized the establishment of the Harris-Galveston Subsidence District in 1975 to regulate and reduce groundwater withdrawals. Since the late 1970s, the U.S. Geological Survey (USGS), in cooperation with the Harris-Galveston Subsidence District, has monitored water-level altitudes and published reports depicting the status of water-level altitudes and long-term water-level changes in the greater Houston area. Following their establishment by the Texas State Legislature, the Fort Bend Subsidence District, Lone Star Groundwater Conservation District, and Brazoria County Groundwater Conservation District, as well as the City of Houston, also became cooperative participants in the project.

This report, prepared by the USGS in cooperation with the Harris-Galveston Subsidence District, City of Houston, Fort Bend Subsidence District, Lone Star Groundwater Conservation District, and Brazoria County Groundwater Conservation District, describes two substantial updates to the ways in which water-level altitudes and water-level changes in the greater Houston area are presented relative to previous USGS reports. The first update involves presenting water-level altitudes and water-level changes as a combined (undifferentiated) representation of the Chicot and Evangeline aquifers. The second update concerns the methods used to depict water-level altitudes and water-level changes in the greater Houston area in interpretive reports. Instead of the manual contouring methods that have historically been used in the annual USGS interpretive report series, geostatistical interpolation methods are used to develop gridded surfaces of water-level altitudes and water-level changes starting with the 2021 annual report on water-level altitudes and water-level changes in the study area published in 2022. As part of the second update, the areal extent of the gridded surfaces was refined through the use of a masking process. In the masking process, grid cells with either extrapolated or interpolated location-specific values representing areas of reduced well density within the well network distribution are not shown. This masking process is used for removing, or hiding, grid cells with estimates of high

uncertainty provided by the interpolation. Estimates of high uncertainty are defined as those where the standard error of the kriging estimate exceeds the overall mean standard error for the entire gridded surface. The standard error most often exceeds the overall mean standard error (as provided by the kriging estimates) in areas of reduced well density or areas where the estimate is extrapolated beyond where there is good data control (such as near the grid boundaries).

Since the formalization of the present-day naming of the Gulf Coast aquifer system aquifers and confining units in the 1960s, the Chicot and Evangeline aquifers have been described as distinct hydrogeologic units for the purpose of water-level mapping. The delineation of these units was largely based on stratigraphic position, grain size, water quality, drill cuttings, and permeability. More recently (2020), the Gulf Coast aquifer system geologic stratigraphy and hydrogeologic unit thicknesses were updated using a coupled chronostratigraphic and lithostratigraphic approach. A confining unit does not separate these two aquifers in the study area, and water-level data from colocated wells screened in these aquifers indicate that there is likely a substantial degree of hydrogeologic connection. Therefore, from a groundwater-flow perspective, these two aquifer units predominantly function as a single unit. Additionally, because of the update to the Gulf Coast aquifer system unit thicknesses, the distribution of wells screened in the Chicot and Evangeline aquifers changed considerably, whereby many wells previously classified as being screened in the Evangeline aquifer were reclassified as being screened in the Chicot aquifer. Because of these factors, the decision was made to combine the Chicot and Evangeline aquifers into a single, undifferentiated hydrogeologic unit for the purposes of assessing water-level altitudes and water-level changes over time.

Colocated well data at four extensometer sites in Harris County indicate that a transition zone from a shallower zone under atmospheric pressure to a deeper zone under artesian pressure exists between about 125 and 225 feet (ft) below land surface (bls). Above the depth interval 125–225 ft bls, water levels have remained relatively stable over time and have not been affected by pressure-head changes within the Chicot and Evangeline (undifferentiated) aquifer that are found when the groundwater is under artesian pressure; any small differences in water levels measured in wells screened in the depth interval 125–225 ft bls are primarily driven by changes in precipitation. Therefore, wells screened above the transition zone that extends to about 250 ft bls were not classified as wells screened in the Chicot and Evangeline aquifers (undifferentiated) and are not planned to be classified as wells screened in the Chicot and Evangeline aquifers (undifferentiated) henceforth for assessing water-level altitudes and water-level changes in the study area. At all of the extensometer sites, water levels among all wells screened in the Chicot and Evangeline aquifers below the transition zone and under artesian pressure were similar on an overall basis during a 40- to 50-year period. The similar water levels among the sites demonstrate a hydraulic connection across a range of depth intervals that has persisted from at least 1980 to 2020 in the Chicot and Evangeline aquifers.

The 2020 water-level altitudes for the Chicot, Evangeline, and Jasper aquifers were re-created in this report as computer algorithms of the contoured datasets as gridded surfaces using the same source data to demonstrate the similarity of results from geostatistical interpolation methods to those from manual contouring methods. In this report, universal kriging methods were used to produce the re-created 2020 water-level-altitude maps for the Chicot, Evangeline, and Jasper aquifers. For the Chicot aquifer in 2020, the universal kriging geostatistical interpolation methods used to develop gridded surfaces of water-level altitudes resulted in estimated water-level altitudes that ranged from –169 to greater than (>) 200 ft above the North American Vertical Datum of 1988 (NAVD 88), and standard error ranged from 10.3 to 97.6 ft with a mean of 21.4 ft. The estimated gridded surface representing 2020 Evangeline aquifer water-level altitudes ranged in estimated water-level altitudes from –285 to >200 ft above NAVD 88, and standard error ranged from 13.1 to 141.0 ft with a mean of 61.1 ft. The estimated gridded surface representing 2020 Jasper aquifer water-level altitudes ranged in estimated water-level altitudes from –206 to >250 ft above NAVD 88, and standard error ranged from 11.3 to 84.8 ft with a mean of 23.4 ft.

Leave-one-out cross validation was performed on each dataset to verify the validity of the kriging model and to determine where the estimated values deviated appreciably from the measured values. For the Chicot aquifer, the residuals for estimated water-level altitudes ranged from –55.7 to 66.1 ft with a mean estimation error of 0.39 ft and a standard deviation of 18.3 ft. For the Evangeline aquifer, the residuals for estimated water-level altitudes ranged from –197.8 to 165.6 ft with a mean estimation error of 0.28 ft and a standard deviation of estimation error of 46.0 ft. For the Jasper aquifer, the residuals for estimated water-level altitudes ranged from –133.2 to 109.8 ft with a mean estimation error of 0.97 ft and a standard deviation of estimation error of 28.9 ft.

After the grids of water-level altitudes were created, estimated water-level altitudes at well locations in the gridded surface for each of the three aquifers were extracted and compared against measured water-level altitudes at the same wells to determine correlations between them. For the 2020 Chicot aquifer water-level altitudes, 173 values were extracted from the estimated gridded surface and produced a mean absolute error of 5.61 ft with a Pearson's correlation coefficient between estimated and measured water-level-altitude values of 0.99 and a root mean square error (RMSE) of 8.13 ft. For the 2020 Evangeline aquifer water-level altitudes, 326 values were extracted from the estimated gridded surface and produced a mean absolute error of 2.68 ft with a Pearson's correlation coefficient between estimated and measured water-level-altitude values of 0.99 and an RMSE of 4.06 ft. For the 2020 Jasper aquifer water-level altitudes, 112 values were extracted from the estimated gridded surface and produced a mean

absolute error of 8.96 ft with a Pearson's correlation coefficient between estimated and measured water-level-altitude values of 0.99 and an RMSE of 13.4 ft.

References Cited

Baker, E.T., Jr., 1979, Stratigraphic and hydrogeologic framework of part of the Coastal Plain of Texas: Texas Department of Water Resources Report 236, 43 p., accessed April 30, 2021, at http://www.twdb.texas.gov/publications/reports/numbered_reports/doc/R236/R236.pdf.

Baker, E.T., Jr., 1986, Hydrology of the Jasper aquifer in the southeast Texas Coastal Plain: Texas Water Development Board Report 295, 64 p., accessed November 30, 2021, at https://www.twdb.texas.gov/publications/reports/numbered_reports/doc/R295/R295.pdf.

Barbie, D.L., Coplin, L.S., and Locke, G.L., 1991, Approximate altitude of water levels in wells in the Chicot and Evangeline aquifers in the Houston area, Texas, January–February 1990: U.S. Geological Survey Open-File Report 91–240, 2 sheets, accessed April 30, 2021, at https://doi.org/10.3133/ofr91240.

Bluebonnet Groundwater Conservation District, 2018, Bluebonnet Groundwater Conservation District groundwater management plan: Bluebonnet Groundwater Conservation District, 179 p., accessed April 30, 2021, at http://www.bluebonnetgroundwater.org/wp-content/uploads/2021/06/APPROVED-MGMT-Plan-20-011.pdf.

Bluebonnet Groundwater Conservation District, 2021, History—Bluebonnet Groundwater Conservation District: Bluebonnet Groundwater Conservation District web page, accessed April 30, 2021, at https://www.bluebonnetgroundwater.org/district/history/.

Bohling, G., 2005, Introduction to geostatistics and variogram analysis: Kansas Geological Survey, v. 1, no. 10, p. 1–20, accessed September 15, 2021, at https://www.academia.edu/23836974/introduction_to_geostatisitics_and_variogram_analysis.

Borrok, D.M., and Broussard, W.P., III, 2016, Long-term geochemical evaluation of the coastal Chicot aquifer system, Louisiana, USA: Journal of Hydrology, v. 533, p. 320–331, accessed April 30, 2021, at https://doi.org/10.1016/j.jhydrol.2015.12.022.

Braun, C.L., and Ramage, J.K., 2020, Status of groundwater-level altitudes and long-term groundwater-level changes in the Chicot, Evangeline, and Jasper aquifers, Houston-Galveston region, Texas, 2020: U.S. Geological Survey Scientific Investigations Report 2020–5089, 18 p., accessed May 25, 2022, at https://doi.org/10.3133/sir20205089.

Braun, C.L., and Ramage, J.K., 2022, Status of water-level altitudes and long-term water-level changes in the Chicot and Evangeline (undifferentiated) and Jasper aquifers, greater Houston area, Texas, 2021: U.S. Geological Survey Scientific Investigations Report 2022–5065, 25 p., accessed August 5, 2022, at https://doi.org/10.3133/sir20225065.

Braun, C.L., Ramage, J.K., and Shah, S.D., 2019, Status of groundwater-level altitudes and long-term groundwater-level changes in the Chicot, Evangeline, and Jasper aquifers, Houston-Galveston region, Texas, 2019: U.S. Geological Survey Scientific Investigations Report 2019–5089, 18 p., accessed May 25, 2022, at https://doi.org/10.3133/sir20195089.

Brazoria County Groundwater Conservation District, 2017, Brazoria County Groundwater Conservation District groundwater management plan: Brazoria County Groundwater Conservation District, 130 p., accessed April 30, 2021, at https://www.bcgroundwater.org/images/bcg/documents/2017/Groundwater-Management-Plan-2017.pdf.

Brazoria County Groundwater Conservation District, 2021, About the district: Brazoria County Groundwater Conservation District web page, accessed April 30, 2021, at https://www.bcgroundwater.org/bcg/About_the_District.asp.

Carr, J.E., Meyer, W.R., Sandeen, W.M., and McLane, I.R., 1985, Digital models for simulation of ground-water hydrology of the Chicot and Evangeline aquifers along the Gulf Coast of Texas: Texas Department of Water Resources Report 289, 101 p., accessed April 30, 2021, at https://www.twdb.texas.gov/publications/reports/numbered_reports/doc/R289/Report289.asp.

Casarez, I.R., 2020, Aquifer extents in the coastal lowlands aquifer system regional groundwater availability study area in Texas, Louisiana, Mississippi, Alabama, and Florida: U.S. Geological Survey data release, accessed April 30, 2021, at https://doi.org/10.5066/P9BH2KG2.

Chowdhury, A.H., and Turco, M.J., 2006, Geology of the Gulf Coast aquifer, Texas, chap. 2 *in* Mace, R.E., Davidson, S.C., Angle, E.S., and Mullican, W.F., eds., Aquifers of the Gulf Coast of Texas: Texas Water Development Board Report 365, p. 23–50, accessed April 30, 2021, at https://www.twdb.texas.gov/publications/reports/numbered_reports/doc/r365/r365_composite.pdf.

Coplin, L.S., 2001, Water-level altitudes in wells completed in the Jasper aquifer, greater Houston area, Texas, spring 2000: U.S. Geological Survey Open-File Report 01–147, 2 p., accessed April 30, 2021, at https://doi.org/10.3133/ofr01147.

Coplin, L.S., and Galloway, D., 1999, Houston-Galveston, Texas—Managing coastal subsidence, *in* Galloway, D., Jones, D.R., and Ingebritsen, S.E., eds., Land subsidence in the United States: U.S. Geological Survey Circular 1182, p. 35–48, accessed April 30, 2021, at https://doi.org/10.3133/cir1182.

Diggle, P.J., and Ribeiro, P.J., Jr., 2007, Model-based geostatistics: New York, Springer, 228 p., accessed November 16, 2021, at https://ethz.ch/content/dam/ethz/special-interest/math/statistics/sfs/Education/Advanced%20Studies%20in%20Applied%20Statistics/course-material-1921/SpatialStatistics/Diggle-Ribeiro-2007.pdf.

Dunlap, L.E., and Spinazola, J.M., 1984, Interpolating water-table altitudes in west-central Kansas using kriging techniques: U.S. Geological Survey Water-Supply Paper 2238, 19 p., accessed October 27, 2021, at https://doi.org/10.3133/wsp2238.

Fisher, J.C., 2013, Optimization of water-level monitoring networks in the eastern Snake River Plain aquifer using a kriging-based genetic algorithm method: U.S. Geological Survey Scientific Investigations Report 2013–5120 (DOE/ID–22224), 74 p., accessed August 15, 2021, at https://doi.org/10.3133/sir20135120.

Fort Bend Subsidence District, 2013, Fort Bend Subsidence District 2013 regulatory plan [amended 2007, 2009, and 2013]: Fort Bend Subsidence District, 14 p., accessed April 30, 2021, at https://fbsubsidence.org/wp-content/uploads/2020/07/FBSD-Regulatory-Plan-Amended-2013.pdf.

Fort Bend Subsidence District, 2021, Fort Bend Subsidence District—District regulatory plan: Fort Bend Subsidence District, accessed April 30, 2021, at https://fbsubsidence.org/planning/regulatory-plan/.

Gabrysch, R.K., 1979, Approximate altitude of water levels in wells in the Chicot and Evangeline aquifers in the Houston area, Texas, spring 1977 and spring 1978: U.S. Geological Survey Open-File Report 79–334, 4 sheets, accessed April 30, 2021, at https://doi.org/10.3133/ofr79334.

Gabrysch, R.K., and Bonnet, C.W., 1975, Land-surface subsidence in the Houston-Galveston region, Texas: Texas Water Development Board Report 188, 19 p., accessed November 1, 2021, at https://www.twdb.texas.gov/publications/reports/numbered_reports/doc/R188.pdf. [Second printing 1977.]

Hammond, W.W., Jr., 1969, Ground-water resources of Matagorda County, Texas: Texas Water Development Board Report 91, 163 p., accessed November 1, 2021, at https://www.twdb.texas.gov/publications/reports/numbered_reports/doc/R91/R91.pdf.

Harris-Galveston Subsidence District, 2013, Regulatory plan 2013: Harris-Galveston Subsidence District, 14 p., accessed April 30, 2021, at https://hgsubsidence.org/wp-content/uploads/2013/07/HGSD-2013-Regulatory-Plan-with-Amendment.pdf.

Harris-Galveston Subsidence District, 2021, Legislative authority: Harris-Galveston Subsidence District web page, accessed April 30, 2021, at https://hgsubsidence.org/about/legislative-authority/.

Hiemstra, P., 2013, automap—Automatic interpolation package—R package version 1.0–14: R Foundation for Statistical Computing software release, accessed September 10, 2021, at https://cran.r-project.org/package=automap.

Hijmans, R.J., 2020, raster—Geographic data analysis and modeling—R package version 3.3–7: R Foundation for Statistical Computing software release, accessed September 10, 2021, at https://cran.r-project.org/package=raster.

Hill, R.T., 1901, Geography and geology of the Black and Grand Prairies, Texas, with detailed description of the Cretaceous formations and special reference to artesian waters, pt. 7 *of* 21st annual report: Washington, D.C., U.S. Geological Survey, 666 p., accessed June 16, 2022, at https://repositories.lib.utexas.edu/handle/2152/78010.

Johnson, M.R., Ramage, J.K., and Kasmarek, M.C., 2011, Water-level altitudes 2011 and water-level changes in the Chicot, Evangeline, and Jasper aquifers and compaction 1973–2011 in the Chicot and Evangeline aquifers, Houston–Galveston region, Texas: U.S. Geological Survey Scientific Investigations Map 3174, 16 sheets, 17 p., accessed April 30, 2021, at https://doi.org/10.3133/sim3174.

Jorgensen, D.G., 1975, Analog-model studies of ground-water hydrology in the Houston district, Texas: Texas Water Development Board Report 190, 84 p, accessed April 30, 2021, at https://www.twdb.texas.gov/publications/reports/numbered_reports/doc/R190/Report190.asp.

Kasmarek, M.C., 1997, Water-level altitudes in wells completed in the Chicot and Evangeline aquifers, Fort Bend County and adjacent areas, Texas, January–March 1990: U.S. Geological Survey Open-File Report 97–784, 2 sheets, accessed April 30, 2021, at https://doi.org/10.3133/ofr97784.

Kasmarek, M.C., 2012, Hydrogeology and simulation of groundwater flow and land-surface subsidence in the northern part of the Gulf Coast aquifer system, Texas, 1891–2009 (ver. 1.1, December 2013): U.S. Geological Survey Scientific Investigations Report 2012–5154, 55 p., accessed April 30, 2021, at https://doi.org/10.3133/sir20125154.

Kasmarek, M.C., Gabrysch, R.K., and Johnson, M.R., 2009, Estimated land-surface subsidence in Harris County, Texas, 1915–17 to 2001: U.S. Geological Survey Scientific Investigations Map 3097, 2 sheets, accessed October 13, 2021, at https://doi.org/10.3133/sim3097.

Kasmarek, M.C., and Houston, N.A., 2007, Water-level altitudes 2007 and water-level changes in the Chicot, Evangeline, and Jasper aquifers and compaction 1973–2006 in the Chicot and Evangeline aquifers, Houston–Galveston region, Texas: U.S. Geological Survey Scientific Investigations Map 2968, 18 sheets, 159 p., accessed April 30, 2021, at https://doi.org/10.3133/sim2968.

Kasmarek, M.C., and Houston, N.A., 2008, Water-level altitudes 2008 and water-level changes in the Chicot, Evangeline, and Jasper aquifers and compaction 1973–2007 in the Chicot and Evangeline aquifers, Houston-Galveston region, Texas: U.S. Geological Survey Scientific Investigations Map 3031, 17 sheets, 4 p., accessed April 30, 2021, at https://doi.org/10.3133/sim3031.

Kasmarek, M.C., Houston, N.A., and Brown, D.W., 2006, Water-level altitudes 2006 and water-level changes in the Chicot, Evangeline, and Jasper aquifers and compaction 1973–2005 in the Chicot and Evangeline aquifers, Houston-Galveston region, Texas: U.S. Geological Survey Open-File Report 2006–1079, 15 sheets, accessed April 30, 2021, at https://doi.org/10.3133/ofr20061079.

Kasmarek, M.C., Houston, N.A., and Ramage, J.K., 2009, Water-level altitudes 2009 and water-level changes in the Chicot, Evangeline, and Jasper aquifers and compaction 1973–2008 in the Chicot and Evangeline aquifers, Houston-Galveston region, Texas (ver. 1.3, March 15, 2011): U.S. Geological Survey Scientific Investigations Map 3081, 16 sheets, 3 p., 2 app., accessed April 30, 2021, at https://doi.org/10.3133/sim3081.

Kasmarek, M.C., Johnson, M.R., and Ramage, J.K., 2010, Water-level altitudes 2010 and water-level changes in the Chicot, Evangeline, and Jasper aquifers and compaction 1973–2009 in the Chicot and Evangeline aquifers, Houston-Galveston region, Texas: U.S. Geological Survey Scientific Investigations Map 3138, 16 sheets, 17 p., 1 app., accessed April 30, 2021, at https://doi.org/10.3133/sim3138.

Kasmarek, M.C., Johnson, M.R., and Ramage, J.K., 2012, Water-level altitudes 2012 and water-level changes in the Chicot, Evangeline, and Jasper aquifers and compaction 1973–2011 in the Chicot and Evangeline aquifers, Houston-Galveston region, Texas: U.S. Geological Survey Scientific Investigations Map 3230, 16 sheets, 18 p., accessed April 30, 2021, at https://doi.org/10.3133/sim3230.

Kasmarek, M.C., Johnson, M.R., and Ramage, J.K., 2013, Water-level altitudes 2013 and water-level changes in the Chicot, Evangeline, and Jasper aquifers and compaction 1973–2012 in the Chicot and Evangeline aquifers, Houston-Galveston region, Texas: U.S. Geological Survey Scientific Investigations Map 3263, 16 sheets, 19 p., accessed April 30, 2021, at https://doi.org/10.3133/sim3263.

Kasmarek, M.C., Johnson, M.R., and Ramage, J.K., 2014, Water-level altitudes 2014 and water-level changes in the Chicot, Evangeline, and Jasper aquifers and compaction 1973–2013 in the Chicot and Evangeline aquifers, Houston-Galveston region, Texas: U.S. Geological Survey Scientific Investigations Map 3308, 16 sheets, 31-p. pamphlet, accessed April 30, 2021, at https://doi.org/10.3133/sim3308.

Kasmarek, M.C., and Lanning-Rush, J., 2004, Water-level altitudes 2004 and water-level changes in the Chicot, Evangeline, and Jasper aquifers and compaction 1973–2003 in the Chicot and Evangeline aquifers, Houston-Galveston region, Texas: U.S. Geological Survey Open-File Report 2004–1084, 13 sheets, accessed April 30, 2021, at https://doi.org/10.3133/ofr20041084.

Kasmarek, M.C., and Ramage, J.K., 2017, Water-level altitudes 2017 and water-level changes in the Chicot, Evangeline, and Jasper aquifers and compaction 1973–2016 in the Chicot and Evangeline aquifers, Houston-Galveston region, Texas: U.S. Geological Survey Scientific Investigations Report 2017–5080, 32 p., accessed April 30, 2021, at https://doi.org/10.3133/sir20175080.

Kasmarek, M.C., Ramage, J.K., Houston, N.A., Johnson, M.R., and Schmidt, T.S., 2015, Water-level altitudes 2015 and water-level changes in the Chicot, Evangeline, and Jasper aquifers and compaction 1973–2014 in the Chicot and Evangeline aquifers, Houston-Galveston region, Texas: U.S. Geological Survey Scientific Investigations Map 3337, 16 sheets, scale 1:100,000, 35-p. pamphlet, accessed April 30, 2021, at https://doi.org/10.3133/sim3337.

Kasmarek, M.C., Ramage, J.K., and Johnson, M.R., 2016, Water-level altitudes 2016 and water-level changes in the Chicot, Evangeline, and Jasper aquifers and compaction 1973–2015 in the Chicot and Evangeline aquifers, Houston-Galveston region, Texas: U.S. Geological Survey Scientific Investigations Map 3365, 16 sheets, scale 1:100,000, 53-p. pamphlet, accessed April 30, 2021, at https://doi.org/10.3133/sim3365.

Kasmarek, M.C., and Robinson, J.L., 2004, Hydrogeology and simulation of ground-water flow and land-surface subsidence in the northern part of the Gulf Coast aquifer system, Texas: U.S. Geological Survey Scientific Investigations Report 2004–5102, 111 p., accessed April 30, 2021, at https://doi.org/10.3133/sir20045102.

Kasmarek, M.C., and Strom, E.W., 2002, Hydrology and simulation of ground-water flow and land-surface subsidence in the Chicot and Evangeline aquifers, Houston area, Texas: U.S. Geological Survey Water-Resources Investigations Report 02–4022, 61 p., accessed April 30, 2021, at https://doi.org/10.3133/wri024022.

Lambeck, K., Esat, T.M., and Potter, E.K., 2002, Links between climate and sea levels for the past three million years: Nature, v. 419, no. 6903, p. 199–206, accessed April 30, 2021, at https://doi.org/10.1038/nature01089.

Lang, J.W., Winslow, A.G., and White, W.N., 1950, Geology and ground-water resources of the Houston district, Texas: Texas State Board of Water Engineers Bulletin 5001, 55 p., accessed April 30, 2021, at https://www.twdb.texas.gov/publications/reports/bulletins/doc/B5001.pdf.

Liu, Y., Li, J., and Fang, Z.N., 2019, Groundwater level change management on control of land subsidence supported by borehole extensometer compaction measurements in the Houston-Galveston region, Texas: Geosciences, v. 9, no. 5, 19 p., accessed April 30, 2021, at https://doi.org/10.3390/geosciences9050223.

Lone Star Groundwater Conservation District, 2020, Groundwater management plan—Adopted April 14, 2020: Lone Star Groundwater Conservation District, 114 p., accessed April 30, 2021, at https://static1.squarespace.com/static/58347802cd0f6854e2f90e45/t/5f5aa373fc64123d4cd68a44/1599775678824/LSGCD+MP+%28Final+Clean%29_Adopted+5.15.20.pdf.

Lone Star Groundwater Conservation District, 2021, Our history—Lone Star Groundwater Conservation District: Lone Star Groundwater Conservation District web page, accessed April 30, 2021, at https://www.lonestargcd.org/history.

Loskot, C.L., Sandeen, W.M., and Follett, C.R., 1982, Ground-water resources of Colorado, Lavaca, and Wharton Counties, Texas: Texas Department of Water Resources Report 270, 199 p., accessed April 30, 2021, at https://www.twdb.texas.gov/publications/reports/numbered_reports/doc/R270/R270.pdf.

Lower Trinity Groundwater Conservation District, 2019, Groundwater management plan: Lower Trinity Groundwater Conservation District, 106 p., accessed April 30, 2021, at https://4596a5d4-d630-4058-8899-b9dd610c192c.filesusr.com/ugd/125bf6_b1700eade64040d7a3791979b153f1d3.pdf.

Lower Trinity Groundwater Conservation District, 2021, What is the Lower Trinity Groundwater Conservation District?: Lower Trinity Groundwater Conservation District web page, accessed April 30, 2021, at https://www.waterwells.info/.

Matérn, B., 1960, Spatial variation—Stochastic models and their application to some problems in forest surveys and other sampling investigations (2d ed.): Berlin, Springer, 144 p., accessed April 30, 2021, at https://pub.epsilon.slu.se/10033/1/medd_statens_skogsforskningsinst_049_05.pdf.

Matheron, G., 1963, Principles of geostatistics: Economic Geology and the Bulletin of the Society of Economic Geologists, v. 58, no. 8, p. 1246–1266, accessed April 30, 2021, at https://doi.org/10.2113/gsecongeo.58.8.1246.

Meyer, W.R., and Carr, J.E., 1979, A digital model for simulation of ground-water hydrology in the Houston area, Texas: Texas Department of Water Resources Limited Publication LP–103, 133 p., accessed April 30, 2021, at https://www.twdb.texas.gov/publications/reports/limited_printing/doc/LP-103/LP-103%20a.pdf.

National Climatic Data Center, 2019, Climate Data Online: National Oceanic and Atmospheric Administration database, accessed October 14, 2019, at https://www7.ncdc.noaa.gov/CDO/CDODivisionalSelect.jsp. [Database moved prior to report publication; accessed April 6, 2022, at https://www.ncdc.noaa.gov/cdo-web/; search interface and search parameters did not change.]

Olea, R.A., 1975, Optimum mapping techniques using regionalized variable theory: Kansas Geological Survey Report No. 2, 137 p., accessed October 27, 2021, at https://www.kgs.ku.edu/Publications/Bulletins/SpA2/SpatialAnalysis2.pdf.

Olea, R.A., 2009, A practical primer on geostatistics (ver. 1.4, December 2018): U.S. Geological Survey Open-File Report 2009–1103, 346 p., accessed October 28, 2021, at https://doi.org/10.3133/ofr20091103.

Paramasivam, C.R., and Venkatramanan, S., 2019, Chapter 3—An introduction to various spatial analysis techniques: GIS and Geostatistical Techniques for Groundwater Science, p. 23–30, accessed April 30, 2021, at https://doi.org/10.1016/B978-0-12-815413-7.00003-1.

Pebesma, E., 2004, Multivariable geostatistics in S—The gstat package: Computers & Geosciences, v. 30, no. 7, p. 683–691, accessed September 10, 2021, at https://doi.org/10.1016/j.cageo.2004.03.012.

Pebesma, E., 2005, sp—R classes and methods for spatial data—R package (ver. 1.4–2): R Foundation for Statistical Computing software release, accessed October 27, 2021, at https://cran.r-project.org/package=sp.

Pebesma, E., 2018, Simple features for R—Standardized support for spatial vector data: R Journal, v. 10, no. 1, p. 439–446, accessed April 30, 2021, at https://doi.org/10.32614/RJ-2018-009.

Pebesma, E., 2020, gstat—Multivariable geostatistics in S—R package (ver. 2.0–6): R Foundation for Statistical Computing software release, accessed September 10, 2021, at https://cran.r-project.org/package=gstat.

Pebesma, E., 2021, sf—Simple features for R—Standardized support for spatial vector data—R package (ver. 0.9–8): R Foundation for Statistical Computing software release, accessed September 10, 2021, at https://cran.r-project.org/package=sf.

Philip, R.D., and Kitanidis, P.K., 1989, Geostatistical estimation of hydraulic head gradients: Ground Water, v. 27, no. 6, p. 855–865.

R Core Team, 2019, R—A language and environment for statistical computing: Vienna, R Foundation for Statistical Computing website, accessed October 28, 2021, at https://www.R-project.org/.

Ramage, J.K., 2022, Depth to groundwater measured from wells completed in the Chicot and Evangeline (undifferentiated) and Jasper aquifers, greater Houston area, Texas, 2021: U.S. Geological Survey data release, https://doi.org/10.5066/P9R6CX2T.

Ramage, J.K., and Braun, C.L., 2020, Groundwater-level altitudes and long-term groundwater-level changes in the Chicot, Evangeline, and Jasper aquifers, Houston-Galveston region, Texas, 2020: U.S. Geological Survey data release, accessed May 25, 2022, at https://doi.org/10.5066/P98IX48O.

Sandeen, W.M., and Wesselman, J.B., 1973, Groundwater resources of Brazoria County, Texas: Texas Water Development Board Report 163, 199 p., accessed November 1, 2021, at http://www.twdb.texas.gov/publications/reports/numbered_reports/doc/R163/R163.pdf.

Sarma, D.D., 2009, Geostatistics with applications in Earth sciences (2d ed.): New York, Springer, 205 p., accessed October 12, 2021, at https://doi.org/10.1007/978-1-4020-9380-7.

Sellards, E.H., Adkins, W.S., and Plummer, F.B., 1932, The geology of Texas, volume 1—Stratigraphy: University of Texas Bulletin 3232, 1,007 p.

Shah, S.D., Ramage, J.K., and Braun, C.L., 2018, Status of groundwater-level altitudes and long-term groundwater-level changes in the Chicot, Evangeline, and Jasper aquifers, Houston-Galveston region, Texas, 2018: U.S. Geological Survey Scientific Investigations Report 2018–5101, 18 p., accessed April 30, 2021, at https://doi.org/10.3133/sir20185101.

Snyder, J.P., 1987, Map projections—A working manual: U.S. Geological Survey Professional Paper 1395, 385 p., accessed November 16, 2021, at https://doi.org/10.3133/pp1395.

Stein, M.L., 1999, Interpolation of spatial data—Some theory for kriging: New York, Springer, 247 p., accessed April 30, 2021, at https://doi.org/10.1007/978-1-4612-1494-6.

Strom, E.W., Houston, N.A., and Garcia, C.A., 2003a, Selected hydrogeologic datasets for the Chicot aquifer, Texas: U.S. Geological Survey Open-File Report 03–297, 1 CD–ROM.

Strom, E.W., Houston, N.A., and Garcia, C.A., 2003b, Selected hydrogeologic datasets for the Evangeline aquifer, Texas: U.S. Geological Survey Open-File Report 03–298, 1 CD–ROM.

Strom, E.W., Houston, N.A., and Garcia, C.A., 2003c, Selected hydrogeologic datasets for the Jasper aquifer, Texas: U.S. Geological Survey Open-File Report 03–299, 1 CD–ROM.

Teeple, A.P., Foster, L.K., Lindaman, M.A., Duncan, L.L., and Casarez, I., 2021, Hydrogeologic data for the development of the hydrogeologic framework of the coastal lowlands aquifer system regional groundwater availability study area in Texas, Louisiana, Mississippi, Alabama, and Florida: U.S. Geological Survey data release, accessed April 30, 2021, at https://doi.org/10.5066/P9PEFY11.

Texas Water Development Board [TWDB], 2020a, Historical water use estimates: Texas Water Development Board web page, accessed October 2020 at http://www.twdb.texas.gov/waterplanning/waterusesurvey/estimates/index.asp.

Texas Water Development Board [TWDB], 2020b, Groundwater Database: Texas Water Development Board database, accessed September 10, 2020, at http://www.twdb.texas.gov/groundwater/data/gwdbrpt.asp.

Texas Water Development Board [TWDB], 2020c, Submitted drillers reports: Texas Water Development Board data viewer, accessed September 10, 2020, at https://www3.twdb.texas.gov/apps/WaterDataInteractive/GroundwaterDataViewer/?map=sdr.

Turcan, A.N., Jr., Wesselman, J.B., and Kilburn, C., 1966, Interstate correlation of aquifers, southwestern Louisiana and southeastern Texas: U.S. Geological Survey Professional Paper 550–D, p. D1–D6, accessed April 30, 2021, at https://doi.org/10.3133/pp550D.

University of Texas, Bureau of Economic Geology, 1968, Geologic atlas of Texas, Beaumont sheet: Austin, University of Texas, Bureau of Economic Geology, scale 1:250,000, accessed May 25, 2022, at https://data.tnris.org/collection/e28d8df6-cd30-4e89-bf0f-833e1ed0e670.

University of Texas, Bureau of Economic Geology, 1974, Geologic atlas of Texas, Austin sheet: Austin, University of Texas, Bureau of Economic Geology, scale 1:250,000, accessed May 25, 2022, at https://data.tnris.org/collection/e28d8df6-cd30-4e89-bf0f-833e1ed0e670.

U.S. Geological Survey, 2021, USGS water data for the Nation: U.S. Geological Survey National Water Information System database, accessed April 30, 2021, at https://doi.org/10.5066/F7P55KJN.

Wentworth, C.K., 1922, A scale of grade and class terms for clastic sediments: Journal of Geology, v. 30, no. 5, p. 377–392, accessed April 5, 2022, at https://doi.org/10.1086/622910.

White, W.N., Livingston, P.P., and Turner, S.F., 1939, Groundwater resources of the Houston-Galveston area and adjacent region, Texas: Prepared by Texas Board of Water Engineers in cooperation with U.S. Geological Survey, 323 p., accessed April 30, 2021, at https://www.twdb.texas.gov/publications/reports/historic_groundwater_reports/doc/M130.pdf.

White, W.N., Rose, N.A., and Guyton, W.F., 1944, Ground-water resources of the Houston district, Texas: U.S. Geological Survey Water-Supply Paper 889–C, 154 p., accessed April 30, 2021, at https://doi.org/10.3133/wsp889C.

Winslow, A.G., and Wood, L.A., 1959, Relation of land subsidence to ground-water withdrawals in the upper Gulf Coast region, Texas: Mining Engineering, v. 11, no. 10, p. 1030–1034.

Wood, L.A., and Gabrysch, R.K., 1965, Analog-model study of ground water in the Houston district, Texas: Texas Water Commission Bulletin 6508, 103 p., accessed April 30, 2021, at https://www.twdb.texas.gov/publications/reports/bulletins/doc/B6508/B6508.pdf.

Yamamoto, J.K., 2000, An alternative measure of the reliability of ordinary kriging estimates: Mathematical Geology, v. 32, no. 4, p. 489–509, accessed December 17, 2021, at https://doi.org/10.1023/A:1007577916868.

Young, S.C., Budge, T., Knox, P., Kalbouss, R., Baker, E., Hamlin, S., Galloway, B., and Deeds, N., 2010, Final report—Hydrostratigraphy of the Gulf Coast aquifer system from the Brazos River to the Rio Grande: Texas Water Development Board report, prepared by URS Corporation, Baer Engineering and Environmental Consulting, Inc., and INTERA, Inc., 203 p., accessed April 30, 2021, at https://www.twdb.texas.gov/publications/reports/contracted_reports/doc/0804830795_Gulf_coast_hydrostratigraphy_wcover.pdf.

Young, S.C., and Draper, C., 2020, The delineation of the Burkeville confining unit and the base of the Chicot aquifer to support the development of the Gulf 2023 groundwater model: Harris-Galveston Subsidence District report, prepared by INTERA, Inc., 75 p., accessed October 27, 2021, at https://hgsubsidence.org/wp-content/uploads/2021/06/Final_HGSD_FBSD_Burkeville_Report_final.pdf.

Young, S.C., Ewing, T., Hamlin, S., Baker, E., and Lupton, D., 2012, Final report—Updating the hydrogeologic framework for the northern portion of the Gulf Coast aquifer system: Texas Water Development Board report, prepared by INTERA, Inc., and Frontera Exploration Consultants, 285 p., accessed April 30, 2021, at https://www.twdb.texas.gov/publications/reports/contracted_reports/doc/1004831113_GulfCoast.pdf.

Young, S.C., Pinkard, J., Basset, R.L., and Chowdhury, A.H., 2014, Final report—Hydrogeochemical evaluation of the Texas Gulf Coast aquifer system and implications for developing groundwater availability models: Texas Water Development Board report no. 1148301233, prepared by INTERA, Inc., and Tetra Tech, 375 p., accessed April 30, 2021, at https://www.twdb.texas.gov/publications/reports/contracted_reports/doc/1148301233.pdf.

Appendix 1

This appendix provides maps depicting the planar surface of 2020 water-level altitudes for the Chicot, Evangeline, and Jasper aquifers in the greater Houston area, Texas. Planar surfaces were prepared by fitting first- and second-order polynomial equations of water-level altitude as a function of *X* and *Y* coordinate pairs. First-order polynomial equations (Olea, 1975, 2009) (eq. 1 in report) produced planar surfaces for the Chicot, Evangeline, and Jasper aquifers (figs. 1.1–1.3). A second-order polynomial equation (Olea, 1975, 2009) (eq. 2 in report) was used to refine the planar surfaces from equation 1 for the Chicot, Evangeline, and Jasper aquifers (figs. 1.4–1.6) to provide a better fit to the water-level-altitude data collected in 2020 (Ramage and Braun, 2020).

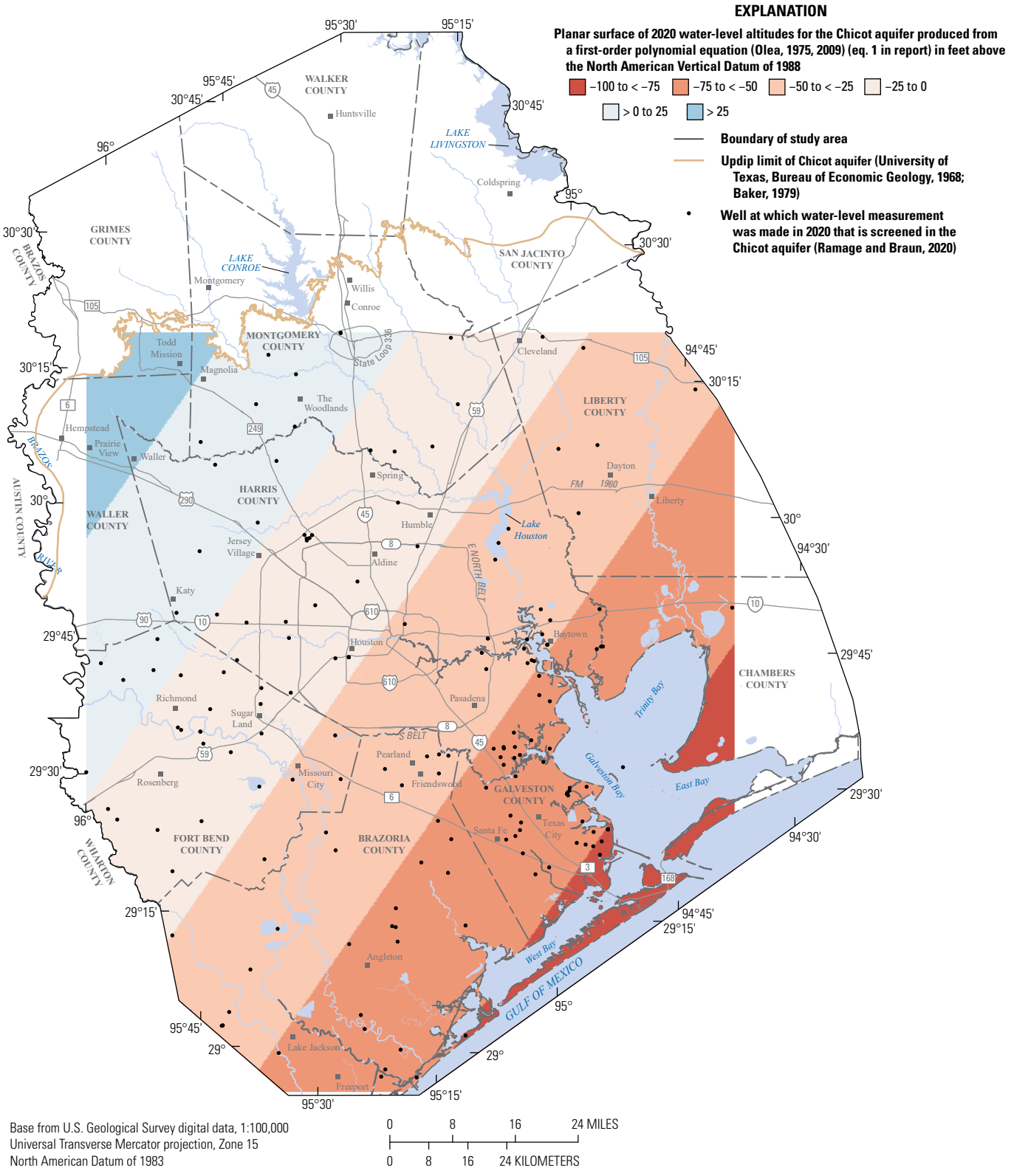

Figure 1.1. Planar surface of 2020 water-level altitudes for the Chicot aquifer in the greater Houston study area, Texas, produced from a first-order polynomial equation.

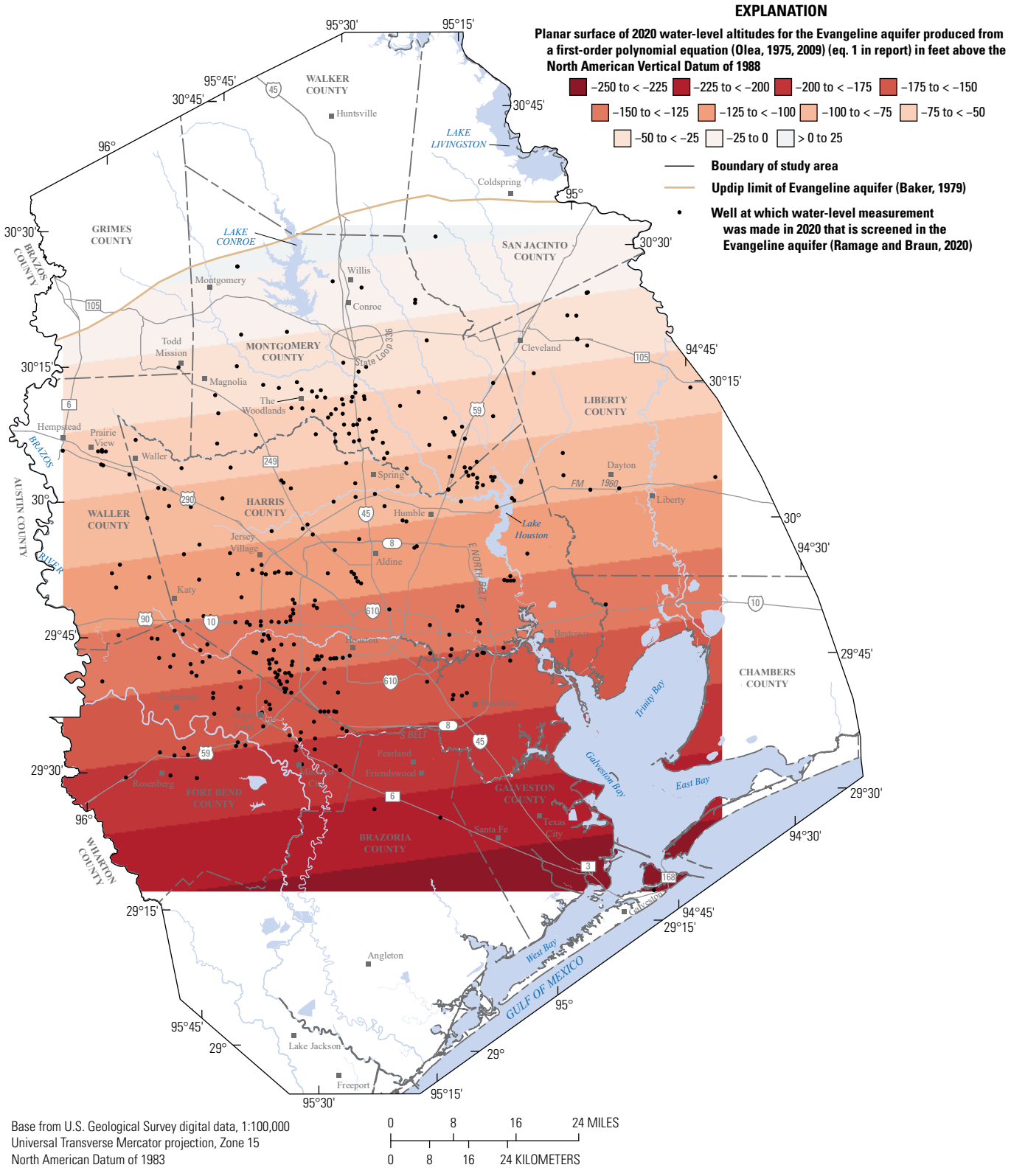

Figure 1.2. Planar surface of 2020 water-level altitudes for the Evangeline aquifer in the greater Houston study area, Texas, produced from a first-order polynomial equation.

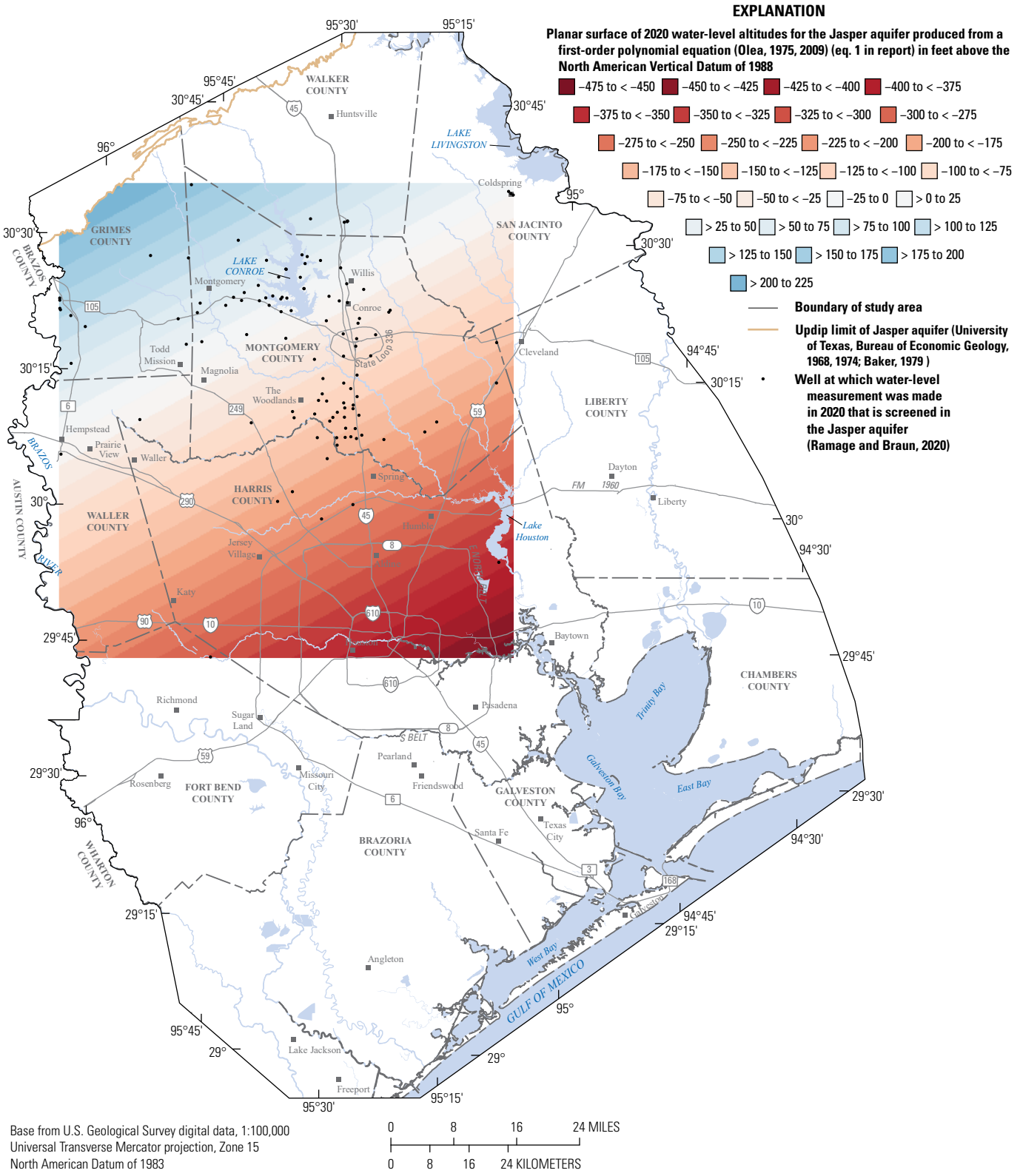

Figure 1.3. Planar surface of 2020 water-level altitudes for the Jasper aquifer in the greater Houston study area, Texas, produced from a first-order polynomial equation.

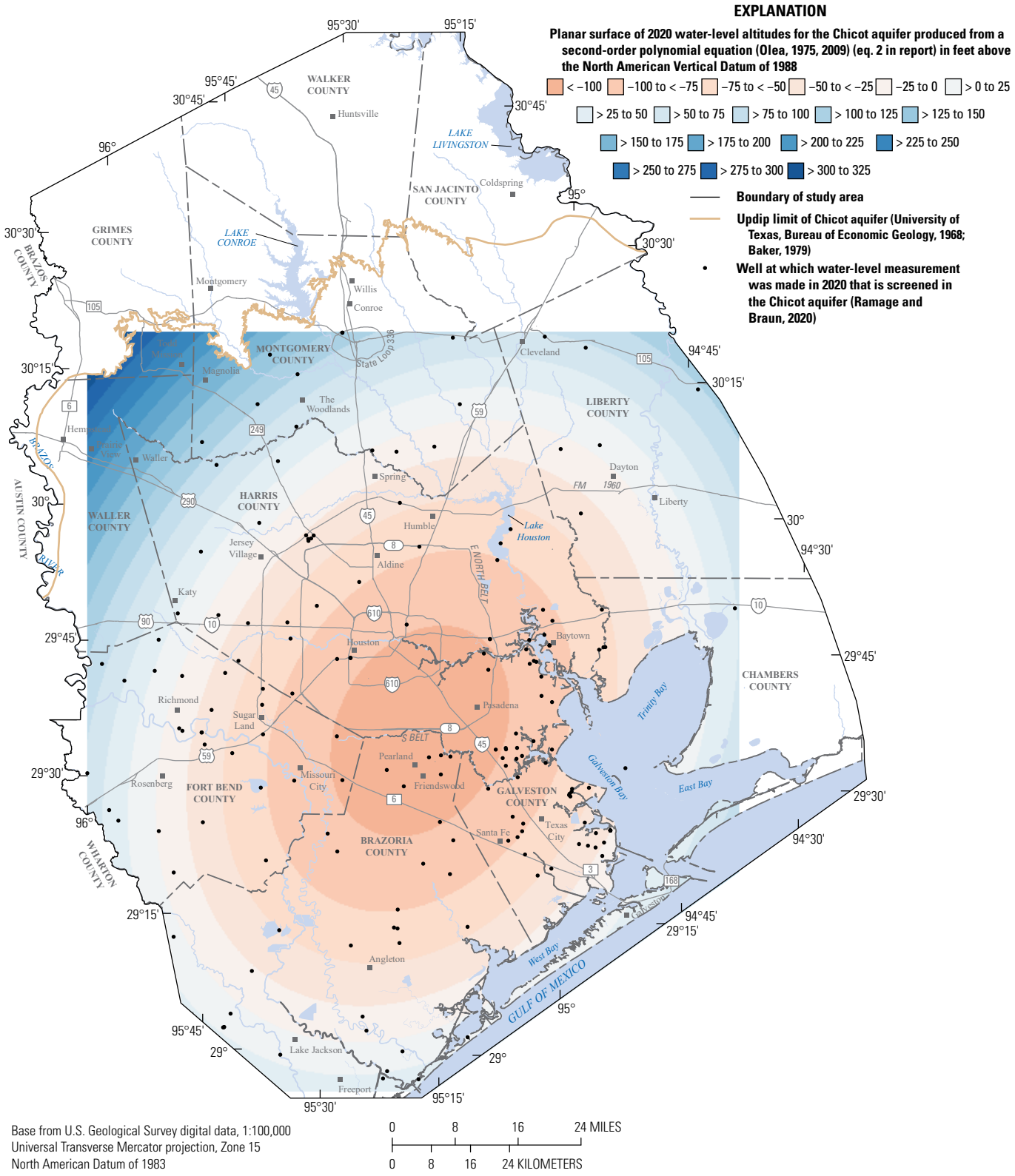

Figure 1.4. Planar surface of 2020 water-level altitudes for the Chicot aquifer in the greater Houston study area, Texas, produced from a second-order polynomial equation.

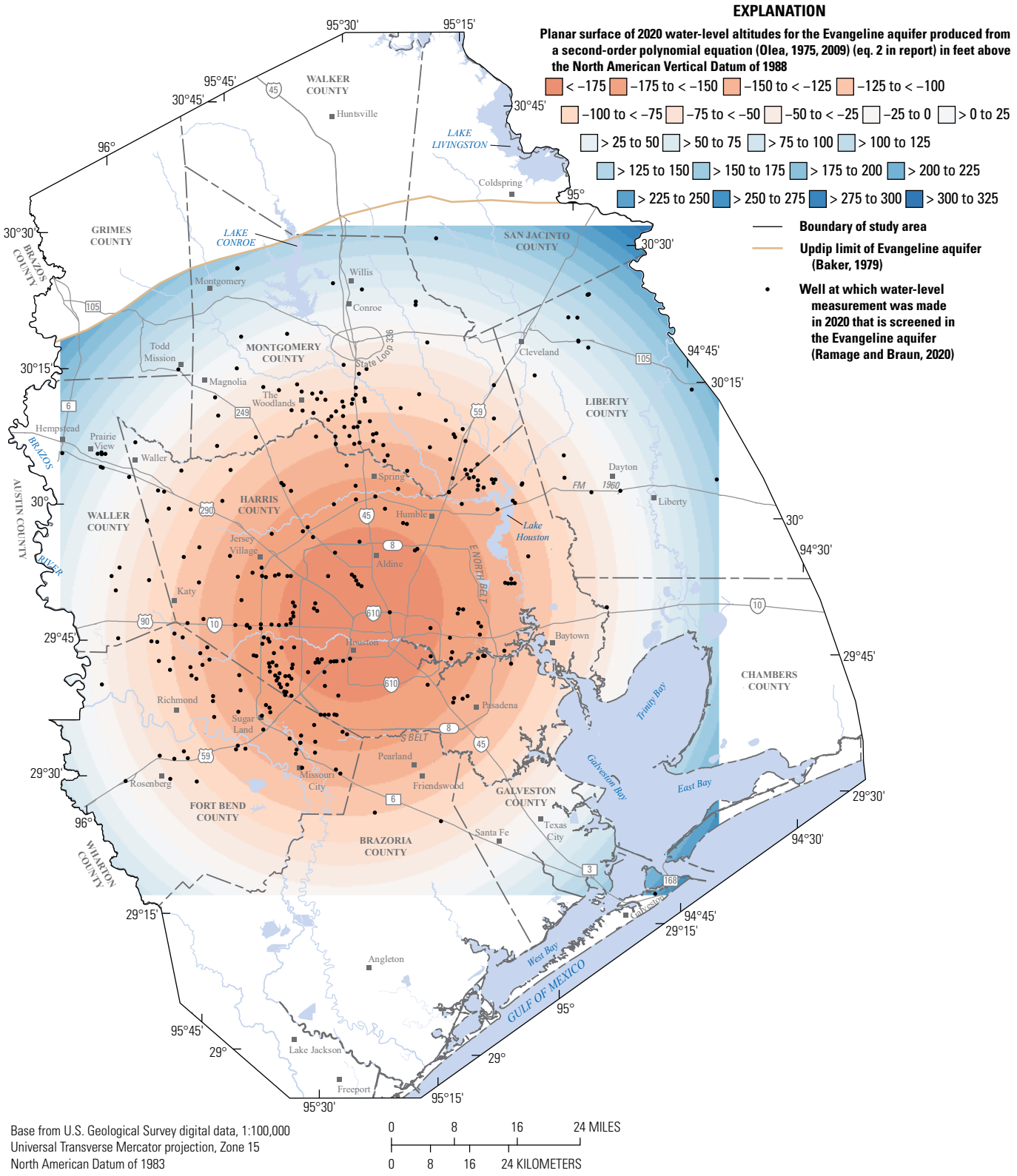

Figure 1.5. Planar surface of 2020 water-level altitudes for the Evangeline aquifer in the greater Houston study area, Texas, produced from a second-order polynomial equation.

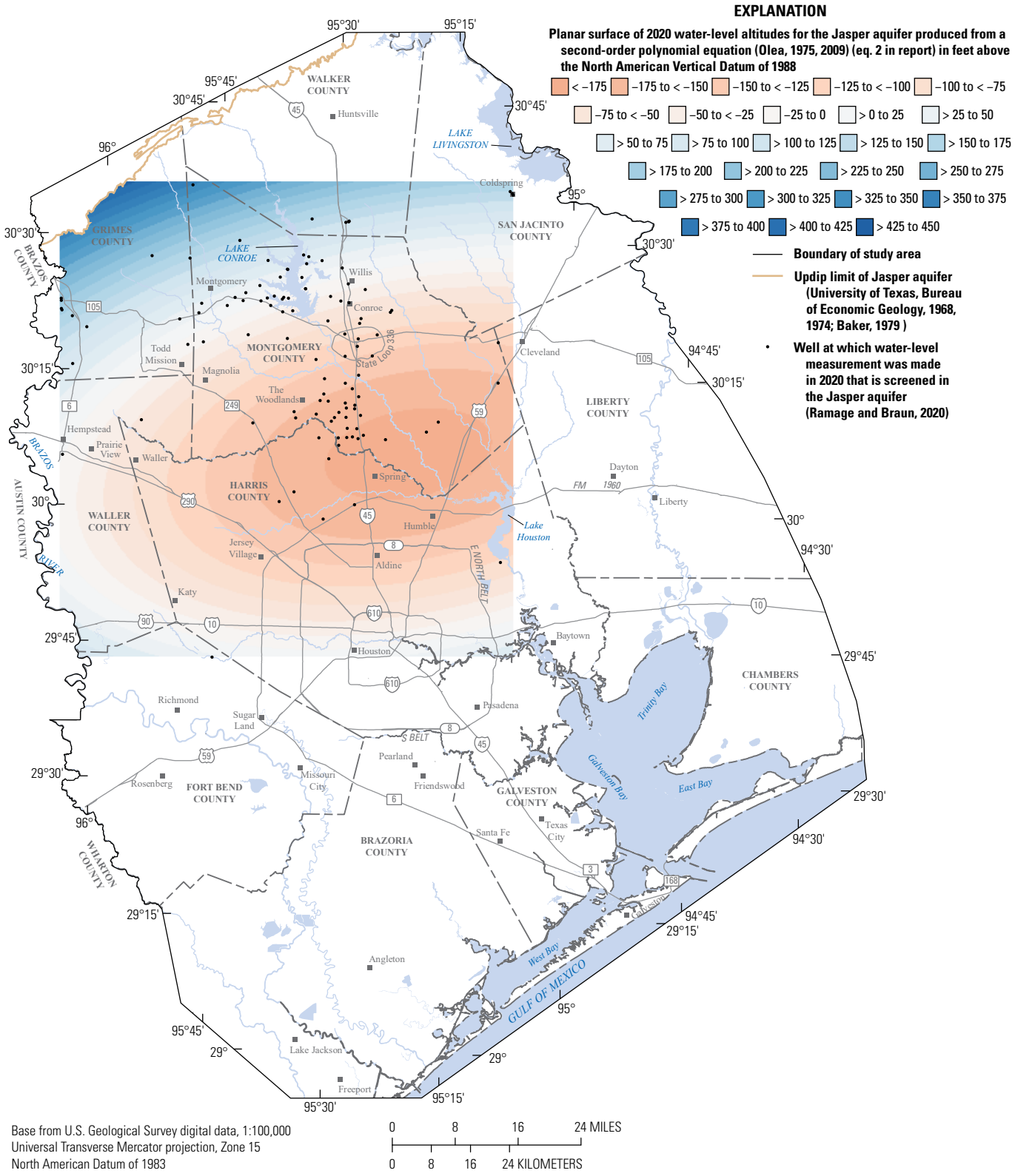

Figure 1.6. Planar surface of 2020 water-level altitudes for the Jasper aquifer in the greater Houston study area, Texas, produced from a second-order polynomial equation.

References Cited

Baker, E.T., Jr., 1979, Stratigraphic and hydrogeologic framework of part of the Coastal Plain of Texas: Texas Department of Water Resources Report 236, 43 p., accessed April 30, 2021, at http://www.twdb.texas.gov/publications/reports/numbered_reports/doc/R236/R236.pdf.

Olea, R.A., 1975, Optimum mapping techniques using regionalized variable theory: Kansas Geological Survey Report No. 2, 137 p., accessed October 27, 2021, at https://www.kgs.ku.edu/Publications/Bulletins/SpA2/SpatialAnalysis2.pdf.

Olea, R.A., 2009, A practical primer on geostatistics (ver. 1.4, December 2018): U.S. Geological Survey Open-File Report 2009–1103, 346 p., accessed October 28, 2021, at https://doi.org/10.3133/ofr20091103.

Ramage, J.K., and Braun, C.L., 2020, Groundwater-level altitudes and long-term groundwater-level changes in the Chicot, Evangeline, and Jasper aquifers, Houston-Galveston region, Texas, 2020: U.S. Geological Survey data release, accessed October 28, 2021, at https://doi.org/10.5066/P98IX48O.

University of Texas, Bureau of Economic Geology, 1968, Geologic atlas of Texas, Beaumont sheet: Austin, University of Texas, Bureau of Economic Geology, scale 1:250,000, accessed May 25, 2022, at https://data.tnris.org/collection/e28d8df6-cd30-4e89-bf0f-833e1ed0e670.

University of Texas, Bureau of Economic Geology, 1974, Geologic atlas of Texas, Austin sheet: Austin, University of Texas, Bureau of Economic Geology, scale 1:250,000, accessed May 25, 2022, at https://data.tnris.org/collection/e28d8df6-cd30-4e89-bf0f-833e1ed0e670.

For more information about this publication, contact
Director, Oklahoma-Texas Water Science Center
U.S. Geological Survey
1505 Ferguson Lane
Austin, TX 78754–4501

For additional information, visit
https://www.usgs.gov/centers/ot-water

Publishing support provided by
Lafayette Publishing Service Center

ISSN 2328-0328 (online)
https://doi.org/10.3133/sir20225064